# การทดสอบในห้องปฏิบัติการเกี่ยวกับคอนกรีตเสริมเส้นใยเหล็ก และ ตัวอย่างการนำมาประยุกต์ใช้ในการศึกษาพฤติกรรมทางด้านโครงสร้างของดาดอุโมงค์

นางสาวทิพพะมาลา มณีวงค์

วิทยานิพนธ์นี้เป็นส่วนหนึ่งของการศึกษาตามหลักสูตรปริญญาวิศวกรรมศาสตร์มหาบัณฑิต

สาขาวิศวกรรมโยธา ภาควิศวกรรมโยธา

คณะวิศวกรรมศาสตร์ จุฬาลงกรณ์มหาวิทยาลัย

ปีการศึกษา 2555

# LABORATORY TESTS ON STEEL FIBER REINFORCED CONCRETE AND THEIR APPLICATION EXAMPLE ON STRUCTURAL PERFORMANCE OF TUNNEL LINING

Miss Thipphamala Manivong

A Thesis Submitted in Partial Fulfillment of the Requirements
for the Degree of master of Engineering  Program in Civil Engineering
Department of Civil Engineering
Faculty of Engineering
Chulalongkorn University
Academic Year 2012

| | |
|---|---|
| หัวข้อวิทยานิพนธ์ | การทดสอบในห้องปฏิบัติการเกี่ยวกับคอนกรีตเสริมเส้นใยเหล็ก และ ตัวอย่างการนำมาประยุกต์ใช้ในการศึกษาพฤติกรรมทางด้านโครงสร้างของดาดอุโมงค์ |
| โดย | นางสาวทิพพะมาลา มณีวงค์ |
| สาขาวิชา | วิศวกรรมโยธา |
| อาจารย์ที่ปรึกษาวิทยานิพนธ์หลัก | ผู้ช่วยศาสตราจารย์ ดร.ธเนศ ศรีศิริโรจนากร |
| อาจารย์ที่ปรึกษาวิทยานิพนธ์ร่วม | ผู้ช่วยศาสตราจารย์ ดร.วิทิต ปานสุข |

---

คณะวิศวกรรมศาสตร์ จุฬาลงกรณ์มหาวิทยาลัย อนุมัติให้นับวิทยานิพนธ์ฉบับนี้เป็นส่วนหนึ่งของการศึกษาตามหลักสูตรปริญญามหาบัณฑิต

…………………………………………….. คณบดีคณะวิศวกรรมศาสตร์
(รองศาสตราจารย์ ดร.บุญสม เลิศหิรัญวงศ์)

คณะกรรมการสอบวิทยานิพนธ์

…………………………………………….. ประธานกรรมการ
(รองศาสตราจารย์ ดร.สุพจน์ เตชวรสินสกุล)

……………………………………….. อาจารย์ที่ปรึกษาวิทยานิพนธ์หลัก
(ผู้ช่วยศาสตราจารย์ ดร.ธเนศ ศรีศิริโรจนากร)

……………………………………….. อาจารย์ที่ปรึกษาวิทยานิพนธ์ร่วม
(ผู้ช่วยศาสตราจารย์ ดร.วิทิต ปานสุข)

…………………………………………….. กรรมการ
(ดร.สุพัฒน์ สุวรรณการ)

ทิพพะมาลา มณีวงค์ : การทดสอบในห้องปฏิบัติการเกี่ยวกับคอนกรีตเสริมเส้นใยเหล็กและ ตัวอย่างการนำมาประยุกต์ใช้ในการศึกษาพฤติกรรมทางด้านโครงสร้างของดาดอุโมงค์ (LABORATORY TESTS ON STEEL FIBER REINFORCED CONCRETE AND THEIR APPLICATION EXAMPLE ON STRUCTURAL PERFORMANCE OF TUNNEL LINING) อ.ที่ปรึกษาวิทยานิพนธ์หลัก: ผศ.ดร.ธเนศ ศรีศิริโรจนากร, อ.ที่ปรึกษาวิทยานิพนธ์ร่วม: ผศ.ดร.วิทิต ปานสุข, 74 หน้า.

งานวิจัยนี้มีวัตถุประสงค์เพื่อศึกษาประสิทธิภาพของคอนกรีตเสริมใยเหล็ก (SFRC) ในงานก่อสร้างเช่นอาคาร, สะพาน, อุโมงค์ ฯลฯ ซึ่งจะแสดงถึงประสิทธิภาพของ SFRC ที่มีและไม่มีสารลดน้ำในคอนกรีตด้วยการทดสอบในห้องปฏิบัติการ ด้วยวิธีการทดสอบกำลังรับแรงอัด กำลังรับแรงดัด และกำลังรับแรงดึง ในตัวอย่างคอนกรีตแบบลูกบาศก์ คาน และบริเคท์ ตามลำดับ คุณสมบัติของ SFRC จะถูกนำไปเปรียบเทียบกับคอนกรีตทั่วไป หลังจากนั้นคุณสมบัติทุกอย่างของ SFRC จากการทดลองจะถูกนำไปใช้กับการออกแบบดาดอุโมงค์ร่วมกับพารามิเตอร์พื้นฐานของดินจากโครงการเขื่อนห้วยลำพันใหญ่ เพื่อใช้เป็นข้อมูลสำหรับการวิเคราะห์ด้วยวิธีไฟไนต์อิลิเมนท์หาพฤติกรรมของดาดอุโมงค์ แบบอุโมงค์ที่ใช้วิเคราะห์มีจำนวนเส้นผ่าศูนย์กลาง 4 ขนาด และมีความหนา 0.5 เมตร งานวิจัยนี้คำนึงถึงน้ำหนักกระทำที่มาจากดินเพียงอย่างเดียวและตรวจสอบความเครียดที่ด้านบน ด้านข้างและด้านล่างของอุโมงค์กับความเค้นดึงที่ได้มาจากการทดสอบในห้องปฏิบัติการ

ภาควิชา ....วิศวกรรมโยธา.... ลายมือชื่อนิสิต ....................

สาขาวิชา ....วิศวกรรมโยธา.... ลายมือชื่อ อ.ที่ปรึกษาวิทยานิพนธ์หลัก....................

ปีการศึกษา ....2555.... ลายมือชื่อ อ.ที่ปรึกษาวิทยานิพนธ์ร่วม....................

## 5370678721 : Civil Engineering Department
KEYWORDS : STEEL FIBER / TUNNEL LINING / SUPER PLASTICIZER

Thipphamala Manivong : LABORATORY TESTS ON STEEL FIBER REINFORCED CONCRETE AND THEIR APPLICATION EXAMPLE ON STRUCTURAL PERFORMANCE OF TUNNEL LINING. ADVISOR : ASST.PROF. TANATE SRISIRIROJANAKORN, Ph.D, CO-ADVISOR : ASST.PROF.DR.VITHIT PANSUK,Ph.D, 74 pp.

The purpose of this research is for studying the performance of Steel Fiber Reinforced Concrete (SFRC) in construction works such as building, bridge, tunnel, etc,. It will present the performance of SFRC with and without super plasticizer by laboratory test on compression, bending and tension test in cube, beam and briquette respectively. The characteristic of SFRC will be found and compared with plain concrete. Next, all of characteristic of SFRC from the test will be applied to the tunnel lining design. The tunnel project case study which is used for this research will be excavated into thick-bedded fine sandstone, locally interbedded with very thin stratified mudstone. In this paper will use the basic parameter of soil from tunnel's site at Huay Lam Phan Ngai Hydropower project (Laos), and apply the basic parameters of material from the laboratory test into Finite Element Method software to analyze and design the performance of lining. Four sizes of tunnel diameter had been applied to the analysis with 0.5 m thickness. This research concerns only the load from the soil, and checks the strain of tunnel lining at crown, invert and spring line of tunnel with the tensile strain from laboratory test.

| | |
|---|---|
| Department...................................... | Student's Signature.......................................... |
| Field of Study............................... | Advisor's Signature.......................................... |
| Academic Year............................. | Co- Advisor's Signature.................................... |

# Acknowledgement

First of all, I would like to say a big thank to AUN/Seed-Net that provide me the scholarship and give me the chance to study at Chulalongkorn University. I would like to thank you to my advisor, Asst. Pro. Dr. Tanate Srisirirojanakorn that supported me everything, suggest a new thing and help me to finish this research. I would like to say thank you to my co-advisor, Asst. Pro. Dr. Vithit Pansuk that gave very good comments and big help about new knowledge that is out of my field. I would like to say thank you to my committees that give the time and knowledge for this research. Last but not least, I would like to thank you all my friends, juniors, and senior that support me everything. At last, I would like to say thank you very much to my parents and family that always support and encourage me while I am study here.

# Content

Page

# Lists of table

Page

Page

# Lists of figure

Page

Page

Page

# Chapter I

# Introduction

## 1. Introduction

In the past, tunnel constructions have been applied to most of the developed countries in the world. It was used for underground transportation such as pathways for mining, developing shorter roads in the mountainous area and diverting or supplying water into the city. In recent years, advancements have been made in constructing tunnels especially, in the materials they use.

The materials used for tunnel construction have been developed continuously such as steel, concrete and Steel Fiber Reinforce Concrete (SFRC). These materials are developed in such a way that it can be used for a long time and it is cost effective. SFRC is new technology in reinforced concrete. It contains steel fiber together with concrete in order to increase the strength of concrete. The technology of SFRC is widely used in the developed countries such as USA, European countries, Japan and Australia, to name a few. They use SFRC for tunnel lining and flooring. In South East Asian countries, there rarely apply this technology for the construction of structures, except Singapore. They use SFRC for the construction of tunnel lining segment. In Thailand, this technology is totally new for the civil engineers. This research provides the characteristics of steel fiber reinforced concrete with the use of the local material. Moreover, this research can provide information on the effectiveness of SFRC in tunneling construction. More so, this research provides the behavior of tunnel lining when SFRC is applied. Furthermore, a comparison between SFRC and plain concrete was made. This is to determine the advantages of SFRC when applied in tunnel lining.

In order to determine the characteristics of SFRC, specimens such as cube, beam and briquette was prepared. These were prepared in 4 batches, 2 of which having different strength and the other 2 contains SFRC with and without plasticizer. Laboratory tests such as tension, compression, and bending moment was performed to obtain the compressive strength, bending strength and tensile strength respectively.

The project related on this research is located on Champasak province, Lao People's Democratic Republic (Lao PDR). Houay Lamphan Ngai Hydropower project is located on Bolaven plateau, southern part of Laos. It covers 2 provinces, the dam located on Xekong province, while the reservoir is on Champasak province. The installed capacity of the Project is 86.7 MW, and the average annual generation capacity is 480GWh. The tunnel is open-face excavation, Horse-shoe Shape under low pressure with the length of 2700 m and 5200 m. The thickness of tunnel lining was 0.5m.

## 2. Purpose of the research

- To know the characteristic of Steel Fiber Reinforced Concrete (SFRC) in terms of axial force (tension and compression) and bending moment, with and without plasticizer.
- To know how to apply the SFRC in to the tunnel construction design.
- To know the behavior of SFRC when the load from the soil is continuously being applied on the tunnel lining segment.

## 3. Limitation of the research

- This research only focuses on the determination of the behavior of SFRC when it was applied to the tunnel lining design of the Huay Lam Phan Ngai hydropower project at Champasak province, Lao PDR. The soil profile and tunnel's properties were based from this hydropower project.
- Studying the characteristic of SFRC by the laboratory test according to ASTM standard.
- Studying the tunnel lining design by numerical method and using structural software (ANSYS) to determine its behavior.
- Studying only on the behavior of lining segments under the load of soil.

## 4. Output

The outputs from this research are enumerated as follows:

- Techniques and methodology of designing and testing SFRC in the laboratory test.
- The characteristic of SFRC with and without super plasticizer and compare it with the plain concrete.
- The methodology of tunnel lining design by using numerical method (ANSYS).
- The behavior of soil and tunnel while using the SFRC.
- Advantages and disadvantages of SFRC when they were applied to tunnel lining.
- The behavior of tunnel lining segment under load of soil.

# Chapter II

## Literature review

1. **Introduction to tunnel**

### 1.1 Type of tunnel lining

There are 3 sections within the tunnel lining that are constantly affected with the load namely: crown, invert, and spring line. A tunnel lining has two parts, primary and secondary lining. Primary lining serves as the main structure and is designed to hold the load of the tunnel. In constructing the primary lining, the segment is installed immediately at the tale of the boring machine. If all the segments of the primary lining is properly installed and forms as a ring, underground water can be prevented to flow inside the tunnel. More so, all forces the tunnel carries will be properly carried by the primary lining. While the secondary lining is responsible on protecting the primary lining from corrosion, and adjusting of the alignment-deviation. It will be installed after the primary lining is finished.

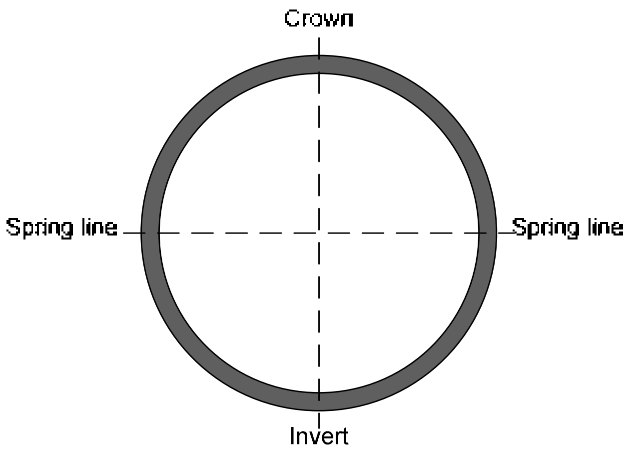


Figure 2.1 Tunnel's element

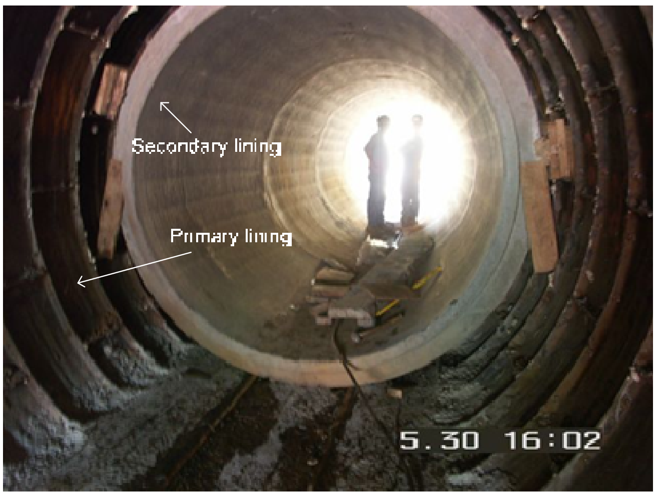


Figure 2.2 Primary lining and secondary lining

### 1.2 Behavior of lining

Normally, the lining construction is designed as an elastic ring which can be deformed. The deformation of the tunnel can vary depending on the properties of lining and the loads effected to the tunnel.

- **Unconfined ring**

For the case of the uniform compression stress, the thickness of the tunnel can resist the deformation enough via the radius as shown in Figure 2.3. For the case of concentrated load occurring at crown and invert, the lining will deform as bloom out at spring line, which the deformation is more than the case of uniform compression stress, as shown in Figure 2.4.

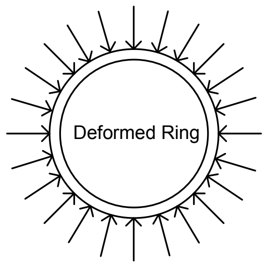


Figure 2.3 The deformation of lining in case of unconfined ring under the uniform load

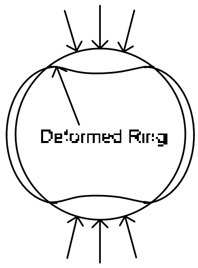


Figure 2.4 The deformation of lining in case of unconfined ring under the concentrated load

- **Partially Confined Ring**

The deformation as shown in Figure 2.5 is the case when the loads occur at the crown and invert are active pressure and passive pressure, respectively. For the deformation of the tunnel, the expansion normally occurs at the spring line. Partially Confined Ring is similar as unconfined ring, but the deformation is smaller.

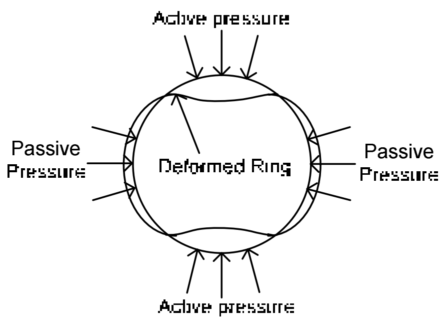


Figure 2.5 The deformation of lining in case of partially confined ring under the concentrated load

- **Fully confined ring**

As shown in Figure 2.6, the active pressure occurs at crown and invert while the passive pressure spread along the lining. In this case, active pressure is a uniform load. If it's not, passive pressure will occur as shown in Figure 2.7 which the deformation of fully confined ring is less than the other case.

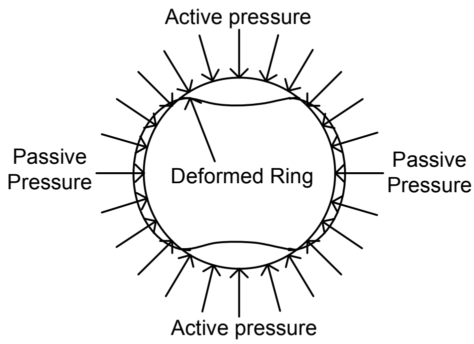


Figure 2.6 The deformation of lining in case of fully confined ring under the concentrated load

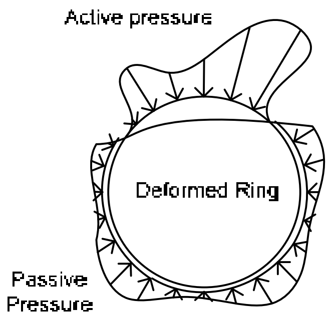


Figure 2.7 The deformation of lining in case of fully confined ring which active pressure is not uniformed under the random load

For the tunnel lining arrangement, in order for the ring to be considered as flexible it is assumed to be a monolithic ring and the moment of inertia is 60-80% of calculated pipe segment in each the same thickness. Normally, the ratio of reinforced concrete tunnel between thickness and radius is 6 to 12% as shown in Figure 2.8.

| (d/R) | $(d/R)^2$ | $q_u$(min) #/ft$^2$=4.8$(d/R)^2$*10$^4$ |
|---|---|---|
| 4 | 640000 | 307 |
| 6 | 2160000 | 1037 |
| 8 | 5120000 | 2456 |
| 10 | 10000000 | 4800 |
| 12 | 17280000 | 8256 |

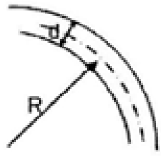


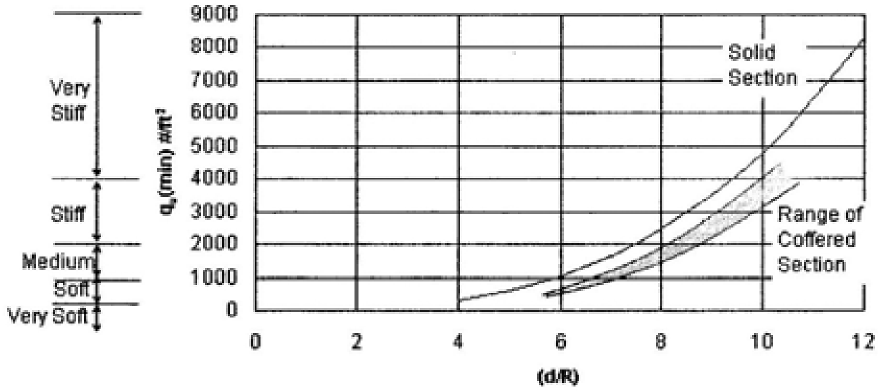


$$\frac{Ei}{R^3} < 5q_u$$

$$q_u > \frac{Ei}{5R^3}$$

$$\text{from } i = \frac{d^3}{12} \text{ for unit tunnel length}$$

$$q_u > \frac{E}{60}\left(\frac{d}{R}\right)^3$$

$$\text{from } E = 2\times10^6\ \#/in^2 \text{ for monolithic concrete segments}$$

$$q_u > \frac{E}{30}\left(\frac{d}{R}\right)^3 \times 10^6\ \#/in^2$$

$$q_u > 4.8E\left(\frac{d}{R}\right)^3 \times 10^6\ \#/in^2$$

Figure2.8 Relationship between the thickness of flexibility ring and $q_u$ minimum.

When there is an internal force present within the tunnel lining it will be considered as an elastic ring. The moment occurring in the lining will be related to the distortion ratio (ΔR/R). The axial force will then be related with the overburden pressure of soil which increases as the depth, the ratio between thickness and radius of tunnel increases as shown in Figure 2.9.

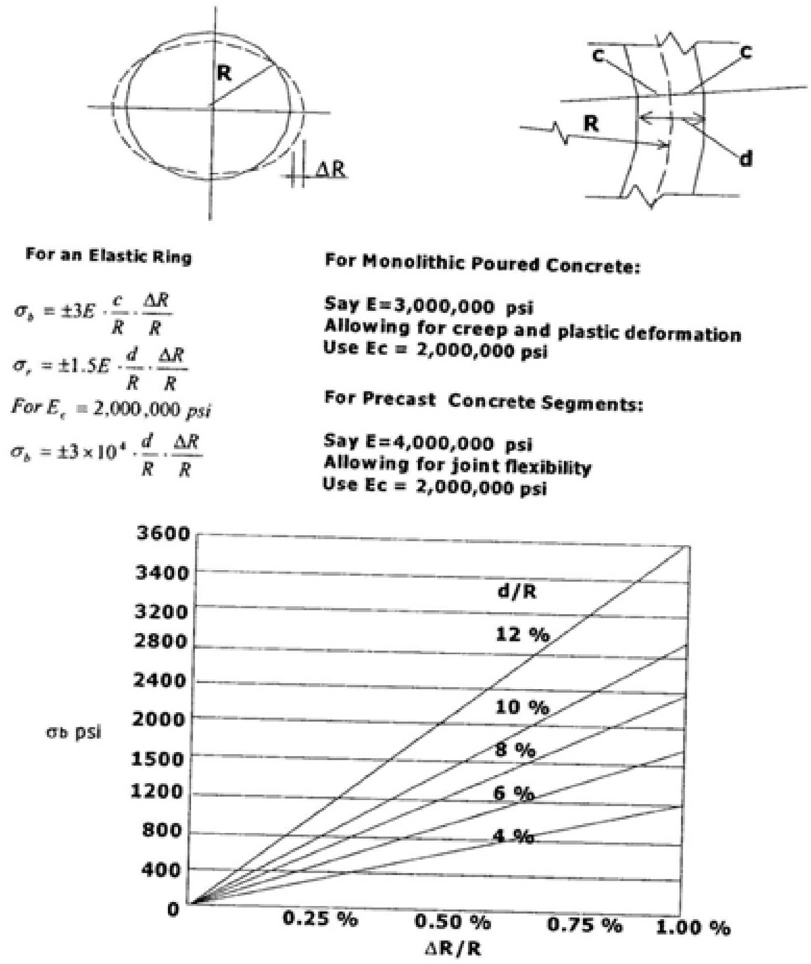


Figure2.9 Relationship between moment in tunnel and deformation ratio.

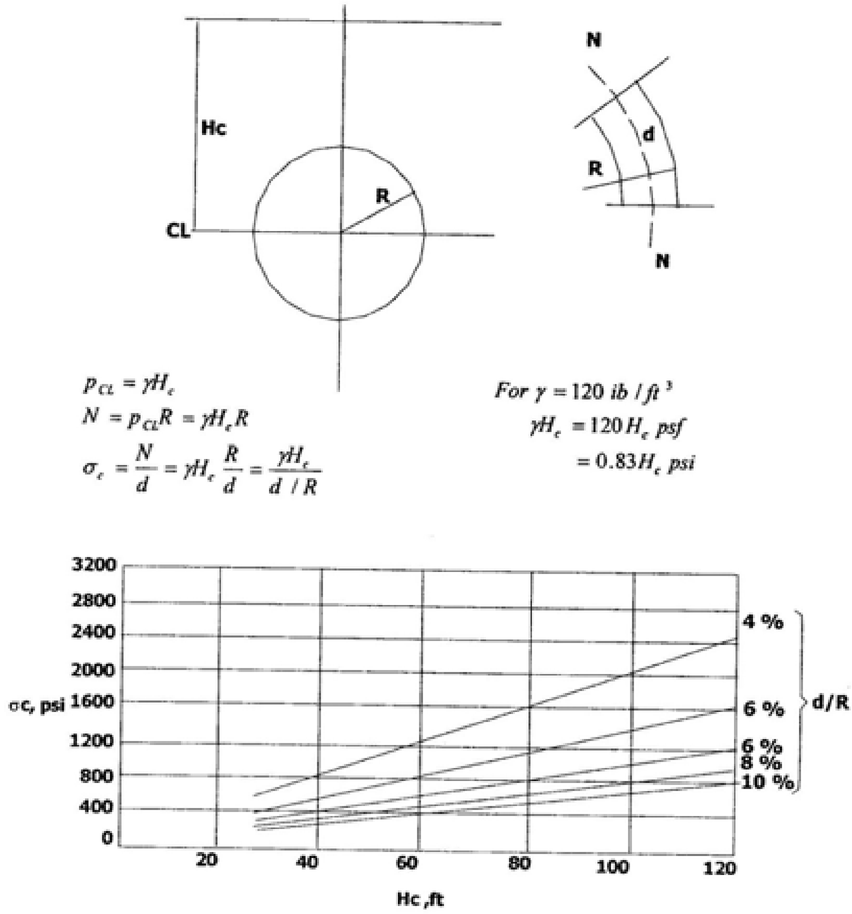


Figure2.10 Relationship between axial force and the depth-size of tunnel

## 2. Introduction to ANSYS

Finite element method is a numerical method which uses computer programming to help engineers analyze the deformation and design of the tunnel lining. The users need to know the basic concept of soil mechanic and calculation criteria. In geotechnical engineering, calculating and designing by finite element method is done by modeling the real behavior of structure by dividing soil and structure into small elements with node point as the area of analysis. In each element, there are stress and strain values that are limited by the boundary condition and the loads present. The user can determine the yield point and deformation value of each element. The appropriate amount and size of each element can be assigned to the structure.

ANSYS is the software that analyzes the behavior of the structure which uses finite element method. Its structural software is from ANSYS, Inc., Canonsburg, Pennsylvania, USA. ANSYS can verify geometric shape, material properties and boundary conditions through graph display before calculation. It can also display the simulation results by multiple ways such as color nephogram, contour and animation display**.** It can perfectly analyze the mechanical behavior of many complex configurations in engineering structures. More so, it can be able to describe crack formation and expansion of the structure. This program can simulate material and geometry nonlinear properties of large-scale complex structure. ANSYS 13.0 was used in this research to analyze the behavior of tunnel lining under large deformation.

## 3. History of Concrete

### 3.1 Plain concrete

In the past, when describing the characteristics of a plain concrete, it is both high compressive strength and low tensile strength. So, in 1849 the French engineer used steel bars (reinforced bars) or pre-stressed steel to help the plain concrete to carry the tensile strength. They called this type of concrete is reinforced concrete. It was used as the main material for construction works especially in constructing buildings. In addition, the failure strain of the plain concrete in tension is so low that the reinforcement has to hold the cracked sections together. A disadvantage of using steel bars is when the maximum bending moment and shear strength are reached then large cracks within the structures can be seen.

### 3.2 Concrete with special material

Since 1960, the innovation of fiber reinforced concrete (FRC) had been carried out by the engineers. Nowadays, FRC is mainly use in shotcrete, flooring and pavement, but it can be adapted to use in the other types of concrete construction such as beam and foundation. Concrete reinforced with fibers (which are usually steel, glass, or plastic fibers) is less expensive than hand-tied rebar and at the same time carries larger tensile strength. Moreover, it can resist corrosion effect without the cover length. The fibers used in FRC material are often divided into 2 categories: low modulus, high elongation; and high strength, high modulus fibers. The following are the different types of fibers generally used in the construction industries.

- Glass-fiber Reinforced Concrete (GFRC): Glass fiber is inexpensive and corrosion-proof, but not as ductile as steel. It can incorporate with continuous lengths or in discontinuous (chopped) lengths. In addition, it's very suitable for the thin concrete segment. Glass fiber reinforced concrete architectural panels have a general appearance of pre-cast concrete panels, but are different in several significant ways. For example, GFRC panels will, on the average, weigh substantially less than pre-cast concrete panels due to their reduced thickness. The low weight of GFRC panels decrease superimposed loads on the building's structural components. The building frame becomes more economical.
- Steel Fiber Reinforced Concrete (SFRC): Steel is the strongest commonly-available fiber, and comes in different lengths (30 to 80 mm in Europe) and shapes (end-hooks). Steel fibers can only be used on surfaces that can tolerate or avoid corrosion and rust stains. In some cases, a steel-fiber surface is faced with other materials.
- Polypropylene Fiber Reinforced (PFR): cement mortar and concrete Polypropylene is one of the cheapest and abundantly available polymers. They are highly resistant to chemical effect. Its melting point is low, so it can tolerate heat from the fire. Polypropylene short fibers in small volume fractions between 0.5 and 15 commercially used in concrete.
- Asbestos Fibers: It is naturally available and it is an inexpensive mineral fiber. This material has been successfully combined with Portland cement paste to form a

widely used product called asbestos cement. Asbestos fibers are thermal mechanical and chemical resistant making them suitable for sheet product pipes, tiles and corrugated roofing elements. Asbestos cement board is approximately two or four times that of unreinforced matrix. However, due to relatively short length (10mm) the fiber have low impact strength.

- Carbon Fibers: Carbon fiber is probably the most impressive addition to the range of fiber available for commercial use. Carbon fiber has very high modulus of elasticity and flexural strength. Even though it is expensive, the strength and stiffness characteristics have been found to be superior even to those of steel. Thus, they are more vulnerable to damage than even glass fiber, and hence are generally treated with resign coating.
- Organic Fibers (Natural Fibers): Organic fiber such as polypropylene or natural fiber may be chemically more inert than either steel or glass fibers. They are also cheaper, especially if naturally obtained. A large volume of vegetable fiber may be used to obtain a multiple cracking composite. The problem of mixing and uniform dispersion may be solved by adding a super plasticizer.

### 3.3 Steel Fiber Reinforce Concrete (SFRC)

During recent years, SFRC has gradually advanced and has now attained acknowledgment in numerous engineering applications. Lately, it has become a more frequent substitute to steel reinforcement.

Concrete is a brittle material with a low tensile strength. Steel Fiber is added in concrete for increasing the tensile strength and its ductility. In addition, it reduces the intensity of the cracks. It provides the large contraction area between concrete and steel compared with the reinforced bar and it also increases shear resistance. Moreover, it helps to minimize the thickness of concrete segment as well as reduce the cost of construction.

The steel fiber has a high elasticity modulus (210.000 MPa), providing a very high tensile strength with a minimum deformation. A very high tensile strength helps the fiber to creep within the concrete without breaking and increasing the capacity of energy absorption. The steel fiber also has a hook which improves the bond between concrete and steel fiber. During construction, it can save time and money on placing the reinforcing fibers.

There are various researches about SFRC which proves that it’s better than reinforced concrete such as the research of Yining Ding et al (2000). The researchers did the laboratory test to find the characteristic of SFRC in the early age. In their article, they studied about the effect of steel fibers in influencing the compressive strength, the duration for the peak load and the energy absorption under uniaxial compressive loading at the early age. The result of their research is at the early age, SFRC can increase the duration of the peak load compared to the plain concrete.

The uses of SFRC over the past thirty years have been so varied and so widespread, that it is difficult to categorize them. The most common applications are pavements, tunnel linings, pavements and slabs, shotcrete (now shotcrete also containing silica fume), airport pavements, bridge deck slab repairs, and so on. There also has been some recent experimental work on roller-compacted concrete (RCC) reinforced with steel fibers.

Table 2.1 Types of Steel Fiber. (Maccaferri, 2008)

| | Flooring and precast fibers | | | Shotcrete fibers | | | |
|---|---|---|---|---|---|---|---|
| Wirand Steel Fiber | FF1 | FF2HS | FF3 | FS9 | FS3N | FS4N | FS7 |
| Length (mm) | 50 | 50 | 50 | 37 | 33 | 33 | 33 |
| Diameter (mm) | 1.00 | 0.90 | 0.75 | 0.75 | 0.75 | 0.60 | 0.55 |
| Min. tensile strength (MPa) | 1100 | 1450 | 1100 | 1100 | 1100 | 1200 | 1200 |
| Aspect ratio L/D | 50 | 56 | 67 | 49 | 44 | 55 | 60 |
| Units/kg (approx) | 3200 | 4000 | 5700 | 7700 | 8700 | 13600 | 16200 |

As shown in Table 2.1, Maccaferri has 3 types of steel fiber for flooring and precast structure, and 4 types for shotcrete structure. Among these types, the main difference is the length and diameter of steel fiber.

**4. How Steel Fiber Reinforced Concrete is applied to the tunnel.**

SFRC is known to be highly resistant to tensile, shear and toughness strength. As well as the decreasing of labor and construction cost. SFRC was incorporated in the tunneling structures around the world such as district heating tunnel in Copenhagen (Thomas Kasper, 2007) and Gold Coast Desalination Tunnels (W Angerer, 2008). Moreover, there were several experiments conducted on using SFRC as a material for tunnel segment lining. For example, the experiments on ductile behavior, the wide cracks, the bridging effect of fiber and so on (see in Table 2.2). Some tunnel projects used SFRC with reinforced bars in order to increase deformation after cracking and the resistance of fire. Moreover, SFRC is used in shotcrete technology to stabilize the resistance of tunnel face and lining.

Table 2.2 The summary of previous papers about SFRC.

| Thesis topic | Authors | Detail | Conclusion | Remarks |
|---|---|---|---|---|
| On the design of steel fiber reinforced concrete tunnel lining segments | L.Sorelli, F. Toutlemon de France, 2005 | Focus on application of SFRC in tunnel lining segment, full scale specimen comparing to RC, tensile test on cylinder drilled out from the specimen. Using numerical method comparing to experiment | Adapting 'strut and tie' analysis to SFRC tunnel design by properly considering the tensile resistance. SFRC can resist the peak load better than RC, as well as fracture energy | SFRC + plain<br>Numerical strut-tie<br>Compression<br>Tension<br>Experiment+ numerical |
| Designing case-in-situ FRC tunnel linings | B. Chiaia, A.P. Fantilli, P. Vallini, Italy, 2008 | Finding suitable steel fiber and steel bar for ductile behavior.<br>Use Euro code,<br>Soil properties by FEM<br>Define ULS & SLS | Fiber reduces the maximum crack width and crack distance, increasing the resistance on corrosion of steel rebar | SFRC + reinforced bar VS plain RC<br>Check: Euro code, ACI |

| Thesis topic | Authors | Detail | Conclusion | Remarks |
|---|---|---|---|---|
| Lining design for the district heating tunnel in Copenhagen with steel fiber reinforced concrete segments | Thimas Kasper, Carola Edvardson, Gerd Wittneben, Dieter Neumann, Germany, 2007 | 3.9m long, inner diameter 4.2 m, 2 steam pipe, 30 cm thick, lining ring 1.5 m wide<br>Use EPB<br>SFRC only<br>100 years service life<br>50°c temperature during operation of pipeline<br>Point bending test for tensile strength.<br>Loading with and without heating of tunnel | Combination between steel fiber and polypropylene fiber can provide fire resistance without any extra method and save cost. | SFRC cannot compete with conventional RC in terms of bending and tensile capacity, bursting capacity under concentrated large load full experiment |
| Design of steel fiber reinforced segmental lining for the Gold Coast Desalination Tunnel | W Angerer, M Chappell, Australia, 2008 | SFRC for intake and discharge tunnel<br>2 km long, 2.8 inner diameter,<br>Trail testing of the segment<br>Brief introduction of SFRC<br>Support rock load and hydrostatic pressure | SFRC have more capacity of tensile than plain reinforced concrete in the first peak crack. | |
| A fracture mechanic-based design method for SFRC tunnel linings | Pruettha Nanakorn, Hideyuki Horii, Shigeru Matsuoka, Japan, 1996 | Estimated load carrying capacity of tunnel lining with various thickness and different kind and volume fraction of fiber<br>Using FEM and experiment | The critical crack length depend on amount of steel fiber | |
| Effect of fiber content on mechanical properties of steel fiber reinforced concrete | Pornpen Limpaninlachat, Pitichoke Thongtrakarn, Withit Pansuk, Thailand, 2553 | JSCE-SF4 standard<br>Effective of SRFC<br>Effect of the arrangement of steel fiber | More steel fiber, more energy absorption, reduce crack, more resistance of bending moment, reduce thickness | No optimum amount of steel fiber |

According to the previous research, most of them research on the peak strength, crack opening and so on. They were figured out that no one study on the flow of SFRC, even the strength of SFRC with special plasticizer (SP). Thus, this research will do the laboratory test on SFRC and SFRC with SP compare with conventional concrete. Moreover, it will be provided to find the behavior of tunnel lining segments especially when it is under large deformation.

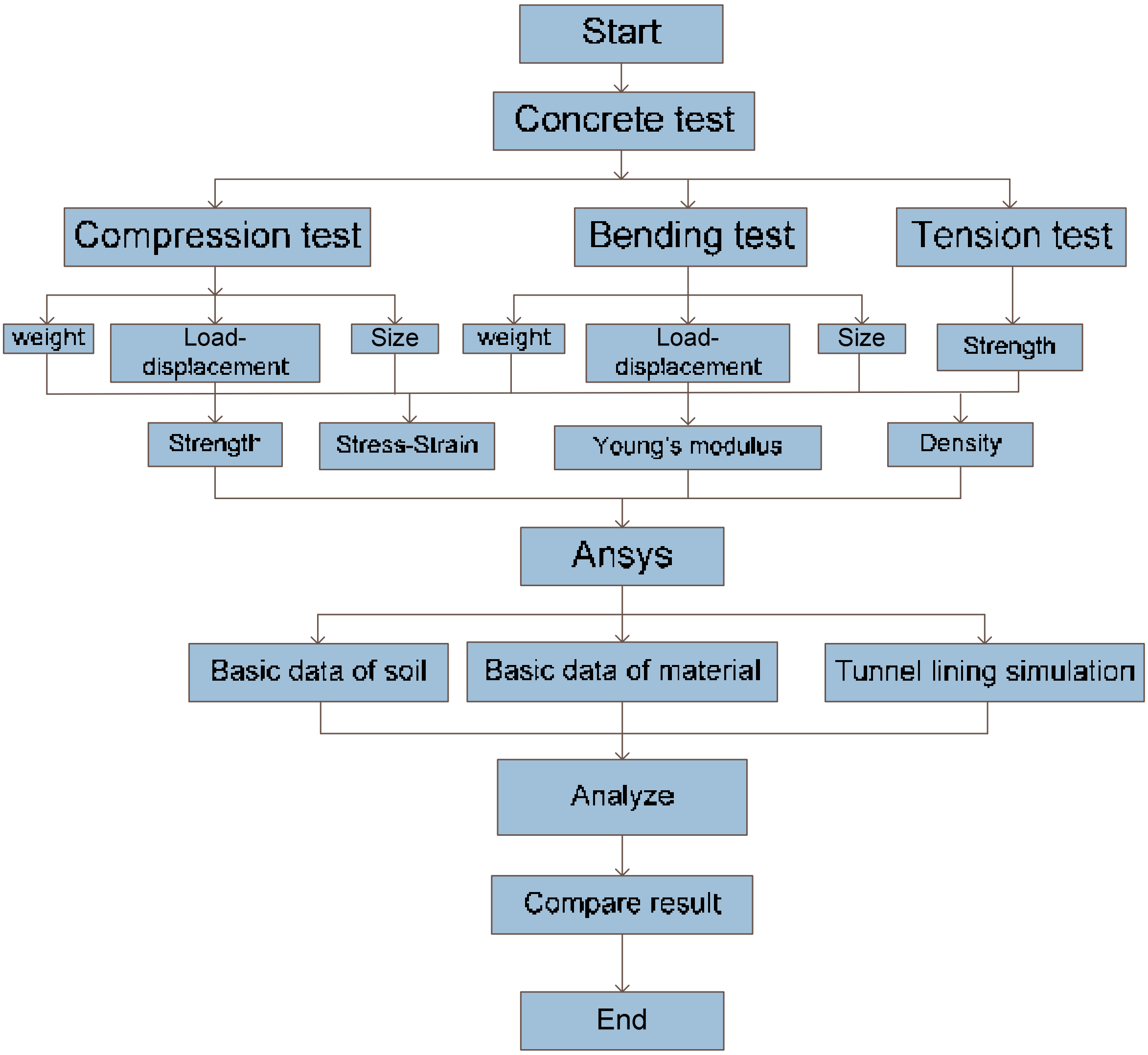


Figure 2.11 Methodology of the research

## Chapter III

## Laboratory test

### 1. Preparing material

In the design of concrete, the main materials are cement, sand and gravel (Figure 3.1). Type I cement was used for the main structure while sand and gravel are local materials. The sand is course sand and the size of gravel is not more than 1 inch (25mm). All of the sand and gravel have been washed for 2 times before mixing. Moreover, they have to be dried up in the oven under a temperature of 100 degree Celsius. In addition, steel fiber and plasticizer were also used in this test.

Steel fiber is under type FF3 which are of 50 cm. diameter, 0.75 cm. long and 5700 pieces per kilogram. The plasticizer (Figure 3.3), whose purpose was to reduce water in concrete to retain or increase the strength of concrete, was used with a proportion of 350 ml per 100 kg of cement. A mixing machine (Figure 3.4) with a 100-liter volume capacity has been utilized.

Figure 3.1 Materials (sand, gravel and cement)


Figure 3.2 Steel fibers (Wirand)

Table 3.1  Types of steel fiber

| Wirand steel fiber | FF1 | FF2HS | FF3 |
|---|---|---|---|
| Length (mm) | 50 | 50 | 50 |
| Diameter (mm) | 1.00 | 0.90 | 0.75 |
| Min. tensile strength (MPa) | 1100 | 1450 | 1100 |
| Aspect ratio L/D | 50 | 56 | 67 |
| Units/kg (approx.) | 3200 | 4000 | 5700 |

There are 2 types of steel fiber used; the first one is for flooring and precast, and the other one is for shotcrete concrete. In this research, the steel fiber for flooring and precast type (batch FF3) was mixed in the concrete whose size is given in Table 3.1

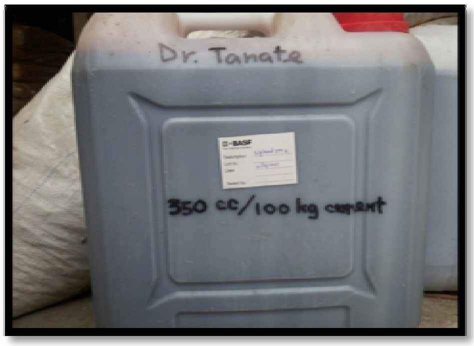


Figure 3.3 Super Plasticizer (Polyheed 779 R, BASFa)

Figure 3.4 Mixing machine

In this experiment, 6 cubes, 6 beams and 3 briquettes had been used for compressive and bending and tension test respectively. For the slump test, the falling depth of SFRC in slump test should not more than 15 cm and for plain concrete should not more than 10 cm.

Figure 3.5 Slump test device


Figure 3.6 RMU Compression Testing machine (serial 85, 3000 kN capacity)

For bending test, the main machine that was used is Instron (Figure 3.7). The ability of this machine is pulling or pushing the load according to the frequency that was set by the user. The initial frequency of this bending test is 0.12 mm/min and was later set to 0.24 mm/min after cracking (in accordance to ASTM C1609/1609M-06).

Due to the old and low version of computer that controls the Instron, the data cannot be transferred. In order to solve this problem, a load cell and LVDT was used to define the load-displacement while a data logger recorded all the data from the bending test.

The Kyowa Hollowed Load Cell (Figure 3.9) has the maximum capacity of 10 tons. Two Kyowa LVDTs (Figure 3.10) with a 2 centimeter maximum length was used to measure the displacement of bending test. In addition, the data recording machine is a data logger (Figure 3.8) that accounts and keeps the data from the load cell and LVDT with a frequency 10 Hz.

Figure 3.7 Instron (Model no. DYNS, Serial no. H 2029, 1000-kN capacity)

Figure 3.8 Data logger (Kyowa Electronic Instruments)

Figure 3.9 Kyowa Hollowed Load Cell (Model BL-10TB, Serial no. AU1170, 10-ton capacity)


Figure 3.10 Kyowa LVDTs (Model DTH-A-20, Serial no. 1930002 and 1930003, 20-mm rated capacity)

2. **Design criteria**

The ASTM C31/C31M was used in mixing and curing the concrete. 320 ksc and 240 ksc strengths of concrete have been designed for this research. A summary of cube and beam specimens is shown in Table 3.2.

Table 3.2 Total amount of specimen

| Strength ksc | Type of specimen | Plain | Steel fiber dosage, FF3 (kg/m$^3$concrete) | | | | | |
|---|---|---|---|---|---|---|---|---|
| | | | 15 | 20 | 25 | 30 | 35 | 40 |
| 240 | Batch No. | 240-0-NSP | 240-15-NSP | 240-20-NSP | 240-25-NSP | 240-30-NSP | 240-35-NSP | 240-40-NSP |
| | Cube | 8 | 8 | 8 | 8 | 8 | 8 | 8 |
| | Beam | 6 | 6 | 6 | 6 | 6 | 6 | 6 |
| | Briquette | 3 | 3 | 3 | 3 | 3 | 3 | 3 |
| 240+SP | Batch No. | 240-0-SP | 240-15-SP | 240-20-SP | 240-25-SP | 240-30-SP | 240-35-SP | 240-40-SP |
| | Cube | 8 | 8 | 8 | 8 | 8 | 8 | 8 |
| | Beam | 6 | 6 | 6 | 6 | 6 | 6 | 6 |
| | Briquette | 3 | 3 | 3 | 3 | 3 | 3 | 3 |
| 320 | Batch No. | 320-0-NSP | 320-15-NSP | 320-20-NSP | 320-25-NSP | 320-30-NSP | 320-35-NSP | 320-40-NSP |
| | Cube | 8 | 8 | 8 | 8 | 8 | 8 | 8 |
| | Beam | 6 | 6 | 6 | 6 | 6 | 6 | 6 |
| | Briquette | 3 | 3 | 3 | 3 | 3 | 3 | 3 |
| 320+SP | Batch No. | 320-0-SP | 320-15-SP | 320-20-SP | 320-25-SP | 320-30-SP | 320-35-SP | 320-40-SP |
| | Cube | 8 | 8 | 8 | 8 | 8 | 8 | 8 |
| | Beam | 6 | 6 | 6 | 6 | 6 | 6 | 6 |
| | Briquette | 3 | 3 | 3 | 3 | 3 | 3 | 3 |

*Remark: Batch No. explanation:

For XXX-YY-ZZZ:

- XXX : target strength, 240 and 320 ksc.

- YY : amount of steel fiber, eg: 0 is no steel fiber.
- ZZZ : with or without super plasticizer , eg: NSP: no super plasticizer.

Table 3.3 Volume fraction of steel fiber

| Steel fiber dosage, FF3(kg/$m^3$concrete) | 0 | 15 | 20 | 25 | 30 | 35 | 40 |
|---|---|---|---|---|---|---|---|
| Volume fraction (%) | 0 | 0.188 | 0.253 | 0.316 | 0.380 | 0.437 | 0.507 |

In 1 $m^3$ of concrete, there is 401.96 kg. cement, 663.92 kg. sand, 1072 kg. gravel, 205 liters water and 1.403 liters of plasticizer. For SFRC, the weight of steel fiber had used to replace the weight of grain materials (sand and gravel) in a haft-haft (table 3.4).

This research contains three types of specimen, cube, beam and briquette. The sizes of all specimens are as figure 3.11, 3.12, and 3.13 respectively.

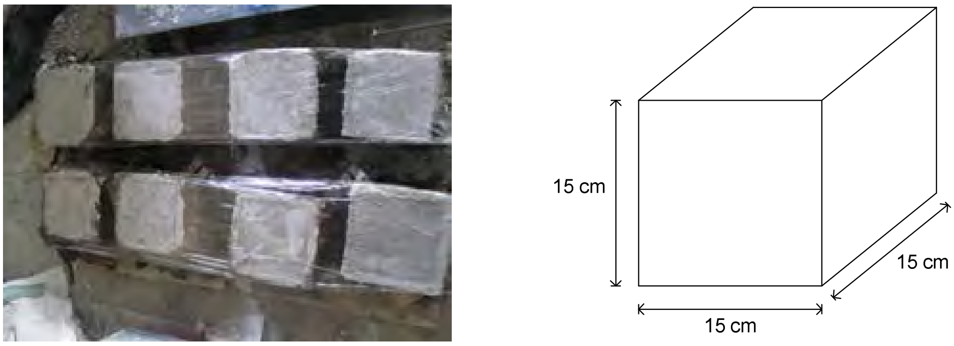


Figure 3.11 Cube specimens

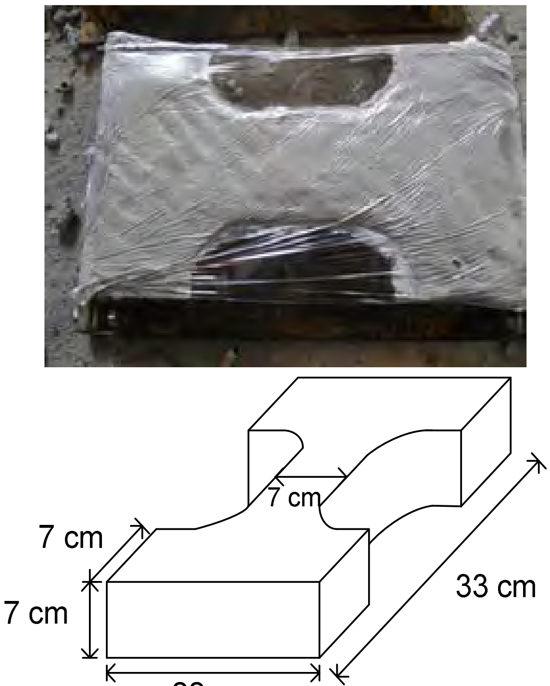


Figure 3.12 Briquette specimen

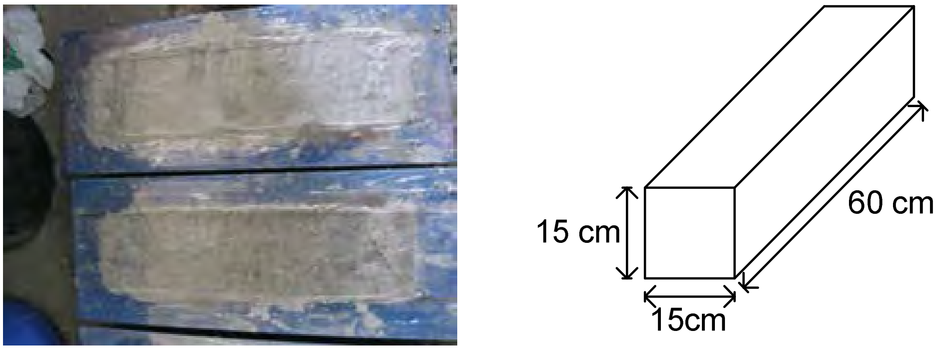


Figure 3.13 Beam specimen

Table 3.4 Concrete mix design

| | | Plant |
|---|---|---|
| Type of cement: | Type 1 | TPI |
| Quantity of cement: | 402 kg/m$^3$ | |
| Water/cement ratio: | 0.509 | |
| Aggregates | | Local meterial |
| Gravel: | 1072 kg/m3 | |
| Sand: | 664 kg/m3 | |
| Admixture | | |
| Super plasticizer: | 1.407 litres/m$^3$ | BASF |
| Steel fiber: | Dosages as listed in table 1 | Maccaferri |

a. Curing method

According to ASTM C192/C 192M-07, all specimens were cured in the tank filled with water.

Figure 3.14 Curing room

## 3. Testing process

a. Slump test

According to ASTM C143/C 143M-08, the slump depth should not be more than 15 cm for the concrete that contains steel fiber, while the slump depth for plain concrete should not be more than 10 cm.

Figure 3.15 Slump test procedure

b. Sieve analysis

Figure 3.16 Sieve devices

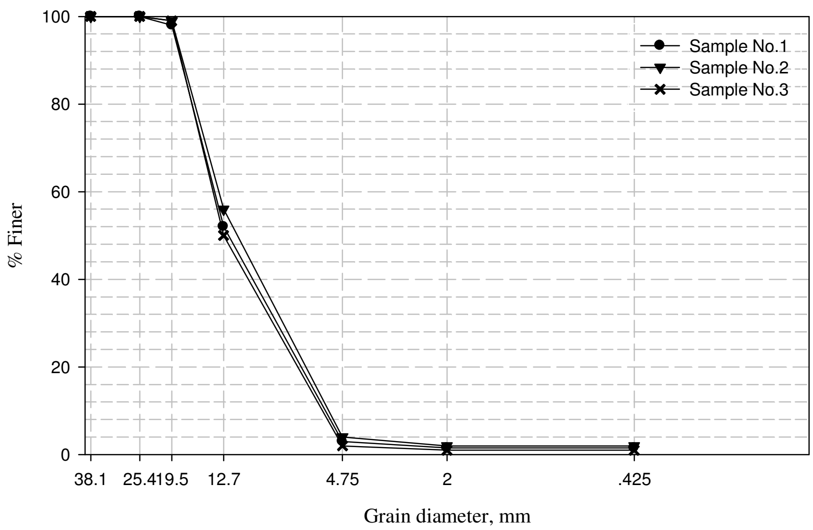


Figure 3.17 Sieve analysis for gravel

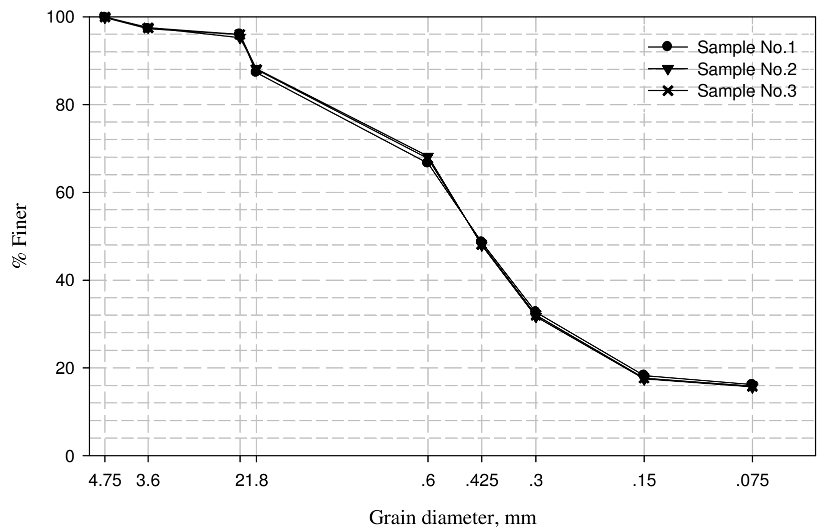


Figure 3.18 Sieve analyses for sand

In conclusion, the size of gravel and sand are 25.4 mm to 0.425 mm, and 4.75 mm to 0.75 mm respectively.

c. Compression test

The dimensions and weight of the concrete block was noted before the test. During the procedure, the load and displacement values were recorded. This was performed by reading the dial gauge, recording the data in the table and plotting the values in a graph.

d. Flexural test

The standard ASTM C 1690/C 1690M-06 is used for the "Flexural Performance of Fiber Reinforced Concrete". According to ASTM C 1690, the size and weight of specimen had to be recorded before and after the test. The beam specimen was installed into the Instron (Figure 3.18) where the LVDTs were installed on both sides of the specimen. The load cell was placed on the top of the specimen that measured the load from Instron. After testing, the sizes of the cracks and the length between the cracks and the supports in every side have to be recorded. Thus, photos in each side of the specimen: top, bottom, left, right, and cracking plan have to be taken (Figure 3.19 to 3.22). The specimens that contain voids and cracks outside L/3 were discarded. The documentation of this test is shown in Figure 3.28-3.31.

Testing procedure:

- Measure size and weight of beam specimen before testing.
- Measure the point of load, support, and LVDT.
- Set the glue (epoxy) to install the LVDT.

Figure 3.19 Beam specimens before testing

- Install the specimen into machine


Figure 3.20 Installing the LVDT and load cell

- Measure size and length of crack, and take photos all side after testing.

Figure 3.21 Right side of the specimen

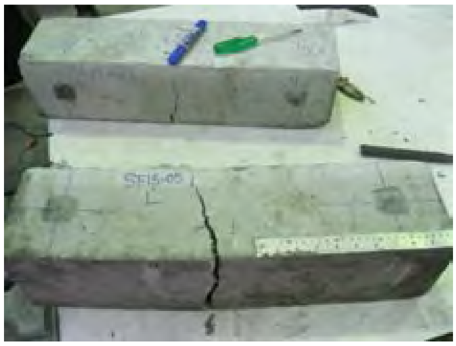

Figure 3.22 Left side of the specimen

Figure 3.23 Bottom side of specimen

Figure 3.24 Fracture plan of specimen

e. Tension test

For tensile test, LVDTs had to be installed to measure the tensile deformation of briquette and the load was read from the machine until it cracks.

Figure 3.25 Installing briquettes and the briquette after tensile testing

## 4. Result

The test results are as the graphs below:

4.1 Fresh concrete

a. Slump test

Table 3.5 Slump test result of each batch

| 240-NSP | slump | 240-SP | slump | 320-NSP | slump | 320-SP | slump |
|---|---|---|---|---|---|---|---|
| 240-0-NSP | 13.0 | 240-0-SP | 13.0 | 320-0-NSP | 10.5 | 315-0-SP | 14.0 |
| 240-15-NSP | 13.5 | 240-15-SP | 15.0 | 320-15-NSP | 10.5 | 320-15-SP | 16.0 |
| 240-20-NSP | 11.5 | 240-20-SP | 15.5 | 320-20-NSP | 10.5 | 320-20-SP | 15.0 |
| 240-25-NSP | 11.0 | 240-25-SP | 15.0 | 320-25-NSP | 11.0 | 320-25-SP | 14.2 |
| 240-30-NSP | 13.0 | 240-30-SP | 14.5 | 320-30-NSP | 11.0 | 320-30-SP | 13.9 |
| 240-35-NSP | 11.7 | 240-35-SP | 16.5 | 320-35-NSP | 12.0 | 320-35-SP | 14.0 |
| 240-40-NSP | 11.0 | 240-40-SP | 15.0 | 320-40-NSP | 10.5 | 320-40-SP | 13.4 |

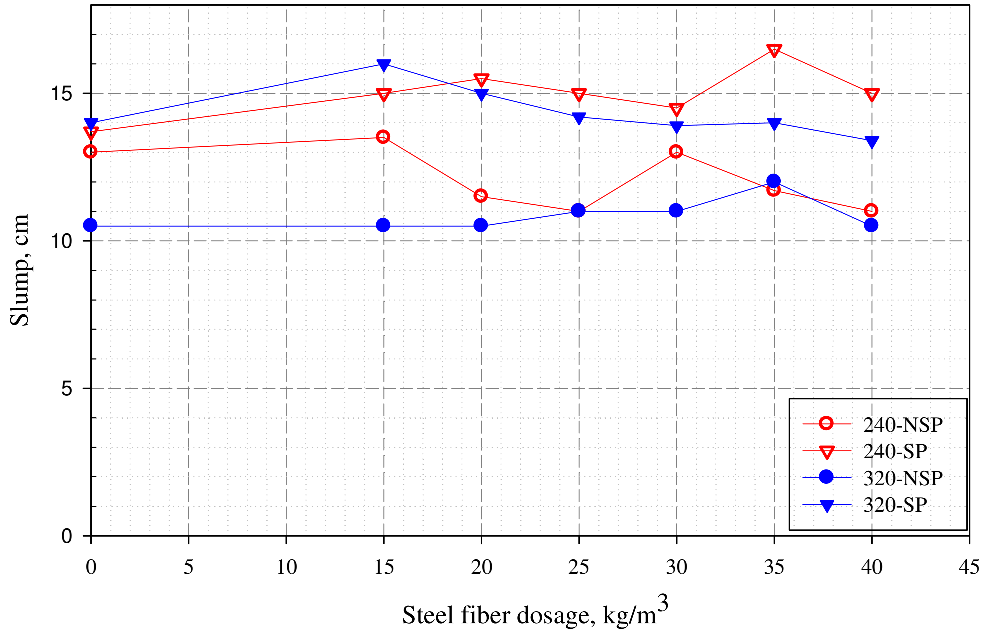


Figure 3.26 Comparison between slumps of each batch

In Figure 3.26, it can be seen that the slump varied from 10 to 17 cm, where the maximum slump is the batch 240-35-SP. It can be deduced that the batches that contains SP have higher slump values than the batches without SP. In other words, the presence of SP makes the concrete flow more easily than the ones without SP.

## 4.2 Hardening of concrete

Table 3.6 Bulk density of cube and beam

| Batch No. | Bulk density ($kg/m^3$) | | Batch No. | Bulk density ($kg/m^3$) | |
|---|---|---|---|---|---|
| | Cube | Beam | | Cube | Beam |
| 240-0-NSP | 2489 | 2432 | 320-0-NSP | 2534 | 2451 |
| 240-15-NSP | 2442 | 2473 | 320-15-NSP | 2499 | 2447 |
| 240-20-NSP | 2404 | 2437 | 320-20-NSP | 2498 | 2454 |
| 240-25-NSP | 2463 | 2437 | 320-25-NSP | 2522 | 2431 |
| 240-30-NSP | 2443 | 2497 | 320-30-NSP | 2487 | 2453 |
| 240-35-NSP | 2475 | 2410 | 320-35-NSP | 2494 | 2410 |
| 240-40-NSP | 2479 | 2470 | 320-40-NSP | 2485 | 2417 |
| 240-0-SP | 2468 | 2457 | 320-0-SP | 2436 | 2384 |
| 240-15-SP | 2489 | 2418 | 320-15-SP | 2534 | 2463 |
| 240-20-SP | 2478 | 2425 | 320-20-SP | 2502 | 2491 |
| 240-25-SP | 2499 | 2452 | 320-25-SP | 2461 | 2460 |
| 240-30-SP | 2508 | 2431 | 320-30-SP | 2497 | 2422 |
| 240-35-SP | 2519 | 2448 | 320-35-SP | 2526 | 2423 |
| 240-40-SP | 2446 | 2436 | 320-40-SP | 2494 | 2435 |

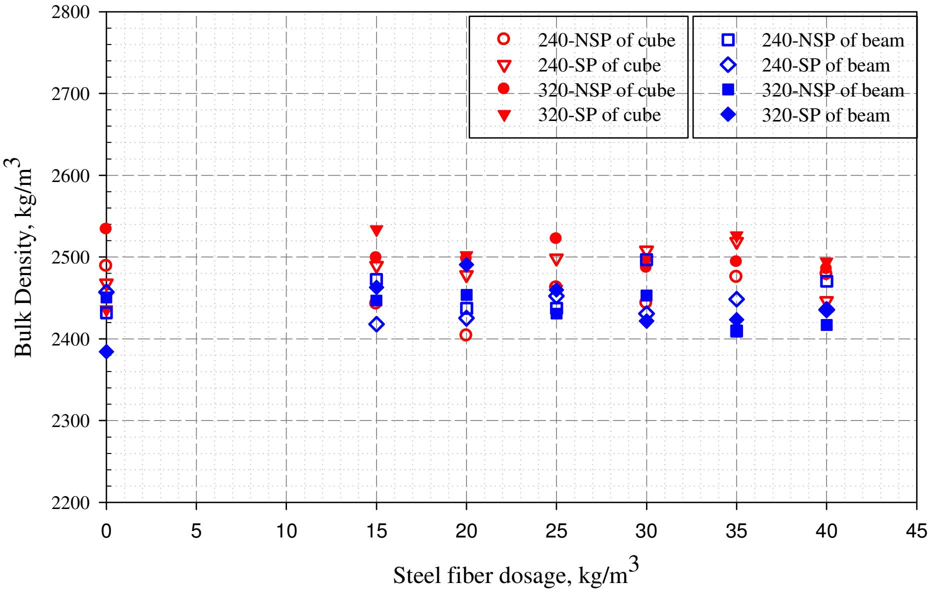


Figure 3.27 Comparison between bulk densities of each batch

According to Figure 3.27, the density of the cube and beam concrete varies from 2400 to 2500 kg/m$^3$.

## 4.3 Compression test

Table 3.7 Compressive strength of each batch

| Batch No. | compressive strength, fc' ksc | Batch No. | compressive strength, fc' ksc |
|---|---|---|---|
| 240-0-NSP | 213 | 320-0-NSP | 306 |
| 240-15-NSP | 254 | 320-15-NSP | 319 |
| 240-20-NSP | 224 | 320-20-NSP | 322 |
| 240-25-NSP | 246 | 320-25-NSP | 319 |
| 240-30-NSP | 232 | 320-30-NSP | 317 |
| 240-35-NSP | 237 | 320-35-NSP | 310 |
| 240-40-NSP | 248 | 320-40-NSP | 315 |
| 240-0-SP | 240 | 320-0-SP | 315 |
| 240-15-SP | 241 | 320-15-SP | 306 |
| 240-20-SP | 235 | 320-20-SP | 323 |
| 240-25-SP | 240 | 320-25-SP | 307 |
| 240-30-SP | 241 | 320-30-SP | 319 |
| 240-35-SP | 251 | 320-35-SP | 312 |
| 240-40-SP | 223 | 320-40-SP | 318 |

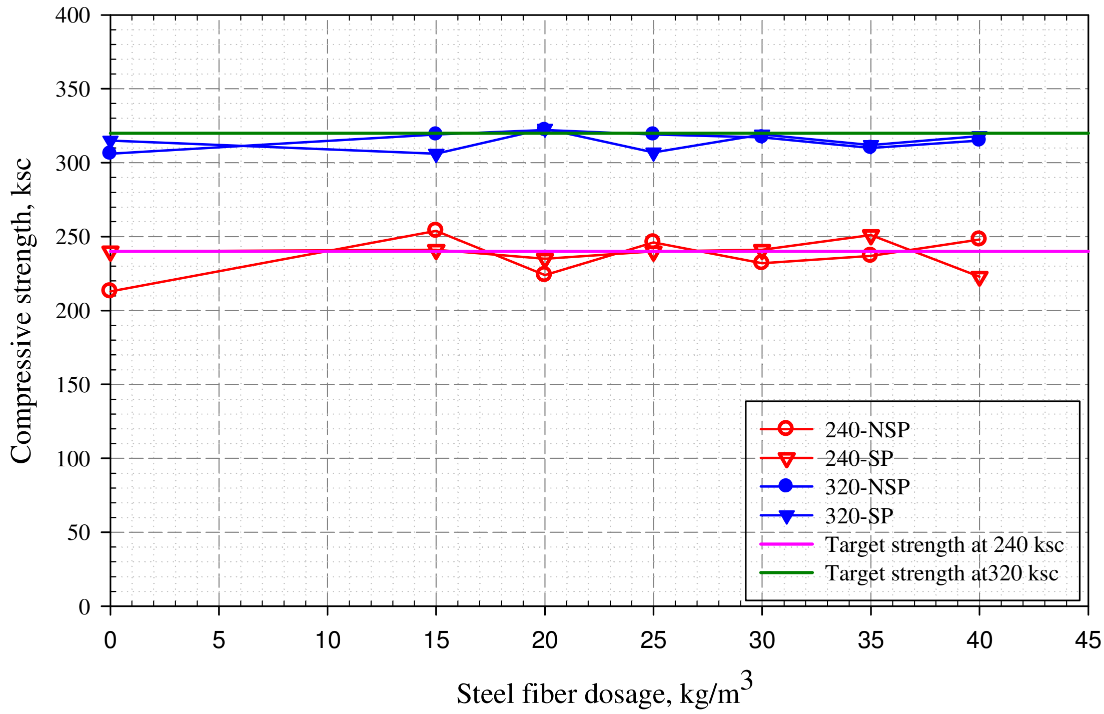


Figure 3.28 Comparison between compressive strength of each batch

In this research, there are two types of concrete design strength, 240 ksc and 320 ksc. Figure 3.28 shows that the concrete compressive strength of each quantity is not far from their design strength.

4.4 Tensile test

Table 3.8 Average tensile strength of each batch

| Batch No. | Strength (ksc) | ft/ fc' | Batch No. | Strength (ksc) | ft/ fc' |
|---|---|---|---|---|---|
| | ft | | | ft | |
| 240-0-NSP | N/A | N/A | 320-0-NSP | 31.02 | 0.10 |
| 240-15-NSP | N/A | N/A | 320-15-NSP | 31.51 | 0.10 |
| 240-20-NSP | N/A | N/A | 320-20-NSP | 36.22 | 0.11 |
| 240-25-NSP | N/A | N/A | 320-25-NSP | 32.35 | 0.10 |
| 240-30-NSP | N/A | N/A | 320-30-NSP | 37.41 | 0.12 |
| 240-35-NSP | N/A | N/A | 320-35-NSP | 31.89 | 0.10 |
| 240-40-NSP | 34.15 | 0.14 | 320-40-NSP | 28.57 | 0.09 |
| 240-0-SP | 25.15 | 0.10 | 320-0-SP | N/A | N/A |
| 240-15-SP | 22.57 | 0.09 | 320-15-SP | 34.80 | 0.11 |
| 240-20-SP | 26.38 | 0.11 | 320-20-SP | 39.65 | 0.12 |
| 240-25-SP | 20.18 | 0.08 | 320-25-SP | 32.74 | 0.11 |
| 240-30-SP | 25.95 | 0.11 | 320-30-SP | 33.17 | 0.10 |
| 240-35-SP | 22.78 | 0.09 | 320-35-SP | 32.15 | 0.10 |
| 240-40-SP | 25.41 | 0.11 | 320-40-SP | 23.26 | 0.07 |

In Table 3.8, N/A is the batch where the specimen dimension does not match with the briquette catcher, making the values unreadable.

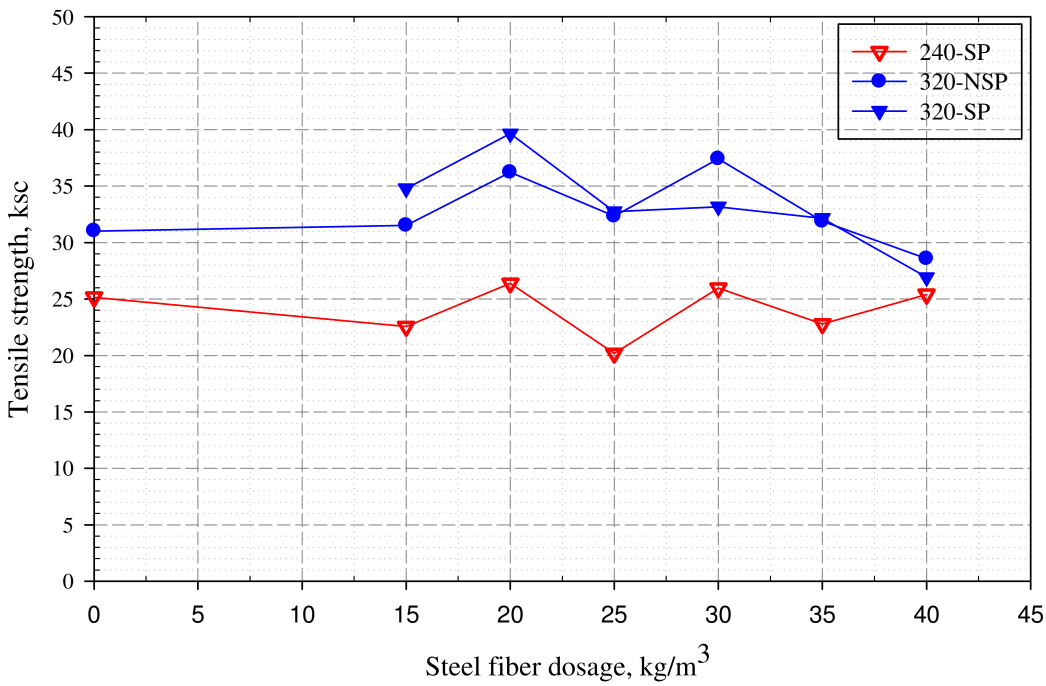


Figure 3.29 Comparison between average tensile strength of each batch

During the tensile strength test, the strengths of certain dosages were not obtained due to difference in dimension of the specimen and the catcher, making the value impossible to acquire. In Figure 3.29, the average tensile strength of the remaining dosages is plotted. It is apparent that the tensile strength is about 8% to 10% of the compressive strength of each batch (Please refer to Table 3.8).

4.5 Flexural test

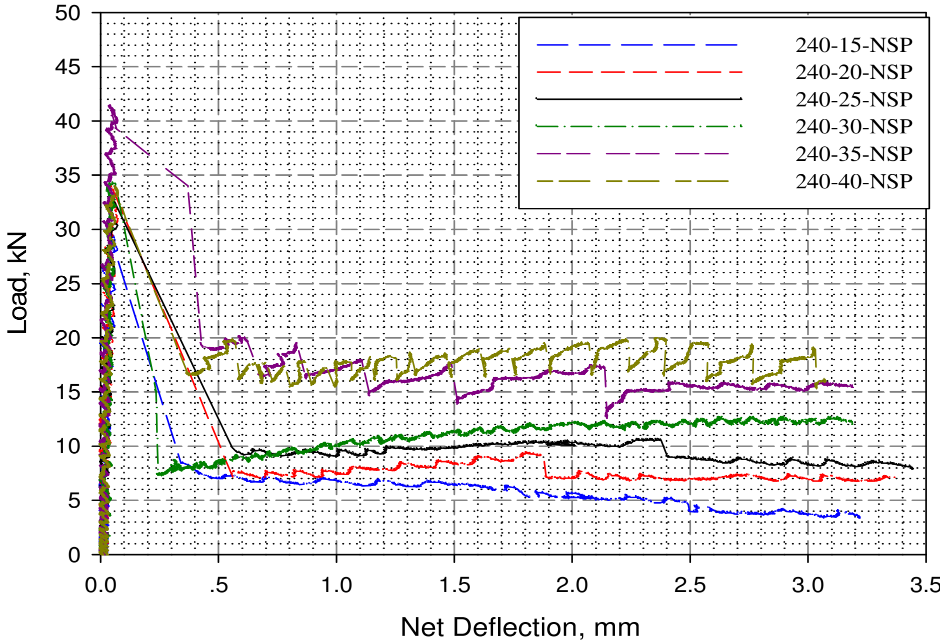


Figure 3.30 Comparison of flexural test between each dosage of batch 240-NSP

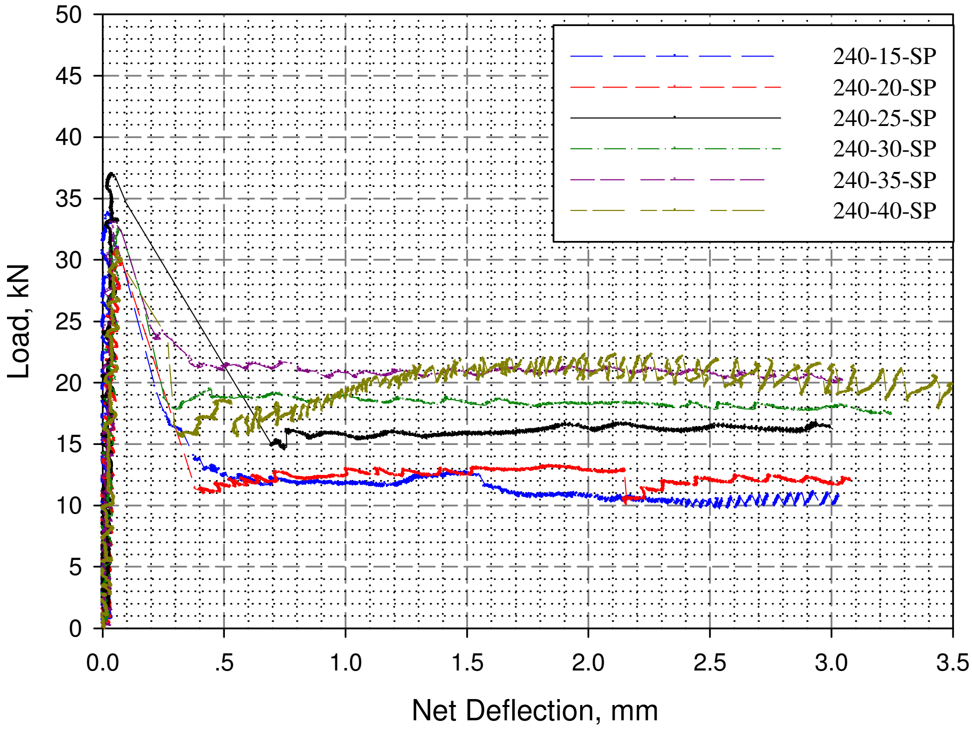


Figure 3.31 Comparison of flexural test between each dosage of batch 240-SP

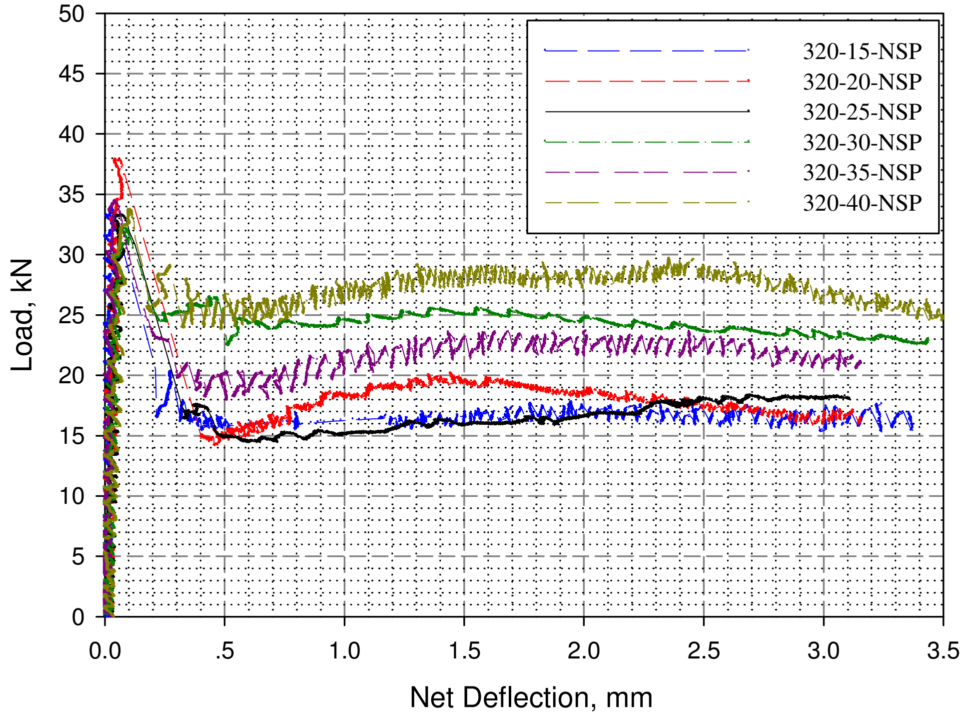


Figure 3.32 Comparison of flexural test between each dosage of batch 320-NSP

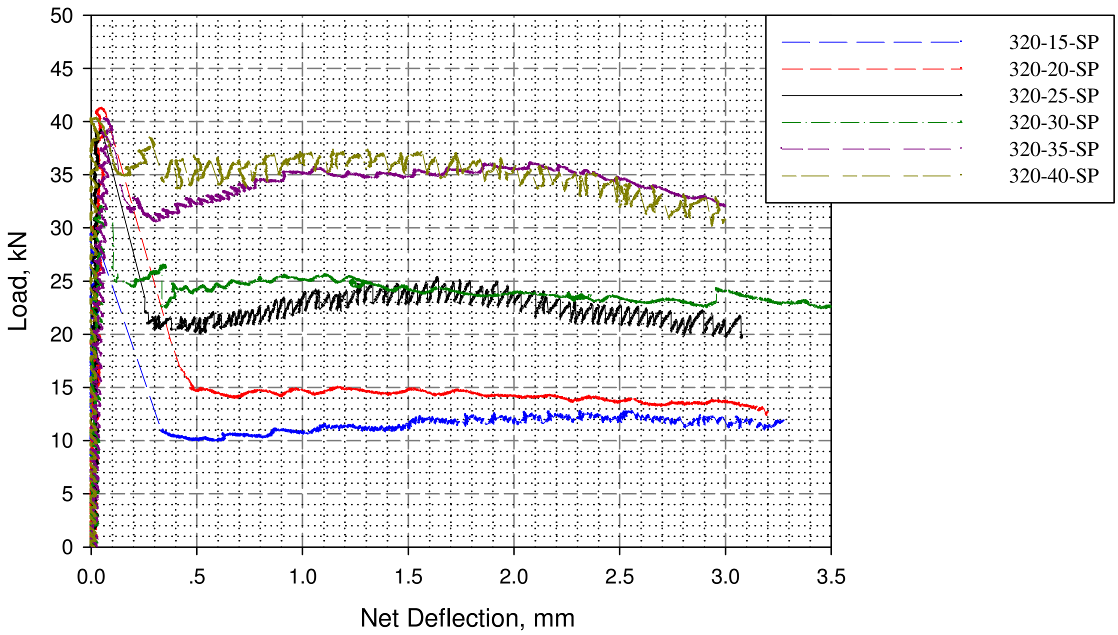


Figure 3.33 Comparison of flexural test between each dosage of batch320-SP

In each dosage, there are 6 specimens. Figures 3.28 to 3.32 show the representatives of each dosage of batch 240-NSP, 240-SP, 320-NSP and 320-SP respectively. From these figures considering the first peak load, it can be observed that the steel fiber has negligible effect. In contrast, it affects the residual load in flexure. When the amount of the steel fiber increased, the residual load increased in every batch. Moreover, comparing figures 3.28 and 3.29, 3.30 and 3.31, it can be seen that the batch that contained SP generated larger peak load and residual load. It can be concluded that SP does not only improve the ability of flow in concrete but also increased the strength of concrete.

In Figure 3.34, it can be observed that the toughness increases as the amount of steel fiber increases with SP.

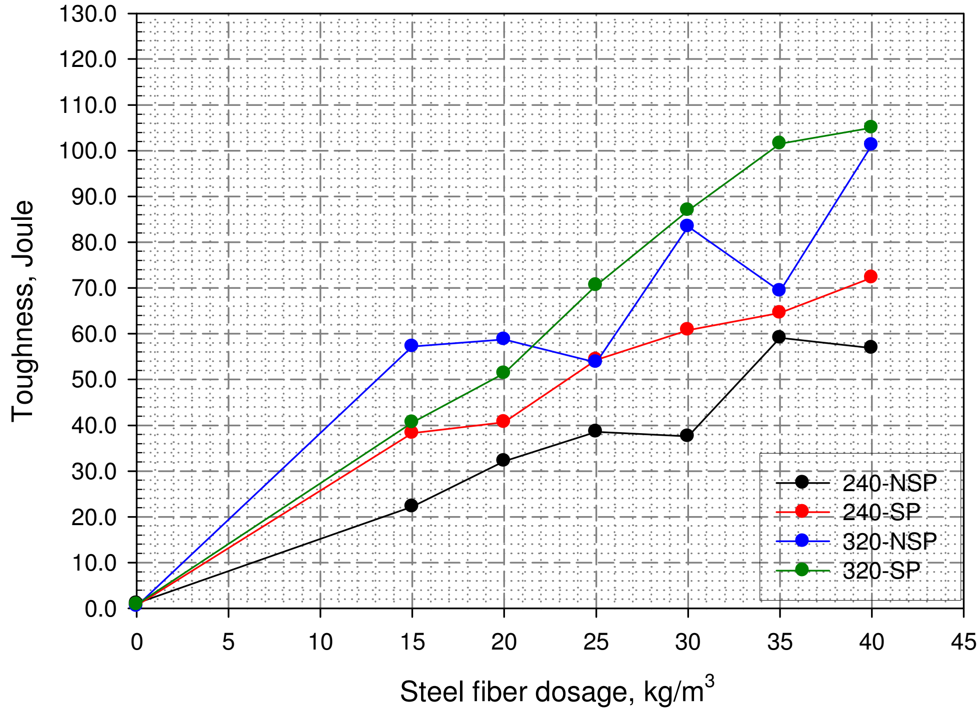


Figure 3.34 Comparison of toughness between each batch

4.6 Normalizing the strength

In this research, it is important to determine whether the design strength of concrete affects its residual strength in flexure. The load (P) at each displacement was divided by the peak load ($P_{peak}$) of each batch and plotted into the graph as shown in Figures 3.33 to 3.36 respectively. Among those graph, for batch without SP, it can be seen that the batch 320-SP has larger residual load than the batch, and the same with the batch with SP. This means that the strength of concrete also improves the resistance of concrete after cracking. For the batch 240-NSP, the range of residual $P/P_{peak}$ is between 20% - 50%, while the batch 320-SP, the range of residual $P/P_{peak}$ is between 50% - 80%. Similarly with the batches with SP, the results above show that the SP helps to increase the strength of concrete. Figures 3.34 and 3.36 also show that the design strength improve the batches with SP to increase the residual load of concrete: 40% - 70% residual strength was obtained for batch 240-SP and 40% - 90% for batch 320-SP.

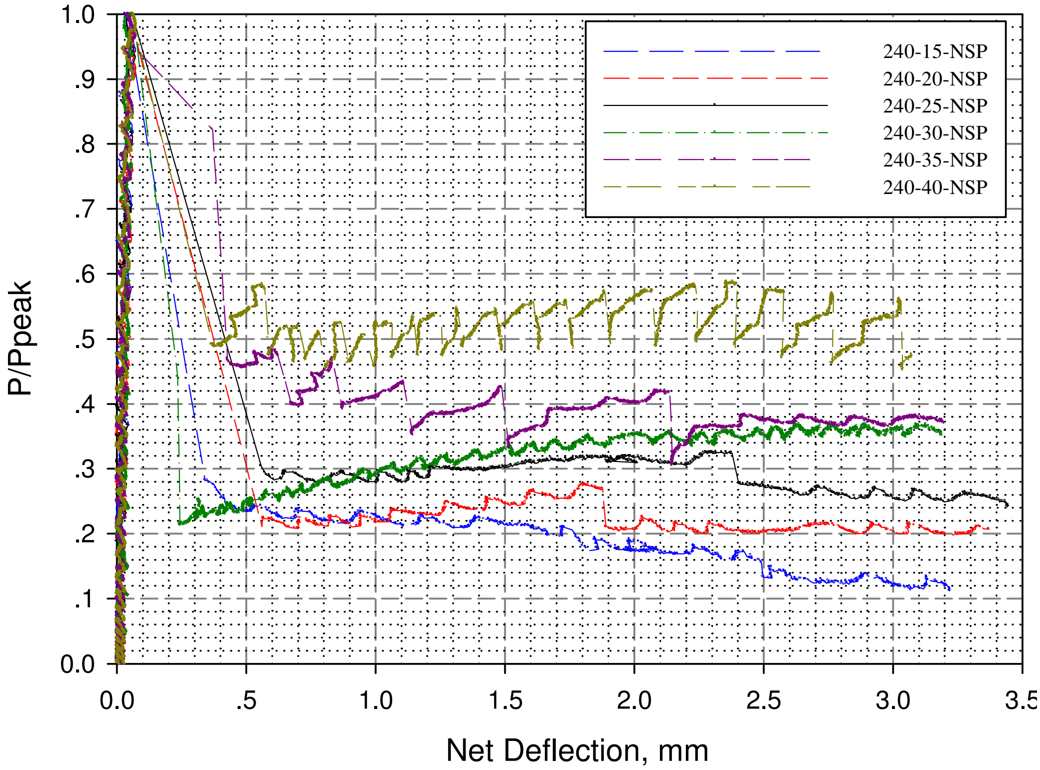


Figure 3.35 Comparison normalizing the load (P) by peak load (Ppeak) in flexural test between each dosage of batch 240-NSP

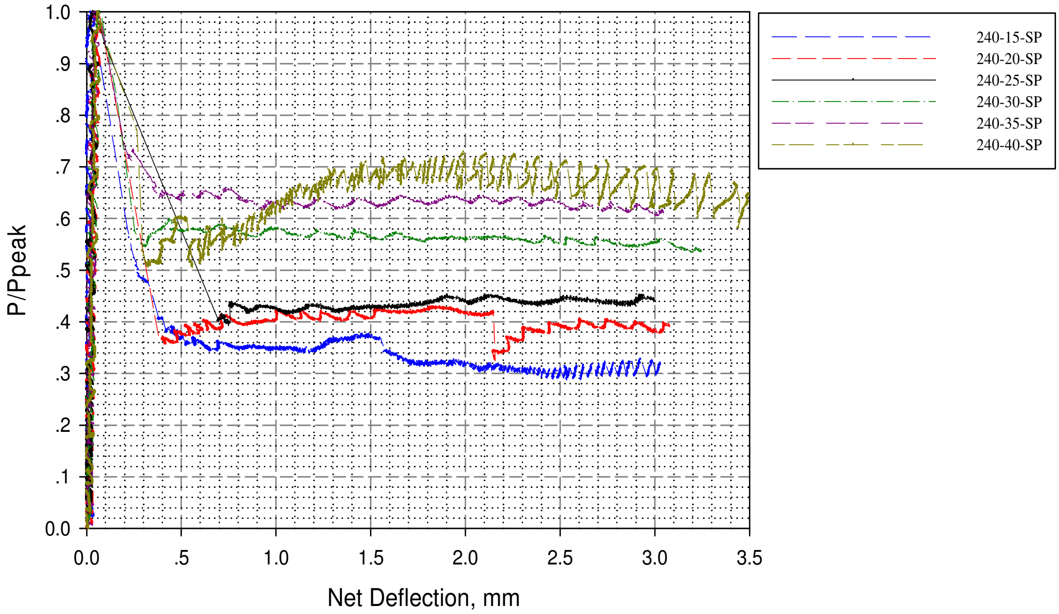


Figure 3.36 Comparison normalizing the load (P) by peak load (Ppeak) in flexural test between each dosage of batch 240-SP

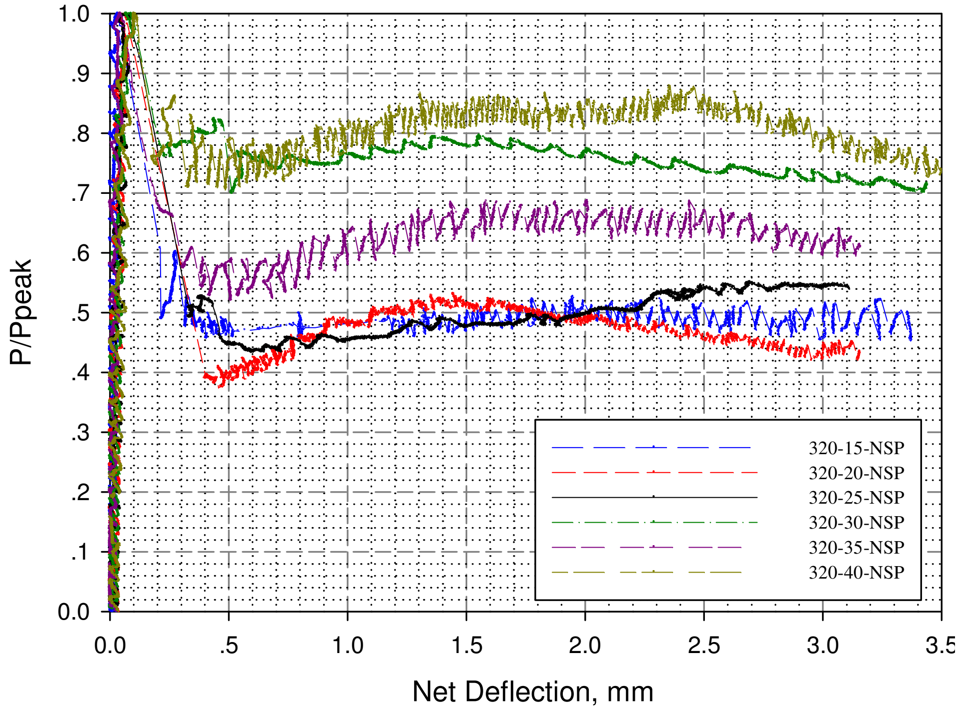


Figure 3.37 Comparison normalizing the load (P) by peak load (Ppeak) in flexural test between each dosage of batch 320-NSP

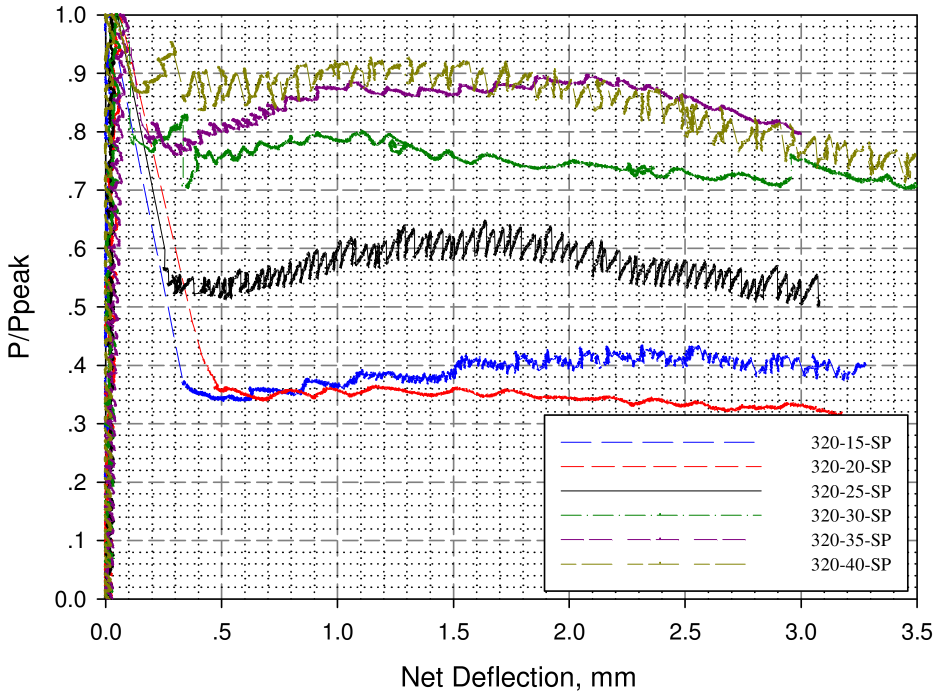


Figure 3.38 Comparison normalizing the load (P) by peak load (Ppeak) in flexural test between each dosage of batch 320-SP

4.7 Specify the dosage for analysis part.

Based on the aim of this research and the result of the toughness in figure 3.32, the batch 320-35-SP is similar to the batch 320-40-SP. Therefore, is has been decided to choose the batch 320-35-SP for the structural analysis in Chapter IV.

All specimens in this batch were divided into 2 groups, 7 days (depending on strength), and 28 days. Details of this batch are listed in Table 3.9.

Table 3.9 All specimen of batch 320-35-SP

| Specimen | All | For 7 days | For 28 days |
|---|---|---|---|
| Cube | 8 | 4 | 4 |
| Beam | 6 | 3 | 3 |
| Briquette | 3 | 3 | 0 |

a). Compression test

Table 3.10 Compression strength of batch 320-35-SP at 7 days and 28 days

| Specimen no. | Compressive strength (ksc) at 7 days | Specimen no. | Compressive strength (ksc) at 28 days |
|---|---|---|---|
| 1 | 262 | 5 | 433 |
| 2 | 335 | 6 | 425 |
| 3 | 291 | 7 | 337 |
| 4 | 320 | 8 | 378 |

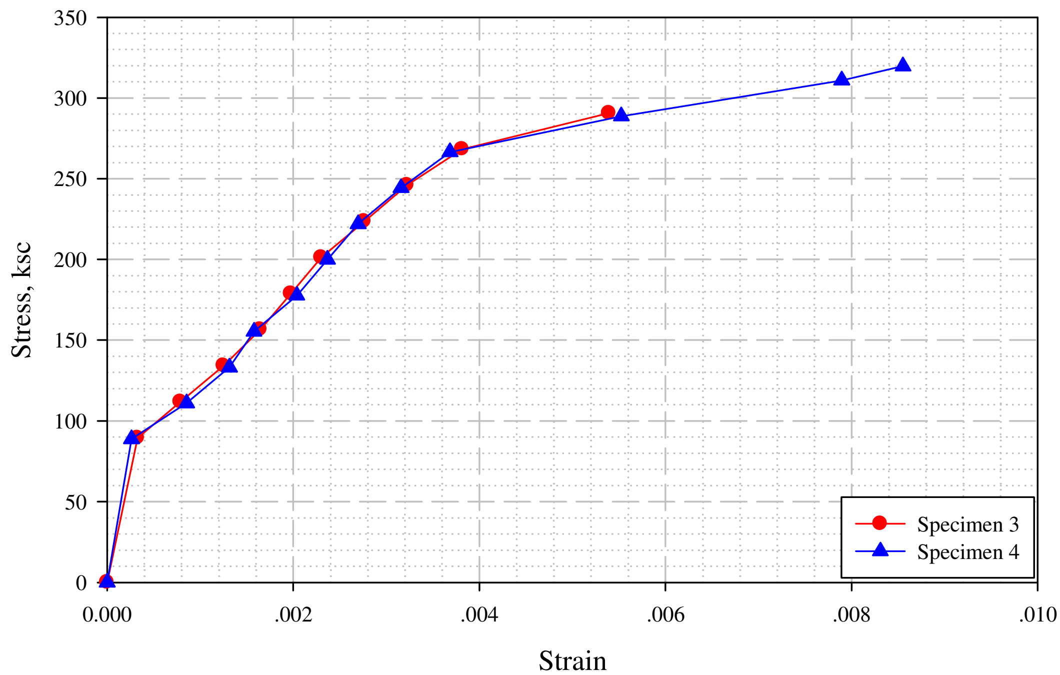


Figure 3.39 The relationship between stress and strain of cube at 7 days

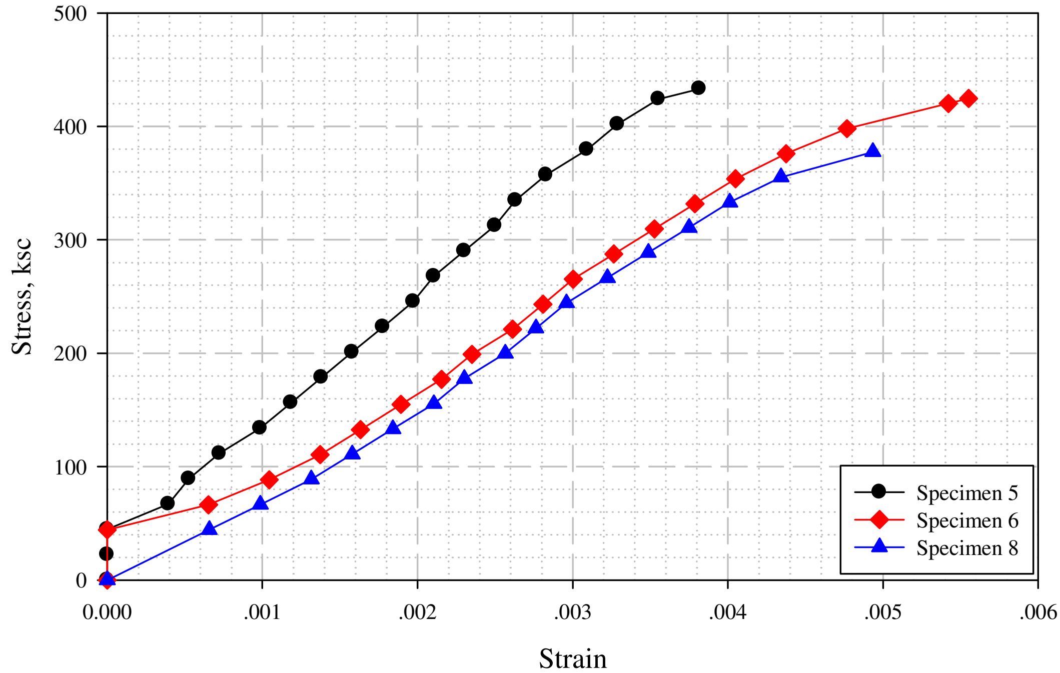


Figure 3.40 The relationship between stress and strain of cube at 28 days

Figure 3.37 and 3.38 show the evolution of the strength of concrete from 7 days to 28 days. Although the design strength is 320 ksc, it can be seen that the compressive of strength of concrete in 28 days is around 380 ksc to 400 ksc with the strain 0.0035 to 0.005.

b). Flexural test

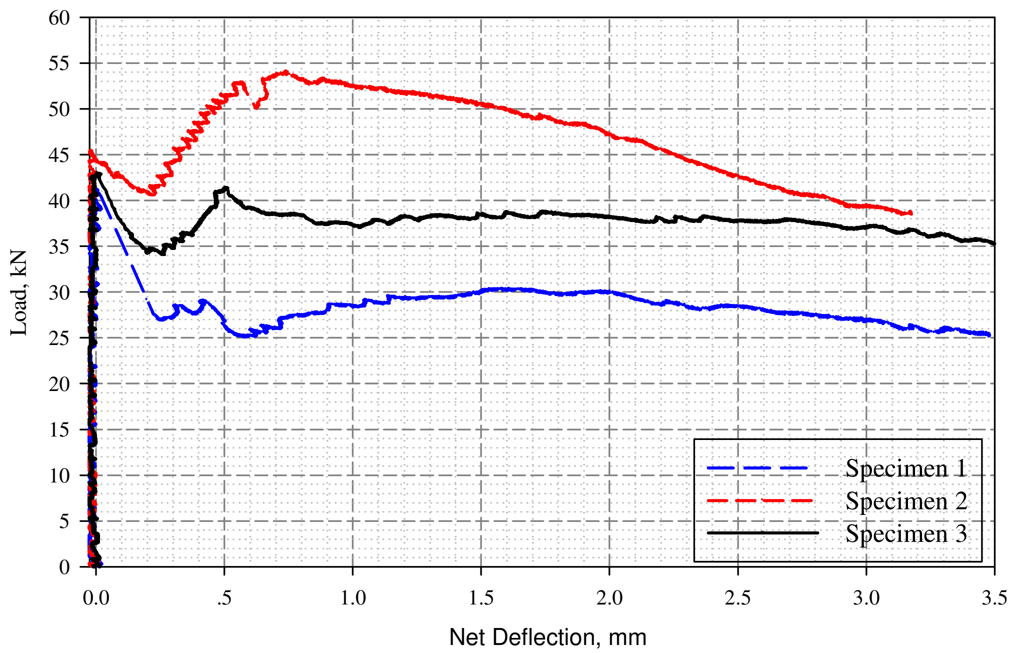


Figure 3.41 Comparing the flexural performance test results of fiber reinforced concrete of batch 320-35-SP at 7 days

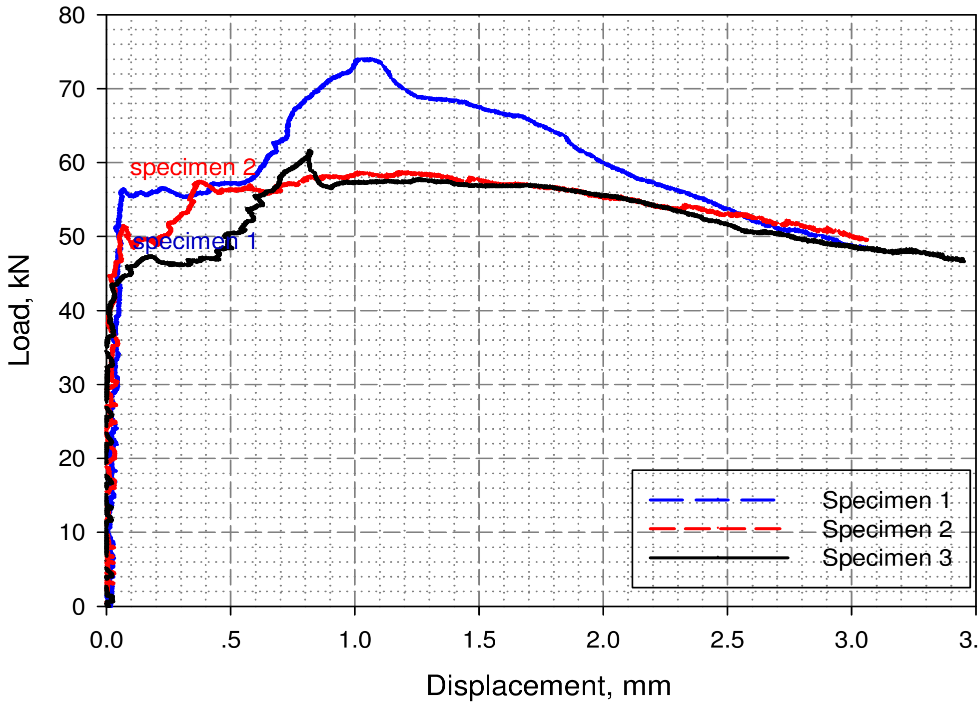


Figure 3.42 Comparing the flexural performance test results of fiber reinforced concrete of batch 320-35-SP at 28 days

According to ASTM 1609C/1609M, the peak load of flexural test has two types: the first load and first peak load. In figure 3.41, for concrete in 7 days, shows that specimen number 1 and 3 has one peak load. While the specimen number 2 has both first peak load and peak load. In addition, the load-displacement curve in figure 3.40 shows that all specimens contain two peak loads.

c). Tensile test

For this test, 3 specimens were used but only the result of two specimens can be analyzed properly. This is due to the unequal size of the catcher and the specimen where the catcher is smaller compared to the specimen. As seen in Figure 3.41, the tensile stress of SFRC is around 20 ksc to 25 ksc. On the other hand the tensile strength is around 10% of the compressive strength. The tensile strain is between 0.032-0.034.

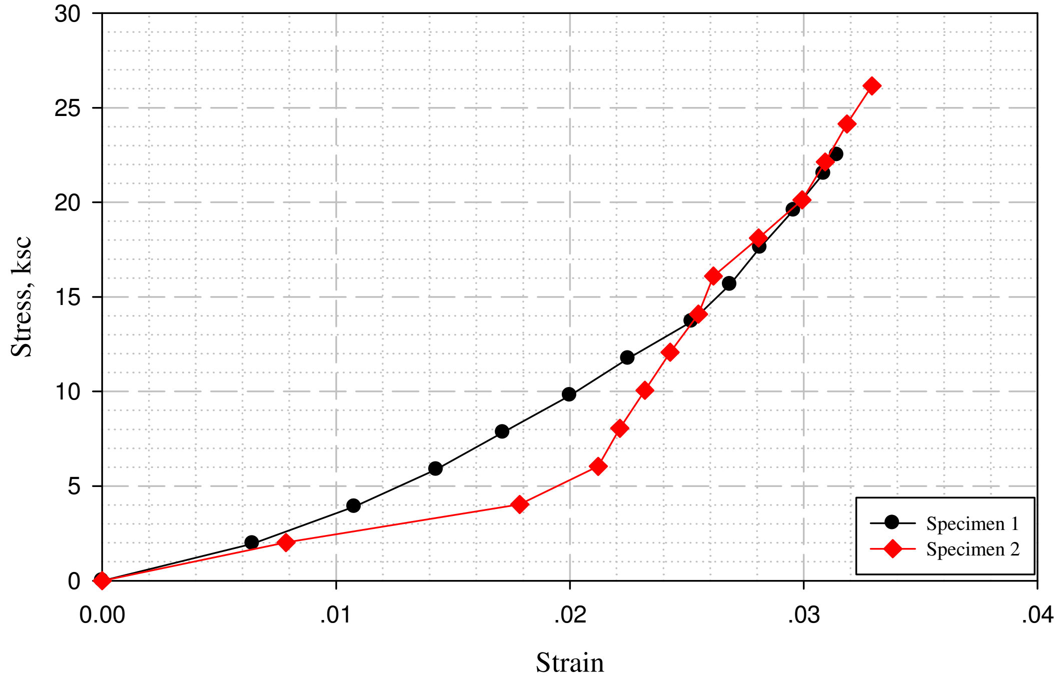


Figure 3.43 The relationship between stress and strain of briquette at 7 days

4.8 Back analysis

Due to lack of equipment in the lab, the process of finding the tensile softening curve from the laboratory was not success. A method from JCI called "**Method of Estimating Tension softening Curve of Concrete**" (JCI-S-001-2003) mentioned that the tensile softening curve can be back analyzed from the flexural test.

The process of this analysis is to divide the beam specimen into 2 sides (symmetrical in both sides), then refine the specimen into nodes and elements (see Figure 3.42. All nodes must have the coordinate of each node, and the elements should define the nodes that build the element. Then the loading node (NLOD), supporting node (NSUP), and LVDT's node (NDEF) should be defined. In addition, the thickness of element, the Young's modulus, Poisson's ratio, and the density of the specimen had been added into the program. Moreover, the load-displacement curve of that specimen from flexural test was also incorporated into the program to find the tensile softening curve of concrete.

According to Figure 3.40, the flexural test of SFRC in 28 days, specimen number 1 has higher residual load than the others. So, this specimen was chosen to be used in back analysis method and the tensile softening curve in Figure 3.43 exhibits the result. For this figure, the tensile strength of concrete is 15.1 N/mm$^2$ and displacement at peak is 0.00259 mm. This value will be used in chapter IV.

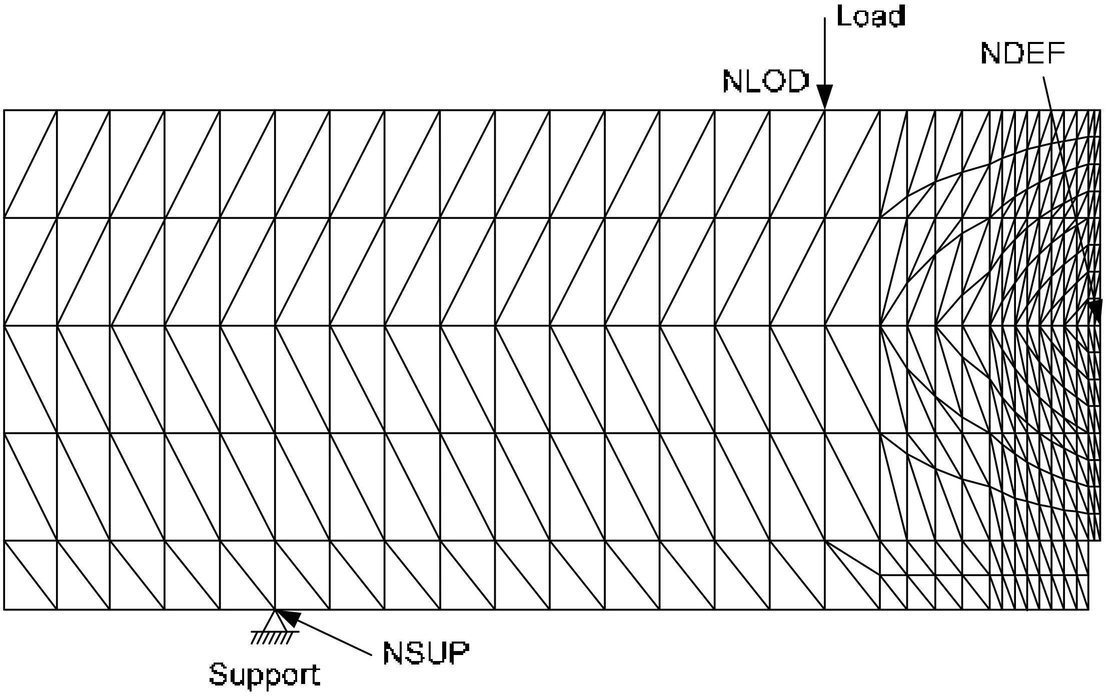


Figure 3.44 Mesh refinements for back analysis method

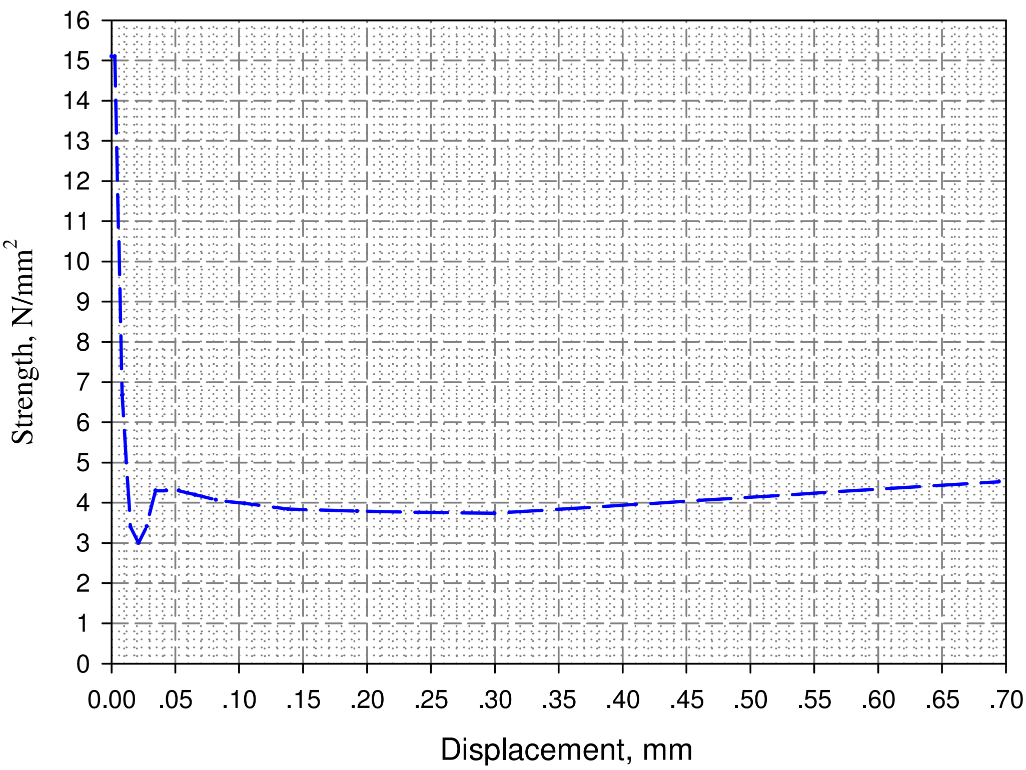


Figure 3.45 Tensile softening curve from back analysis method

## 4.9 Conclusion

According to the laboratory test result, it can be concluded that for:

a) Fresh concrete

- The slump of concrete without SP is in the range between 10 to 13 cm, and the concrete with SP is 14 to 17 cm. The batch that contains SP has more slump than the batch without SP. It means that with SP, the concrete easily flows to the mould better than the one without SP.

b) Hardening concrete

- The bulk density of any dosage is in the similar value which is in the range between 2400 and 2550 kg/m$^3$.
- In the compression test, the steel fiber does not have any remarkable effect to the strength of concrete in any dosage, and not far from design strength.
- For the peak load in the flexural test, the strength of concrete is relatively close to one another. It can be said that the steel fiber does not have any significant effect to the peak load of concrete.
- For residual load at 0.75 mm and 3 mm net deflection, the strength of concrete is increasing with the increase in amount of steel fiber. For the concrete with SP, the strength of concrete is higher than the one without SP.
- The batch that contains SP has larger peak load and residual load. It means that SP does not only improve the ability of flow in concrete, it increases the strength of concrete as well.
- For tensile strength, the specimen capacity reaches around 8% to 10% of compressive strength of each batch.
- When the amount of steel fiber increased with the addition of SP, the toughness of each dosage increased respectively.

c) Normalizing the strength

- Based on $P/P_{peak}$, the higher strength of concrete will result to better post-cracking resistance.

# Chapter IV

## Tunnel lining analysis (case study)

### 1. Introduction to the project.

The project related to this research is located on Champasak province, Lao PDR. Houay Lamphan Ngai Hydropower Project is situated on Bolaven plateau which is in the southern part of Laos. The project covers 2 provinces. The dam located on Xekong province, while the reservoir is on Champasak province. The installed capacity of the project is 88 MW and the average annual generation capacity is 480GWh. There are 4 different sizes of tunnel diameter as shown in Table 4.6. The considered tunnel installed in the project is positioned in between thick-bedded fine sandstone and locally interbedded very thin stratified mudstone. The soil layer that was applied to this research is shown in Tables 4.2 and 4.3, and was summarized in Table 4.4.

### 2. Tunnel parameters

2.1 Basic parameter

Basic parameters of soil and tunnel lining that were used in Ansys are stated below. The tunnel lining was analyzed in static mode, linear isotropic property, and 2 dimensional analyses.

2.1.1 Tunnel lining parameter

According to the laboratory test in chapter III, the parameters that were used in the analysis are stated in Table 4.1. Young's modulus and Poisson's ratio calculation are shown in the appendix. The compression Young's modulus was calculated from the slope of compression stress-strain curve, and the Poisson's ratio was calculated from the elongation of the cube in x-axis and y-axis. The Bending Young's modulus was back calculated from equation (4.2).

$$\delta_1 = \frac{23P_1 l^3}{1296EI}\left[1 + \frac{216d^2(1+\mu)}{115L^2}\right] \quad \text{……………………………………………...(4.1)}$$

$$\rightarrow E = \frac{23P_1 l^3}{1296\delta_1 I}\left[1 + \frac{216d^2(1+\mu)}{115L^2}\right] \quad \text{……………………………………………...(4.2)}$$

Where: δ1 = the first peak deflection, mm
P1 = the first-peak load, N
L = the span length, mm
E = the estimated modulus of elasticity of the concrete,
I = the cross-sectional moment of inertia, mm4
d = the average depth of specimen at the fracture, as oriented for testing, mm
μ = Poisson's ratio

For a Poisson's ratio of 0.20 and a d to L ratio of 1/3, the value of the portion of the equation in brackets is 1.25.

Table 4.1 Young's modulus and Poisson's ratio of each type of specimen

| Specimen | E, Mpa | | Poisson's ratio | |
|---|---|---|---|---|
| | 7 days | 28 days | 7 days | 28 days |
| cube | 9646 | 10592 | 0.28 | 0.23 |
| beam | 233672 | 35490 | | |
| briquette | 1361 | | | |

*See more in appendix

2.1.2 Soil parameter

The soil layer of this project contains 4 layers, when looking at the density and water content; they can be concluded in 2 main layers: $Q_{edl}$ and $N_2$.

Table 4.2 Basic parameters of soil

| soil layer | | depth | ρ | σ | Wn | $W_l$ | Wp | Ip |
|---|---|---|---|---|---|---|---|---|
| | | m | g/cm3 | kN/m3 | % | % | % | |
| 7 | ZK01 | 3.2 | 1.62 | 51 | 35.5 | 74.9 | 37.7 | 37.2 |
| | ZK01 | 8.4 | 1.68 | 137 | 36.2 | 72.6 | 39.9 | 32.7 |
| 8 | ZK02 | 10.6 | 1.59 | 171 | 49.1 | 90.8 | 50.2 | 40.6 |
| | ZK02 | 14.8 | 1.59 | 236 | 48.7 | 92.6 | 50.2 | 42.4 |
| 9 | ZK03 | 21 | 1.61 | 334 | 37.4 | 79.1 | 37 | 42.1 |
| | ZK03 | 29.2 | 1.6 | 463 | 41.1 | 100.7 | 45.7 | 55 |
| 10 | K1 | 32.2 | 1.99 | 522 | 14.6 | 35.9 | 20.1 | 15.8 |
| | K2 | 38.2 | 2.04 | 642 | 16.8 | 36.7 | 20.4 | 16.3 |
| | K3 | 46.2 | 2.06 | 803 | 17.1 | 41.3 | 22 | 19.3 |
| | K4 | 53.2 | 2.12 | 949 | 20.9 | 31.7 | 18.6 | 13.1 |
| | K5 | 130 | 2.12 | 2546 | 23.5 | 30.1 | 18 | 12.1 |

Table 4.3.Basic parameters of soil (continue)

| Soil layer | | Depth | Density | Unit weight | Cohesion | Friction angle | Undrained modulus | Poisson's ratio |
|---|---|---|---|---|---|---|---|---|
| | | | ρ | γ | Cu | φ | E | v |
| | | M | g/cm3 | kN/m3 | kN/m2 | degree | kPa | assume |
| 7 | ZK01 | 3.2 | 1.62 | 15.9 | 58.52 | 12 | 11798 | 0.25 |
| | ZK01 | 8.4 | 1.68 | 16.5 | 59.85 | 12 | 13727 | 0.25 |
| 8 | ZK02 | 10.6 | 1.59 | 15.6 | 63.36 | 15.2 | 11704 | 0.2 |
| | ZK02 | 14.8 | 1.59 | 15.6 | 63.36 | 15.2 | 11208 | 0.15 |
| 9 | ZK03 | 21 | 1.61 | 15.8 | 52.36 | 27.9 | 9328 | 0.25 |
| | ZK03 | 29.2 | 1.6 | 15.7 | 52.36 | 27.9 | 7140 | 0.25 |

| Soil layer | | Depth | Density | Unit weight | Cohesion | Friction angle | Undrained modulus | Poisson's ratio |
|---|---|---|---|---|---|---|---|---|
| | | | ρ | γ | Cu | φ | E | v |
| | | M | g/cm3 | kN/m3 | kN/m2 | degree | kPa | assume |
| 10 | K1 | 32.2 | 1.99 | 19.5 | 88.5 | 31.5 | 42009 | 0.26 |
| | K2 | 38.2 | 2.04 | 20.0 | 80.5 | 34.6 | 37040 | 0.26 |
| | K3 | 46.2 | 2.06 | 20.2 | 82.1 | 33.8 | 31904 | 0.26 |
| | K4 | 53.2 | 2.12 | 20.8 | 28.1 | 32.7 | 16088 | 0.26 |
| | K5 | 110 | 2.12 | 20.8 | 100.4 | 36.6 | 62231 | 0.26 |

Table 4.4 Summary soil's parameters used in Ansys

| soil | Density | Unit Weight | cohesion | Friction angle | Young's modulus (undrained) | Poisson's ratio |
|---|---|---|---|---|---|---|
| | P | Γ | C | φ | E | v |
| | kg/m3 | kN/m3 | N/m2 | degree | N/m2 | |
| $Q_{edl}$ | 1615 | 15.84 | 58302 | 18.37 | 21635074 | 0.23 |
| $N_2$ | 2066 | 20.27 | 64580 | 33.84 | 65745678 | 0.26 |

## 3. Applying into ANSYS

Ansys is a flexible program which is suitable for solving engineering problems by using finite element method to obtain results. It includes a lot of failure criteria that the user can choose as much as possible whichever is suitable to the problem.

- Use Mechanical APDL (ANSYS)
- Design as plane strain, linear isotropic structure.
- Tunnel shape: circular.

### 3.1.1 Geometry

According to the Training Course on Computational Geotechnics, 2012, the width and the depth of the soil surrounding the tunnel structure is shown in Figure 4.1. The distance from ground surface to the center of tunnel is 110 m. The coordinates of each boundary point is given in Table 4.5, while the tunnel geometry is shown in Figure 4.2.

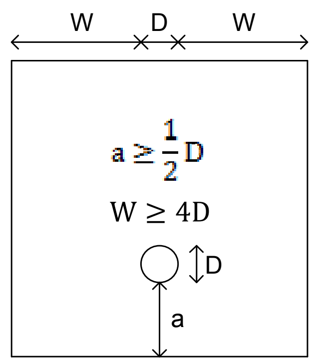


Figure 4.1 Model boundary of tunnel

Table 4.5 Coordinate of each point in the structure

| Point | x (m) | y (m) |
|---|---|---|
| A | 0 | 0 |
| B | 35 | 0 |
| C | 35 | -130 |
| D | 0 | -130 |
| E | 0 | -30 |
| F | 35 | -30 |
| G | 0 | -110 |

Table 4.6 Tunnel's dimension

| Point | D (m) |
|---|---|
| G1 | 2 |
| G2 | 2.5 |
| G3 | 3 |
| G4 | 3.2 |

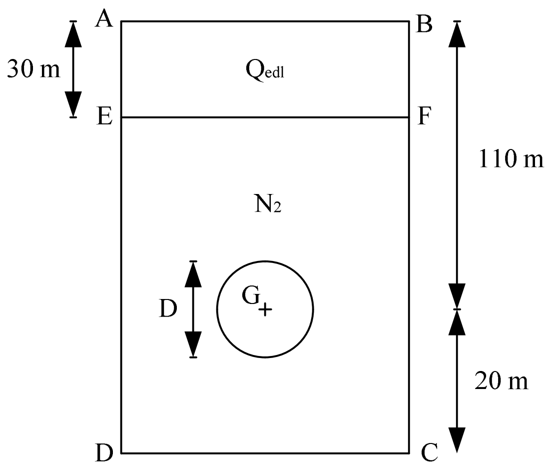


Figure 4.2 Geometry of structure

### 3.1.2 Element type

Element PLANE 183 represented the real behavior of soil and concrete. PLANE 183 is a 2-D 8-node solid structure; 2 degrees of freedom in each node (see Figure 4.3). It can support the gravity load applied to each node of the element. The failure criterion that supports this element is the Extended Drucker-Prager that will be discussed in subchapter 3.1.3.

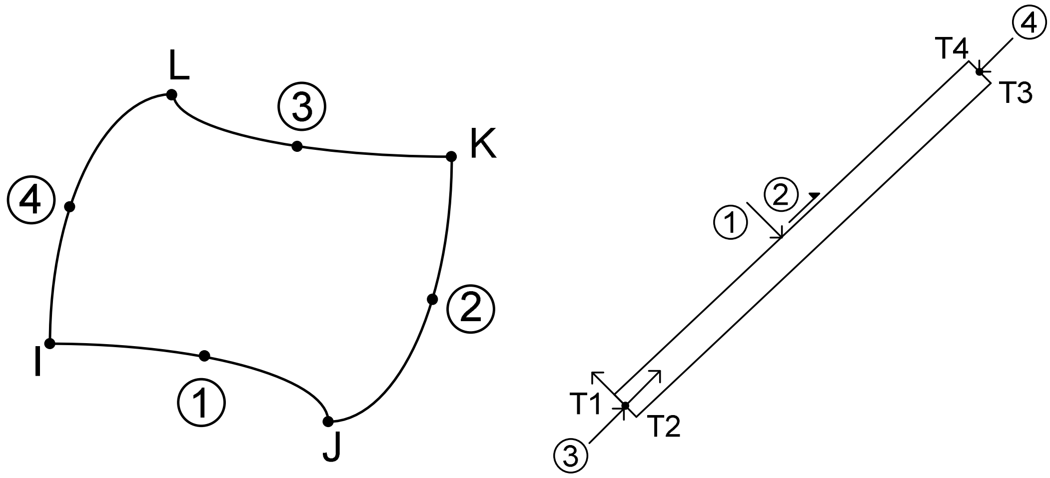


Figure 4.3 PLANE183

3.1.3 Material properties

Parameters for material properties were divided into 2 parts; linear elasticity and non linear elasticity. For linear elasticity, the parameters needed are density, Young's modulus and Poisson's ratio (shown in Table 4.4). For non linear elasticity, Ansys has various failure criteria that the user needed to understand. The user used the suitable failure criteria based on the material composition incorporated in the structure. In this research, the failure criterion of Extended Drucker-Prager (EDP) was chosen to represent the behavior of tunnel lining. Before getting the parameters of EDP, the parameter of Drucker-Prayger (DP) was calculated and then the parameters of EDP: Linear yield function and Linear Potential Flow function was found (Table 4.7).

- Failure criteria

The Drucker-Prager failure criterion is suitable for soil, rock, and concrete. It was developed from the Mohr-Coulomb law. As shown in Figure 4.4, the failure surface can be drawn on the principal stress in 3 axes because of the failure criteria of DP associated with the behavior of concrete when the load was applied.

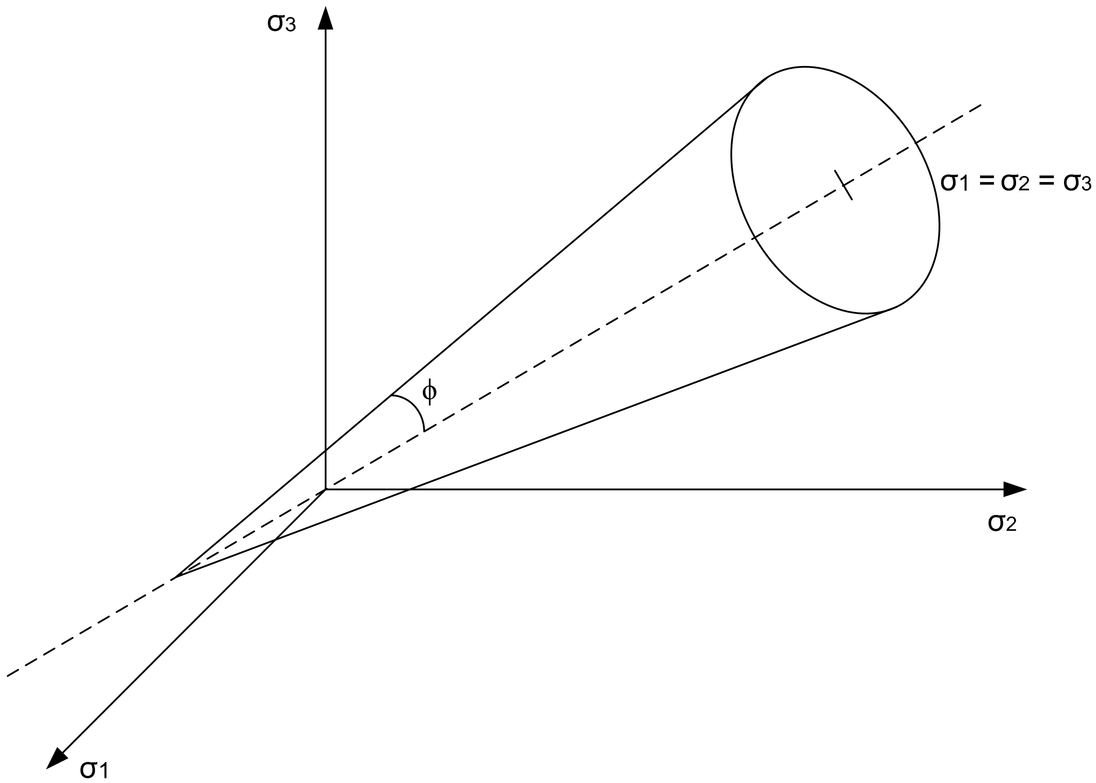


Figure 4.4 Failure plane surface of Druker-Prager failure criteria

$$F = 3\beta\sigma_m + \left[\frac{1}{2}\{s\}^T[M]\{s\}\right]^{\frac{1}{2}} - \sigma_y = 0 \quad \text{..............................................(4.3)}$$

Where F = yield function

$$[M] = \begin{bmatrix} I_{3\times3} & 0 \\ 0 & 2I_{3\times3} \end{bmatrix}$$

$\{s\}$ = Deviatoric stress vector = $\{\sigma\} - \sigma_m\{1\ 1\ 1\ 0\ 0\ 0\}^T$

$\beta$ = material constant

$\sigma_m$ = Mean stress = $\frac{\sigma_1+\sigma_2+\sigma_3}{3}$

$\sigma_y$ = yield parameter

The variable $I_{3x3}$ that appear in $[M]$ is an identity matrix with size 3x3 and average stress (F) occurred in equation 4.3 is calculated from 3 main principal stress axes. Furthermore, the material constant can also be applied in a form of DP failure criteria into two variables which are Cohesion (C) and internal friction angle (ϕ) that can be calculated from the equations below:

$$\beta = \frac{2\sin\emptyset}{\sqrt{3}(3-\sin\emptyset)} \quad \text{.......(4.4)}$$

$$\sigma_y = \frac{6C\cos\emptyset}{\sqrt{3}(3-\sin\emptyset)} \quad \text{.......(4.5)}$$

Cohesion and internal friction angle are not the only criteria that are associated with the DP failure. The Dilatancy angle is also a concern, which is the variable that controls the direction of the plastic strain and the associated flow rule as stated in the equation below.

Yield surface of DP is a circular cone when $\beta$ and $\sigma_y$ reach the outer cone of the Mohr-Coulomb surface. If $\sigma_e$ reaches $\sigma_y$, concrete becomes plastic and flow rule will affect the DP.

$$\{d\varepsilon^{Pl}\} = \lambda\left\{\frac{\partial Q}{\partial \sigma}\right\} \quad \text{.......(4.6)}$$

Where $\{d\varepsilon^{Pl}\}$ = transition of plastic strain vector

$\left\{\frac{\partial Q}{\partial \sigma}\right\}$ = transition rate of yield function compare with stress state

$\lambda$ = plastic multiplier

The material related to the flow rule is the material with the transition of plastic strain vector perpendicular with failure plane. The DP is dependent on the association of the flow rule. If the DP is associated with the flow rule, the friction angle is equal to the Dilatancy angle and causes volume expansion. On the other hand, the non-associated flow rule causes less volumetric expansion if the Dilatancy angle is less than friction angle and no volumetric expansion if Dilatancy angle is zero. The transition rate of yield function and stress vector can be calculated as:

$$\left\{\frac{\partial F}{\partial \sigma}\right\} = \beta\{1\,1\,1\,0\,0\,0\}^T + \frac{\{s\}}{\left[\frac{1}{2}\{s\}^T[M]\{s\}\right]^{\frac{1}{2}}} \quad \text{.......(4.7)}$$

Where F = yield function

$$[M] = \begin{bmatrix} I_{3\times3} & 0 \\ 0 & 2I_{3\times3} \end{bmatrix}$$

$\{s\}$ = Deviatoric stress vector = $\{\sigma\} - \sigma_m\{1\,1\,1\,0\,0\,0\}^T$

$\beta$ = material constant

When the material constant that comes from the internal friction angle is not equal with the material constant that come from the Dilatancy angle ($\beta|_{\phi=\phi} \neq \beta|_{\phi=\phi f}$), the material is not associated with the flow rule. The volumetric expansion decreases as the Dilatancy angle decreases until the material doesn't have volumetric expansion where the Dilatancy is zero. Figure 4.5 show the associated and non-associated flow rule of the material.

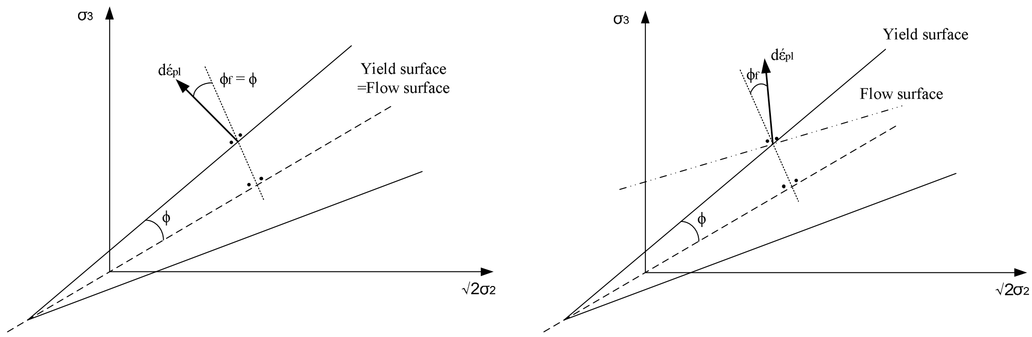


a. Associated flow rule b. Non- Associated flow rule

Figure 4.5 Associate and Non-Associate flow rule diagram

According to Prasertsri.T (2012), the flow rule of concrete is not associated with the failure criteria and the dilatancy angle is zero which means that there is no volumetric expansion. Mirmiran et al (2000) used the equations that define cohesion value and internal friction angle by unconfined strength of concrete. Rochette and Labossiere (1997) defined that:

$$C = \left(f'_{co} - 5\sqrt{3}\right)\frac{3 - sin\emptyset}{6cos\emptyset} \quad \text{(4.8)}$$

$$\emptyset = sin^{-1}\left(\frac{3}{1+\frac{2f'_{co}}{\sqrt{3}}}\right) \quad \text{(4.9)}$$

Where $f'_{co}$ = unconfined strength of concrete (MPa)

In this research, two materials are considered: soil and concrete. A 2-D finite element using PLANE183 to simulate the soil and concrete structure that can be applied with EDP was used. For the element PLANE183, another failure criterion called Extended Drucker-Prager, EDP (Mirmiran et al, 2000) is needed. The difference between DP and EDP are the parameters that will be added into the program. The parameters have two main parts; the yield function part and the plastic flow potential function. Each part has three types of function: linear, power law, and hyperbolic (Ansys element reference, 2009), wherein linear function has been used for this study.

Linear yield function:

$$C_1 = \sqrt{3}\beta = \frac{2sin\emptyset}{3 - sin\emptyset} \quad \text{(4.10)}$$

$$C_2 = \sqrt{3}\sigma_y = \frac{6C(cos\emptyset)}{3 - sin\emptyset} \quad \text{(4.11)}$$

Linear Plastic Flow Potential Function (Sheldon Imaoka, 2008):

$$Q = \frac{6sin\emptyset_f}{3 - sin\emptyset_f} \quad \text{(4.12)}$$

Where Dilatancy angle: $\varnothing_f = \frac{\varnothing}{2}$

$$\varnothing_f = \varnothing \rightarrow \text{Associated Flow Rule}$$

$$\varnothing_f \neq \varnothing \rightarrow \text{Non-Associated Flow Rule}$$

Table 4.7 DP and EDP parameters of concrete for Ansys

| Lining | | compressive strength, fcu | DP | | | | | EDP | | |
|---|---|---|---|---|---|---|---|---|---|---|
| | | | C | ϕ | ϕf | β | σy | C1 | C2 | Q |
| | | Mpa | MPa | degree | degree | | MPa | | MPa | |
| Plain | 320-0-SP | 31 | 10.49 | 21.64 | 10.82 | 0.16 | 12.84 | 0.28 | 22.24 | 0.40 |
| SFRC | 320-35-SP | 40 | 14.99 | 16.88 | 8.44 | 0.12 | 18.33 | 0.21 | 31.76 | 0.31 |
| IN SITU | C25 | 25 | 7.77 | 26.29 | 13.14 | 0.20 | 9.43 | 0.35 | 16.34 | 0.49 |

Table 4.8 Basic parameters of concrete for Ansys

| AT 28 DAYS | DENSITY, kg/m3 | | | E, Mpa | | | POISSON'S RATIO | | | SOURCE |
|---|---|---|---|---|---|---|---|---|---|---|
| | COM | BEND | TEN | COM | BEND | TEN | COM | BEND | TEN | |
| PLAIN | 2456 | 2434 | - | - | 32784 | - | 0.23 | | | LAB TEST |
| SFRC | 2510 | 2365 | | 10592 | 35490 | 1494 | 0.23 | | | LAB TEST |

### 3.1.4 Boundary condition

There are 2 types of boundary condition that will be chosen to be applied to this research. The B1 is fixed only x-axis at the side and fixed all axes at the bottom of the geometry, while B2 concerns only the bottom of geometry by fix all the axis at the middle and fix at y-axis at the corner of geometry.

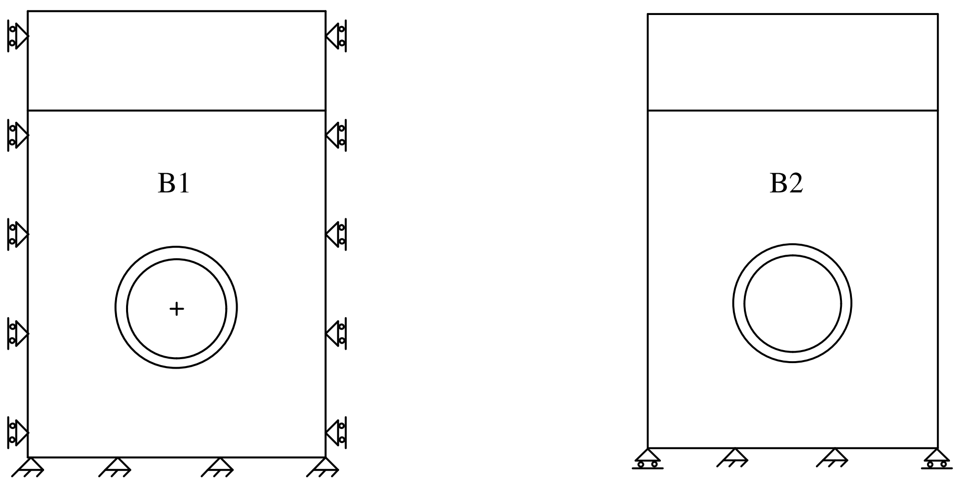


Figure 4.6 Boundary condition

Both boundary conditions will be checked for convergence with the empirical method in 3.1.5. The stress will be plotted into the graph in Figure 4.8.

### 3.1.5 Empirical method

According to Obert and Duvall (1967), the stress of soil at any position of the tunnel can be calculated in the process as shown below. The data from the equations was used to calculate and obtain the results to be compared in Figure 4.8. The stress results are shown in Table 4.9 and 4.10.

- Vertical stress: $S_v = \gamma h$ ……………………………………….(4.13)

- Horizontal stress: $S_h = mS_v$ ……………………….(4.14)

$$m = \frac{\nu}{1-\nu} \quad \text{……………………………………….. (4.15)}$$

Which $\gamma$ = unit weight of soil, N/m$^3$

h = depth of tunnel at point concerned, m

$\nu$ = Poisson's ratio of soil

- Radial stress:

$$\sigma_r = \left(\frac{S_h+S_v}{2}\right)\left(1-\frac{a^2}{r^2}\right)+\left(\frac{S_h-S_v}{2}\right)\left(1-\frac{4a^2}{r^2}+\frac{3a^4}{r^4}\right)cos2\theta \quad \text{.. (4.16)}$$

- Tangential stress:

$$\sigma_\theta = \left(\frac{S_h+S_v}{2}\right)\left(1+\frac{a^2}{r^2}\right)-\left(\frac{S_h-S_v}{2}\right)\left(1+\frac{3a^4}{r^4}\right)cos2\theta \quad \text{... (4.17)}$$

- Shear stress:

$$\sigma_\theta = \left(\frac{S_h-S_v}{2}\right)\left(1+\frac{2a^2}{r^2}-\frac{3a^4}{r^4}\right)sin2\theta \quad \text{………………..(4.18)}$$

Where a = radius of tunnel, m.

r = the distance from center of tunnel to the point concerned, m.

$\theta$ = the angle between x-axis and the point concerned, degree.

Table 4.9 Vertical and horizontal stress by empirical method

| Diameter | radius | Thickness | Sv, N/m2 | | | Sh, N/m2 | | |
|---|---|---|---|---|---|---|---|---|
| D, m | a, m | m | σc | Σi | σs | σc | σi | σs |
| 2 | 1 | 0.5 | 2066290 | 2127092 | 2096691 | 725994 | 747357 | 736675 |
| 2.5 | 1.25 | 0.5 | 2061223 | 2132159 | 2096691 | 724214 | 749137 | 736675 |
| 3 | 1.5 | 0.5 | 2056156 | 2137226 | 2096691 | 722433 | 750917 | 736675 |
| 3.2 | 1.6 | 0.5 | 2054130 | 2139253 | 2096691 | 721721 | 751629 | 736675 |

Table 4.10 Axial stress and tangential stress by empirical method

| Diameter | a | r | radial stress | | | tangental stress | | |
|---|---|---|---|---|---|---|---|---|
| | | | Σr | | | σθ | | |
| D, m | m | m | Σc | σi | σs | σc | σi | σs |
| 2 | 1 | 1.5 | 651533 | 670705 | 912974 | 949377 | 977313 | 3129296 |
| 2.5 | 1.25 | 1.75 | 508409 | 525906 | 870614 | 912732 | 944144 | 3350524 |
| 3 | 1.5 | 2 | 407237 | 423294 | 824333 | 870914 | 905252 | 3539052 |
| 3.2 | 1.6 | 6.6 | 375008 | 390548 | 805823 | 853920 | 889307 | 3606519 |

*Remark: c = at crown of tunnel.
i = at invert of tunnel.
s = at spring line of tunnel.

## 4. Analysis result

- Understanding of data

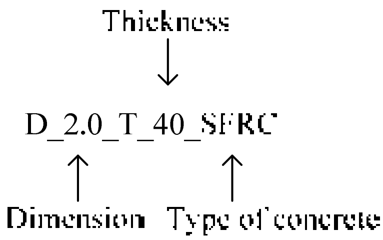


Figure 4.7 Data explanation

4.1 Convergence check

The convergence was checked from the boundary condition which was appropriate to the analysis by plotting the tunnel analysis result from 2 types of boundary condition. The axial stress of tunnel analysis from Ansys was compared with the tangential stress from the empirical method. In addition, this convergence checked the appropriate amount of elements that was used in Ansys.

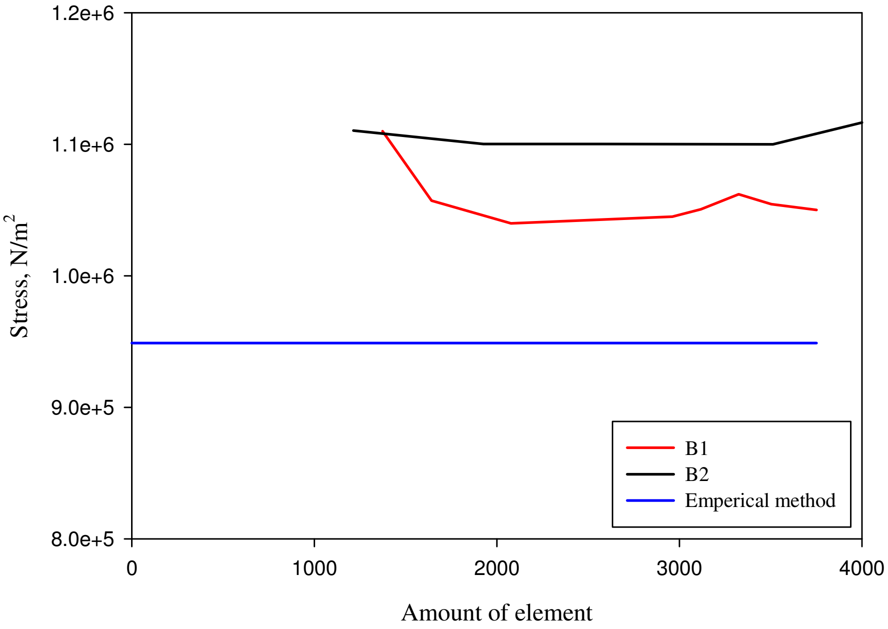


Figure 4.8 Convergence check by boundary condition and amount of elements

According to Figure 4.8, it can be seen that B1 has the result closer to the empirical method than B2. B1 is far from empirical method about 9%, while B2 is about 14%. With this figure, it showed that the suitable amount of element is 2000 elements, and this number of elements was used into the analysis in Ansys.

## 4.2 Analysis result

After solving the problem in Ansys, the stain at each node was plotted as a list and the strain was chosen according to the segment position (see Figure 4.9) of each tunnel diameter. The strain chosen from the list is the axial strain at x-axis and y-axis. The strain that contains a negative sign (-) is tensile strain, while the other (+) is compressive strain. The maximum strain is obtained from the discussion in chapter III. The tensile deformation at peak tensile softening curve (see Figure 3.43), 0.000259 mm, is divided by the crack opening (3 mm). The maximum strain is -8.63E-04. The axial strain from Ansys was compared with the maximum strain as shown in Table 4.11 to 4.14. Moreover, the strains of the tunnel segment at each position were plotted in Figure 4.11 to 4.14.

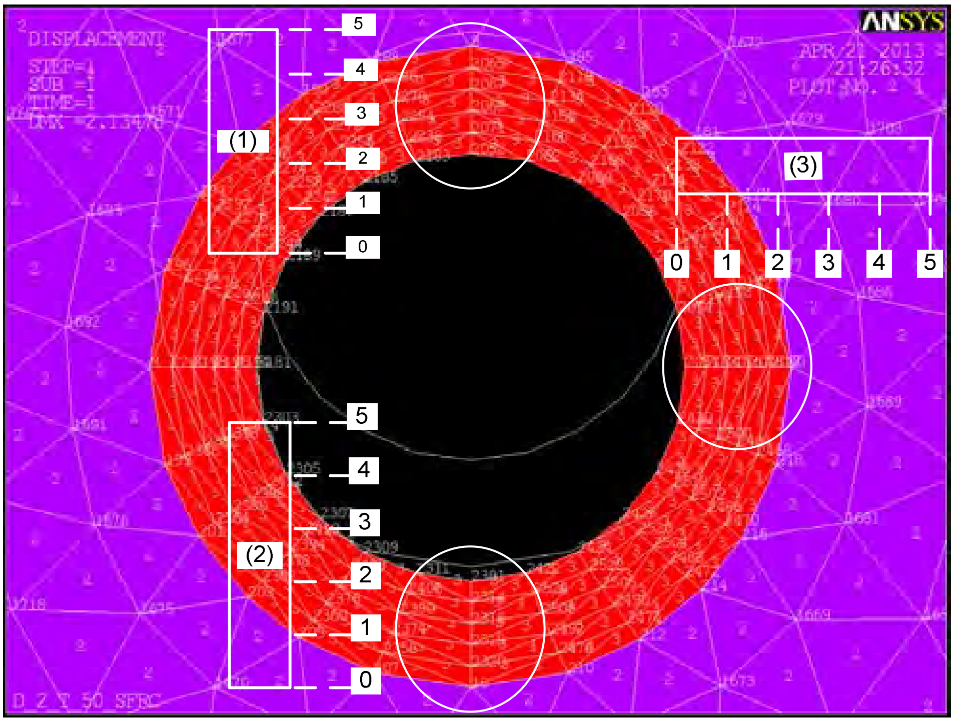


Figure 4.9 Tunnel's position

Table 4.11 Strain at crown, invert, and spring line of tunnel lining D_2.0_T_50 and Max strain

| D_2.0_T_50 | NODE | STRAIN | | MAX STRAIN |
|---|---|---|---|---|
| | | x | y | |
| (1) Crown | 8 | -5.03E-04 | 7.02E-05 | -8.63E-04 |
| | 2065 | -3.66E-04 | 6.55E-05 | |
| | 2067 | -2.14E-04 | 5.34E-05 | |
| | 2069 | -3.73E-05 | 2.68E-05 | |
| | 2071 | 1.84E-04 | -2.79E-05 | |
| | 2052 | 4.74E-04 | -1.34E-04 | |
| (2) Invert | 2301 | 4.74E-04 | -1.34E-04 | -8.63E-04 |
| | 2314 | 1.83E-04 | -2.78E-05 | |
| | 2316 | -3.91E-05 | 2.68E-05 | |
| | 2318 | -2.16E-04 | 5.32E-05 | |
| | 2320 | -3.70E-04 | 6.51E-05 | |
| | 10 | -5.07E-04 | 6.97E-05 | |
| (3) Spring line | 2051 | 2.69E-04 | -9.15E-04 | |
| | 2074 | 1.14E-04 | -5.75E-04 | |
| | 2076 | 2.12E-05 | -3.15E-04 | |
| | 2078 | -3.47E-05 | -1.09E-04 | |
| | 2080 | -7.02E-05 | 6.77E-05 | |
| | 7 | -9.31E-05 | 2.23E-04 | |

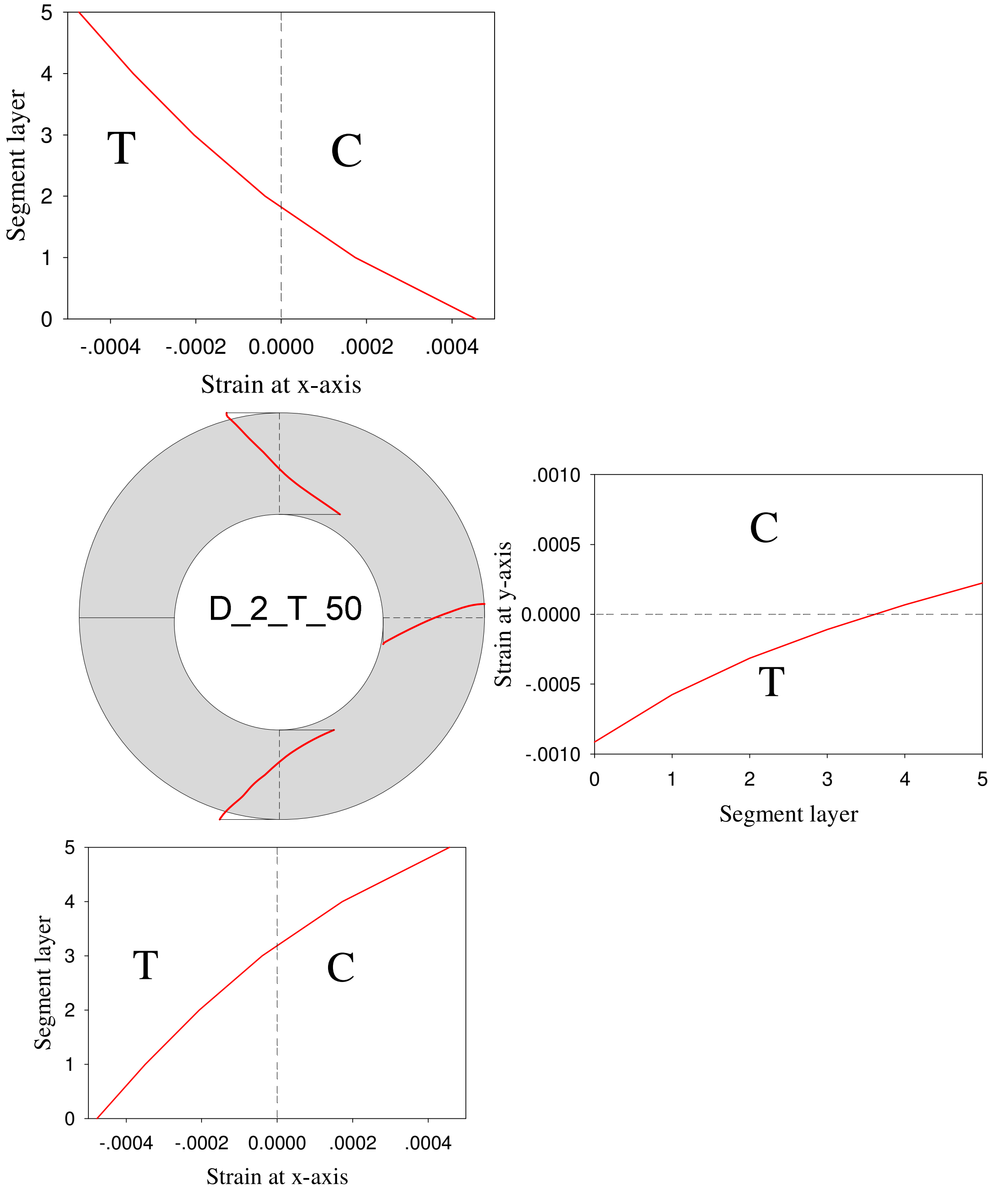


Figure 4.11 Strain at crown, invert, and spring line of tunnel lining D_2.0_T_50

Table 4.12 Strain at crown, invert, and spring line of tunnel lining D_2.5_T_50 and Max strain

| D_2.5_T_50 | NODE | STRAIN | | MAX STRAIN |
|---|---|---|---|---|
| | | x | y | |
| (1) Crown | 8 | -2.91E-05 | 5.42E-06 | -8.63E-04 |
| | 2025 | -2.07E-05 | 4.74E-06 | |
| | 2027 | -1.13E-05 | 3.49E-06 | |
| | 2029 | -5.19E-07 | 1.37E-06 | |
| | 2031 | 1.24E-05 | -2.22E-06 | |
| | 2012 | 2.77E-05 | -7.92E-06 | |
| (2) Invert | 2261 | 2.78E-05 | -7.93E-06 | |
| | 2274 | 1.23E-05 | -2.21E-06 | |
| | 2276 | -6.10E-07 | 1.38E-06 | |
| | 2278 | -1.14E-05 | 3.50E-06 | |
| | 2280 | -2.09E-05 | 4.74E-06 | |
| | 10 | -2.93E-05 | 5.41E-06 | |
| (3) Spring line | 2011 | 1.21E-05 | -4.32E-05 | |
| | 2034 | 7.14E-06 | -3.15E-05 | |
| | 2036 | 1.34E-06 | -1.54E-05 | |
| | 2038 | -1.94E-06 | -3.47E-06 | |
| | 2040 | -4.15E-06 | 6.95E-06 | |
| | 7 | -5.59E-06 | 1.61E-05 | |

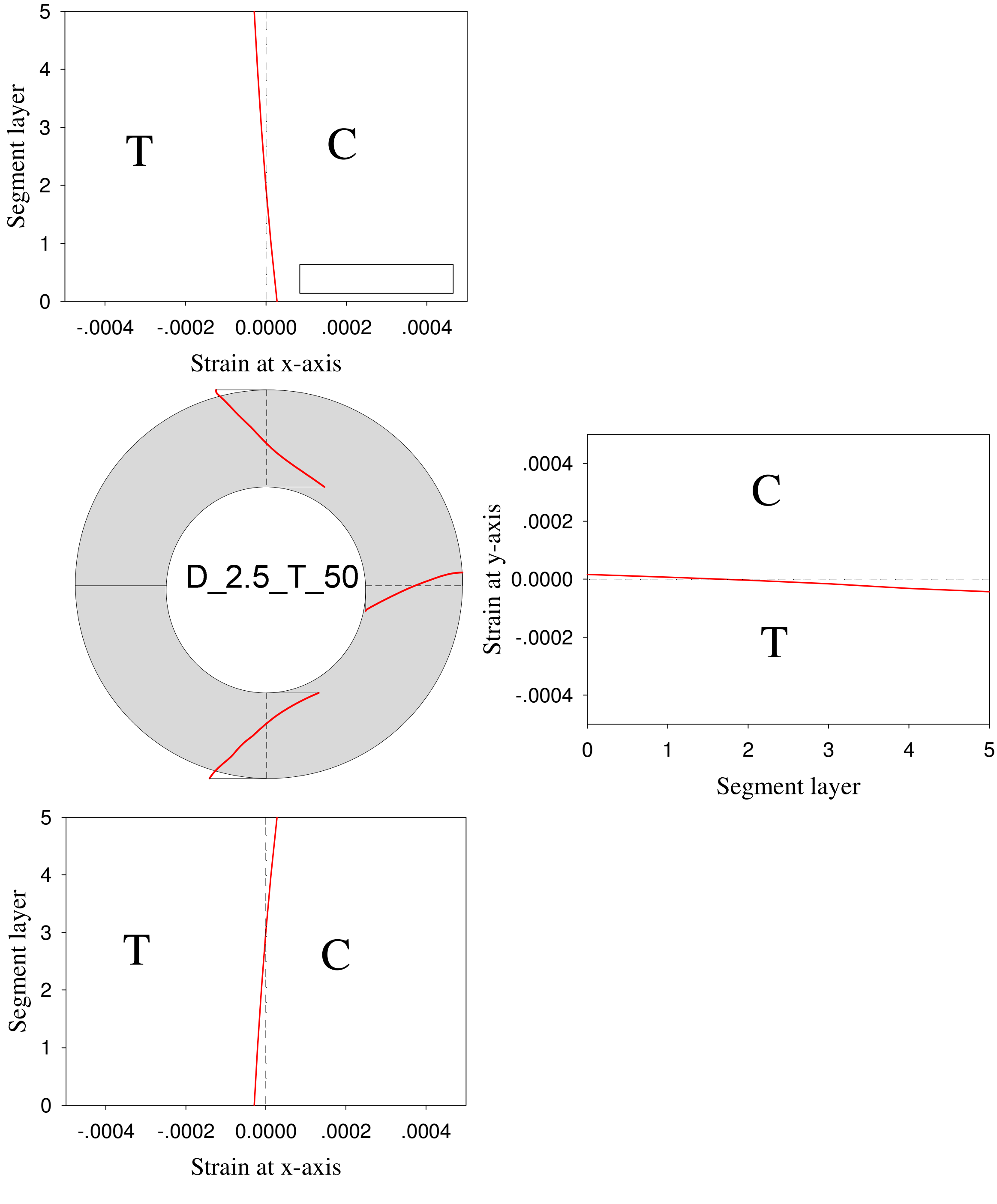


Figure 4.12 Strain at crown, invert, and spring line of tunnel lining D_2.5_T_50

Table 4.13 Strain at crown, invert, and spring line of tunnel lining D_3.0_T_50 and Max strain

| D_3_T_50 | NODE | STRAIN | | MAX STRAIN |
|---|---|---|---|---|
| | | x | y | |
| (1) Crown | 8 | -4.03E-05 | 8.51E-06 | -8.63E-04 |
| | 1969 | -2.82E-05 | 7.20E-06 | |
| | 1971 | -1.45E-05 | 4.96E-06 | |
| | 1973 | 7.78E-07 | 1.56E-06 | |
| | 1975 | 1.86E-05 | -3.69E-06 | |
| | 1956 | 3.85E-05 | -1.10E-05 | |
| (2) Invert | 2025 | 2.01E-06 | -9.83E-06 | |
| | 2218 | 1.86E-05 | -3.69E-06 | |
| | 2220 | 6.68E-07 | 1.58E-06 | |
| | 2222 | -1.47E-05 | 4.98E-06 | |
| | 2224 | -2.85E-05 | 7.22E-06 | |
| | 10 | -4.07E-05 | 8.53E-06 | |
| (3) Spring line | 1955 | 1.40E-05 | -4.39E-05 | -8.63E-04 |
| | 1978 | 1.05E-05 | -4.29E-05 | |
| | 1980 | 2.45E-06 | -2.12E-05 | |
| | 1982 | -2.59E-06 | -3.35E-06 | |
| | 1984 | -6.04E-06 | 1.23E-05 | |
| | 7 | -8.32E-06 | 2.61E-05 | |

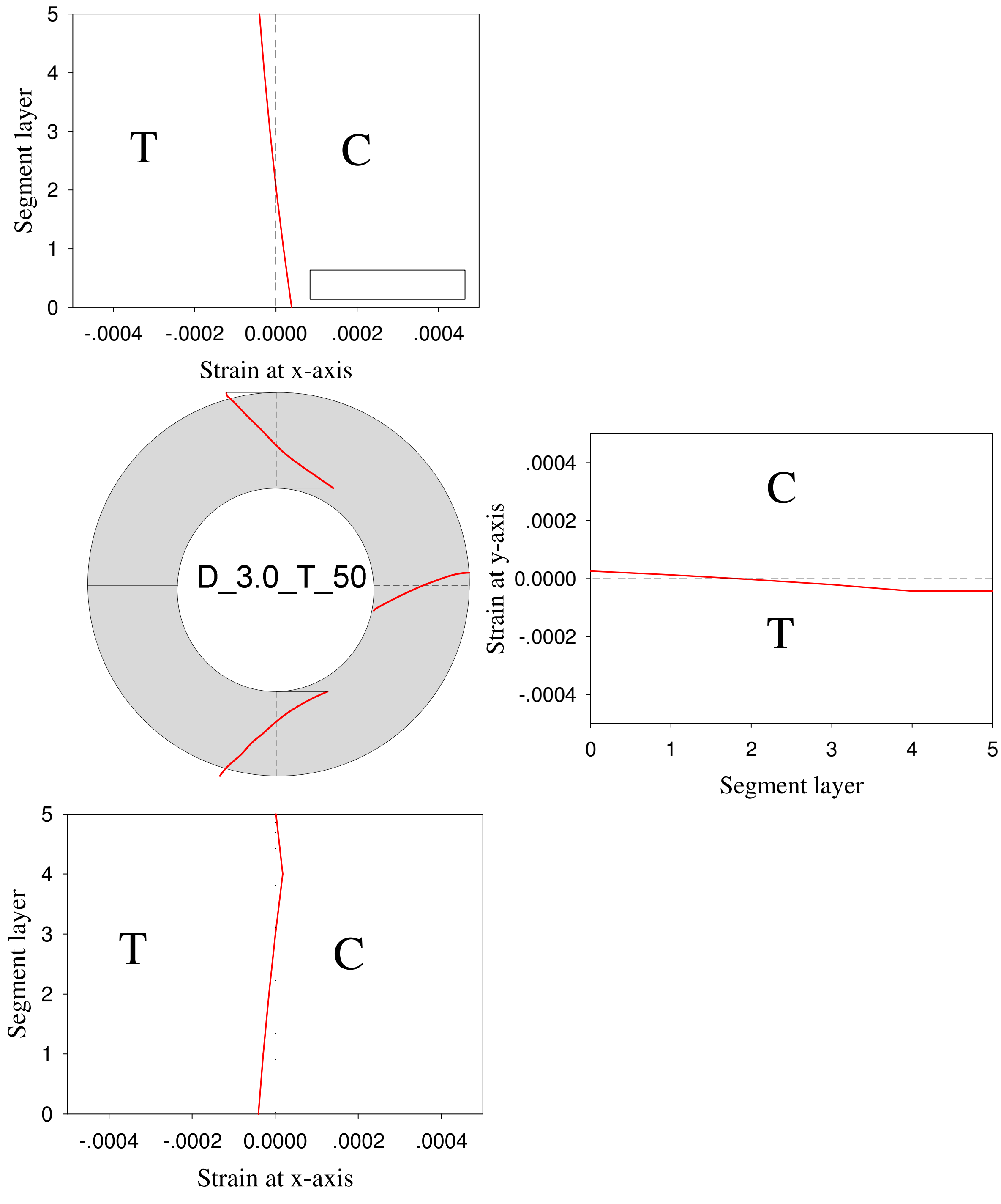


Figure 4.13 Strain at crown, invert, and spring line of tunnel lining D_3.0_T_50

Table 4.14 Strain at crown, invert, and spring line of tunnel lining D_3.2_T_50 and Max strain

| D_3.2_T_50 | NODE | STRAIN | | MAX STRAIN |
|---|---|---|---|---|
| | | x | y | |
| (1) Crown | 8 | -4.61E-05 | 1.01E-05 | -8.63E-04 |
| | 1957 | -3.19E-05 | 8.44E-06 | |
| | 1959 | -1.58E-05 | 5.66E-06 | |
| | 1961 | 2.16E-06 | 1.50E-06 | |
| | 1963 | 2.55E-05 | -5.93E-06 | |
| | 1944 | 3.51E-05 | -1.01E-05 | |
| (2) Invert | 2193 | 3.51E-05 | -1.01E-05 | |
| | 2206 | 2.55E-05 | -5.94E-06 | |
| | 2208 | 2.06E-06 | 1.52E-06 | |
| | 2210 | -1.60E-05 | 5.70E-06 | |
| | 2212 | -3.22E-05 | 8.48E-06 | |
| | 10 | -4.65E-05 | 1.01E-05 | |
| (3) Spring line | 1943 | 1.46E-05 | -4.39E-05 | |
| | 1966 | 1.20E-05 | -4.58E-05 | |
| | 1968 | 3.40E-06 | -2.53E-05 | |
| | 1970 | -2.81E-06 | -3.85E-06 | |
| | 1972 | -7.02E-06 | 1.50E-05 | |
| | 7 | -9.81E-06 | 3.15E-05 | |

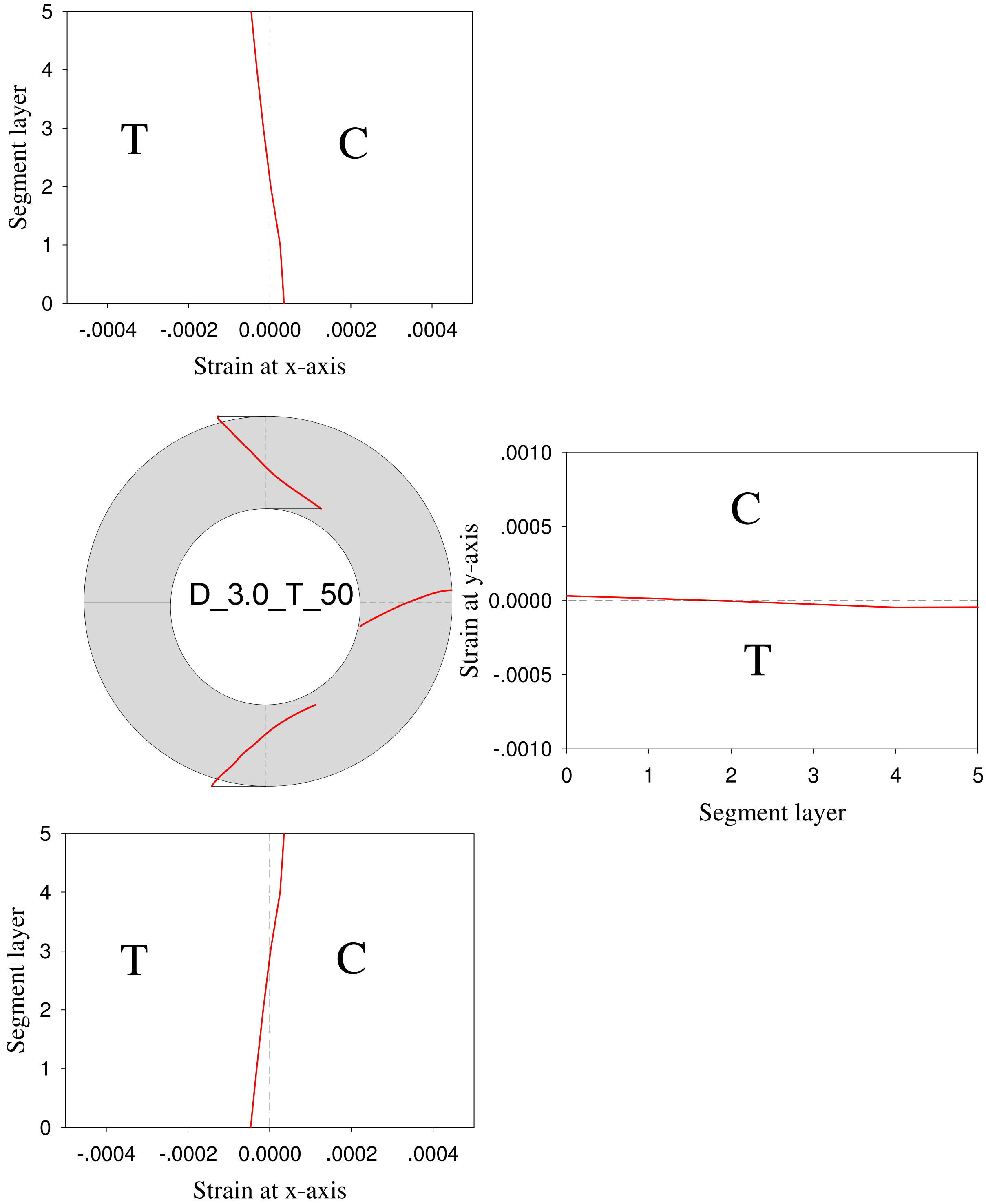


Figure 4.14 Strain at crown, invert, and spring line of tunnel lining D_3.2_T_50

## 5. Conclusion

When looking at the strain of crown, invert, and spring line of the tunnel lining, almost all strains occurred is smaller than the maximum strain from the laboratory experiment. This means that from the load applied to the tunnel lining, only the concrete resist all the load. The steel fiber does not yet support the concrete to counteract with the load. In contrast, only the load at node 2051, internal spring line of D_2.0_T_50 has the tensile strain more than the maximum strain. This means that it exceeded the serviceability criteria of the concrete, but it didn't exceed the ultimate tensile strain of the SFRC yet. The diameter of tunnel lining also affects the strain values, wherein the smaller diameter results into larger strain compared to the tunnel lining with bigger diameter which resulted into smaller strain.

# Chapter V

# Conclusion

The purpose of this research is to study the characteristic of steel fiber reinforce concrete and it will be applied to the case study of tunnel structure in order to study the behavior of tunnel lining. The laboratory test, 3 types of specimen that contain cube, beam and briquette had been test to figure out the characteristic of SFRC under compression, tension, and bending. The design strength of concrete was divided by 2 strengths, 240 ksc and 320 ksc. The amount of steel fiber had been varied into 6 dosages: 0 (no steel fiber), 15, 20, 25, 30, 35, and 40 kg/$m^3$ concrete respectively. Then they were mixed in 2 batches, with SP and without SP.

For the case study of tunnel lining analysis, the diameter of the tunnel divided in 4 sizes, 2 m, 2.5 m, 3.0 m, and 3.2 m with 0.5 m thickness. The depth of tunnel is 110 m from the ground surface. Only the load from the soil applied to tunnel lining segment. Ansys is the finite element analysis program was used to analyze the behavior of tunnel lining under the load of soil. The entire plane in the project was divided by 2000 elements which is appropriate for the analysis.

## 1. Laboratory test

Nowadays, the steel fiber is a new material to add into the concrete in order to increase the strength of concrete after crack either decreases the covering of concrete segment. This research tell that when the amount of steel fiber in concrete increase, the residual strength of concrete also increase. In addition, the super plasticizer (SP) that usually added into SFRC not only helps the better flow ability, but also helps to increase the strength of concrete. Moreover, the design strength of concrete also effect to the residual strength of SFRC.

## 2. Tunnel lining analysis (case study)

When applying the load to the tunnel lining, only the concrete resist the entire load. The steel fiber not yet helps concrete to tolerant with the load. In contrast, only the load at node 2051, internal spring line of D_2.0_T_50 has the tensile strain more than the maximum strain about 6%. The strain exceeded the serviceability criteria of the concrete, but it didn't exceed the ultimate tensile strain of the SFRC yet. The diameter of tunnel lining also have effect with the strain, the smaller diameter has larger strain than the bigger diameter.

## 3. Future work

Even this research study only the characteristic of SFRC and behavior of tunnel lining under serviceability criteria, there are lot of advantage of SFRC (especially the behavior of tunnel lining under ultimate criteria). First of all, steel fiber is easier for transferring from the warehouse to the construction filed compared to the reinforced bar. Next, when it's applied to the tunnel lining segment, it reduces the crack happening during the transportation. In addition, it helps to reduce the covering depth compare to conventional reinforced concrete. Moreover, steel fiber can save the cost of labor to tied the reinforced bar. And so on. If you want to do further work from this research, the characteristic of SFRC under the ultimate strength should be figure out.

## References

<u>Thai</u>

ทศพร ประเสริฐศรี, 2555, การวิเคราะห์กำลังและความเหนียวของทรงกระบอกคอนกรีตที่ถูกโอบรัดบางส่วนด้วยพอลิเมอร์เสริมเส้นใย, ปริญญาวิศวกรรมศาสตรมหาบัณฑิต, สาขาวิชาวิศวกรรมโยธา ภาควิชาวิศวกรรมโยธา, คณะวิศวกรรมศาสตร์ จุฬาลงกรณ์มหาวิทยาลัย

พรเพ็ญ ลิมปนิลชาติ, ปิติโชค ทองตระการ, วิทิต ปานสุข, 2553, อิทธิพลของปริมาณเส้นใยที่มีต่อคุณสมบัติเชิงกลของคอนกรีตเสริมเส้นใยเหล็ก, การประชุมวิชาการวิศวกรรมโยธาแหงชาติครั้งที่ 15.

## English

B. Chiaia, A.P. Fantilli, P. Vallini, 2008, designing cast-in-situ FRC tunnel lining, Tailor made concrete structures.

Bernardino Chiaia, Alessandro P. Fantilli, Paolo Vallini, 2009, combining fiber-reinforced concrete with traditional reinforcement in tunnel linings, Engineering Structures 31, 1600-1606.

Japan society of civil engineers, 1996, Japanese standard for shield tunnel (the third edition).

John Poh, Kiang Hwee Tan, Graeme Laurence Peterson, Dazhi Wen, structural testing of steel fiber reinforced concrete (SFRC) tunnel lining segments in Singapore.

L. Sorelli, F. Toutlemonde, 2005, on the design of steel fiber reinforced concrete tunnel lining segment, 11th international conference on fracture, Italy.

M. Colombo, M. di Prisco, L. Mazzaleni, 2009, sprayed tunnel linings: a comparison between several reinforcement solutions, Materials and structures 42, 1295-1311.

Mirmiran, Amir, Kenneth Zagers, and Wenqing Yuan. "Nonlinear finite element modeling of concrete confined by fiber composites." Finite Elements in Analysis and Design 35.1 (2000): 79-96.

Pornpen Limpaninlachat, Pitichoke Thongtrakarn, Withit Pansuk, 2010, EFFECT OF FIBER CONTENT ON MECHANICAL PROPERTIES OF STEEL FIBER REINFORCED CONCRETE, 15th national conference, Ubonrachathanee.

Pruettha Nanakorn, Hideyuki Horii, Shigeru Matsuoka, 1996, a fracture mechanics-based design method for SFRC tunnel linings, J.Materials Conc. Struct., Pavements No.532/V-30, 221-223.

RELEASE, ANSYS. 11.0 Users Manual, Swanson Inc. Canongsburg, PA, 2008.

Sadeghian, Pedram, Ali R. Rahai, and Mohammad R. Ehsani. "Numerical modeling of concrete cylinders confined with CFRP composites." Journal of Reinforced Plastics and Composites 27.12 (2008): 1309-1321.

Sheldon Imaoka, 2008, Sheldon's ANSYS.NET Trips and Tricks: Drucker-Prayger Model

Thomas Kasper et al, 2007, lining design for the district heating tunnel in Copenhagen with steel fiber reinforced concrete segment, tunnel lining and underground space technology, Germany.

Victor C.Li, Mohamed Maalej, 1996, toughening in cement based composites. Part II: Fiber Reinforced Concrete Cementitious Composites, cement and concrete composites 18, 239-249.

W. Angerer, M. Chappell, 2008, Design of steel fiber reinforced segmental lining for the gold coast destinations tunnels, 13th Australian Tunneling Conference, Melbourne, p.463-470.

Yining Ding, Wolfgang Kusterle, 2000, Compressive stress-strain relationship of steel fibre-reinforced concrete at early age. Cement & concrete research 30, 1573-1579.

# Appendix

# 1 . Compressive test:

| Batch No. | Slump (cm) | Cube specimens | | | Beam specimens | | | Age (day) | Average Cube Compressive strength (ksc) |
|---|---|---|---|---|---|---|---|---|---|
| | | Bulk density (kg/m3) | Number of specimen | COV (%) | Bulk density (kg/m3) | Number of specimen | COV (%) | | |
| 240-0-NSP | 13.0 | 2489 | 8 | 1.06 | 2432 | 6 | 1.40 | 7 | 213 |
| 240-15-NSP | 13.5 | 2442 | 8 | 1.69 | 2473 | 6 | 1.07 | 7 | 254 |
| 240-20-NSP | 11.5 | 2404 | 6 | 0.64 | 2437 | 6 | 1.44 | 7 | 224 |
| 240-25-NSP | 11.0 | 2463 | 6 | 0.98 | 2437 | 6 | 1.83 | 7 | 246 |
| 240-30-NSP | 13.0 | 2443 | 8 | 1.64 | 2497 | 6 | 1.93 | 7 | 232 |
| 240-35-NSP | 11.7 | 2475 | 8 | 1.37 | 2410 | 6 | 1.24 | 7 | 237 |
| 240-40-NSP | 11.0 | 2479 | 4 | 3.73 | 2470 | 6 | 1.42 | 8 | 248 |
| 240-0-SP | 13.0 | 2468 | 4 | 2.38 | 2457 | 6 | 1.10 | 6 | 240 |
| 240-15-SP | 15.0 | 2489 | 4 | 0.76 | 2418 | 6 | 0.78 | 5 | 241 |
| 240-20-SP | 15.5 | 2478 | 4 | 1.79 | 2425 | 6 | 0.59 | 5 | 235 |
| 240-25-SP | 15.0 | 2499 | 4 | 0.88 | 2452 | 6 | 0.52 | 6 | 240 |
| 240-30-SP | 14.5 | 2508 | 4 | 1.20 | 2431 | 6 | 1.04 | 6 | 241 |
| 240-35-SP | 16.5 | 2519 | 4 | 1.66 | 2448 | 6 | 2.05 | 5 | 251 |
| 240-40-SP | 15.0 | 2446 | 4 | 2.66 | 2436 | 6 | 1.51 | 5 | 223 |
| 320-0-NSP | 10.5 | 2534 | 4 | 2.19 | 2451 | 6 | 0.72 | 10 | 306 |
| 320-15-NSP | 10.5 | 2499 | 4 | 2.26 | 2447 | 6 | 0.66 | 10 | 319 |
| 320-20-NSP | 10.5 | 2498 | 4 | 1.40 | 2454 | 6 | 0.42 | 10 | 322 |
| 320-25-NSP | 11.0 | 2522 | 4 | 1.05 | 2431 | 6 | 0.53 | 11 | 319 |
| 320-30-NSP | 11.0 | 2487 | 4 | 1.92 | 2453 | 6 | 1.09 | 10 | 317 |
| 320-35-NSP | 12.0 | 2494 | 4 | 1.87 | 2410 | 6 | 0.89 | 10 | 310 |

| Batch No. | Slump (cm) | Cube specimens | | | Beam specimens | | | Age (day) | Average Cube Compressive strength (ksc) |
|---|---|---|---|---|---|---|---|---|---|
| | | Bulk density (kg/m3) | Number of specimen | COV (%) | Bulk density (kg/m3) | Number of specimen | COV (%) | | |
| 320-40-NSP | 10.5 | 2485 | 4 | 2.30 | 2417 | 6 | 0.82 | 10 | 315 |
| 320-0-SP | 14.0 | 2436 | 7 | 1.46 | 2384 | 6 | 2.20 | 7 | 315 |
| 320-15-SP | 16.0 | 2534 | 4 | 2.19 | 2463 | 6 | 1.30 | 8 | 306 |
| 320-20-SP | 15.0 | 2502 | 4 | 1.10 | 2491 | 6 | 1.46 | 7 | 323 |
| 320-25-SP | 14.2 | 2461 | 4 | 2.32 | 2460 | 6 | 1.57 | 7 | 307 |
| 320-30-SP | 13.9 | 2497 | 4 | 1.62 | 2422 | 6 | 2.07 | 7 | 319 |
| 320-35-SP | 14.0 | 2526 | 4 | 1.57 | 2423 | 6 | 2.35 | 7 | 312 |
| 320-40-SP | 13.4 | 2494 | 4 | 1.64 | 2435 | 6 | 1.75 | 7 | 318 |

## 2 . Flexural test:

| Specimen<br>no | First-Peak load<br>$P_1$<br>kN | Peak load<br>Pp<br>kN | Net deflection at first peak load<br>$\delta_1$<br>mm | Net deflection at peak load<br>$\delta_P$<br>mm | First-Peak strength<br>$f_1$<br>Mpa | Peak strength<br>fp<br>Mpa | Residual load at L/600<br>$P^D_{600}$<br>kN | Residual strength at L/600<br>$f^D_{600}$<br>Mpa | Residual load at L/450<br>$P^D_{450}$<br>kN | Residual strength at L/450<br>$f^D_{450}$<br>Mpa | Residual load at L/150<br>$P^D_{150}$<br>kN | Residual strength at L/150<br>$f^D_{150}$<br>Mpa | Modulus of elasticity under bending<br>E<br>Mpa | Toughness<br>$T^D_{150}$<br>Joule | Equivalent Flexural Strength Ratio<br>$R^D_{T,150}$<br>% | Fracture offset<br>mm | remark |
|---|---|---|---|---|---|---|---|---|---|---|---|---|---|---|---|---|---|
| 1-240-0-NSP | 39 | 39 | 0.06 | 0.06 | 5.00 | 5.00 | 0 | 0.00 | 0 | 0.00 | 0 | 0.00 | 89820 | 1 | 1.0 | not available | |
| 2-240-0-NSP | 32 | 32 | 0.05 | 0.05 | 4.10 | 4.10 | 0 | 0.00 | 0 | 0.00 | 0 | 0.00 | 89171 | 1 | 1.0 | not available | |
| 3-240-0-NSP | 37 | 37 | 0.05 | 0.05 | 4.80 | 4.80 | 0 | 0.00 | 0 | 0.00 | 0 | 0.00 | 109021 | 1 | 1.0 | not available | |
| 4-240-0-NSP | 32 | 32 | 0.06 | 0.06 | 4.15 | 4.15 | 0 | 0.00 | 0 | 0.00 | 0 | 0.00 | 83358 | 1 | 1.5 | not available | |
| 5-240-0-NSP | 34 | 34 | 0.05 | 0.05 | 4.45 | 4.45 | 0 | 0.00 | 0 | 0.00 | 0 | 0.00 | 96646 | 1 | 1.5 | not available | |
| 6-240-0-NSP | 31 | 31 | 0.04 | 0.04 | 3.90 | 3.90 | 0 | 0.00 | 0 | 0.00 | 0 | 0.00 | 112118 | 1 | 1.0 | not available | |
| 1-240-15-NSP | 30 | 30 | 0.03 | 0.03 | 3.60 | 3.60 | 7 | 0.85 | 7 | 0.85 | 4 | 0.45 | 120016 | 21 | 24.0 | not available | |
| 2-240-15-NSP | 35 | 35 | 0.04 | 0.04 | 4.50 | 4.50 | 17 | 2.25 | 14 | 1.85 | 13 | 1.70 | 134572 | 47 | 45.5 | not available | |
| 3-240-15-NSP | 35 | 35 | 0.07 | 0.07 | 4.45 | 4.45 | 9 | 1.15 | 8 | 1.05 | 5 | 0.65 | 77159 | 29 | 28.0 | not available | |
| 4-240-15-NSP | 34 | 34 | 0.03 | 0.03 | 4.15 | 4.15 | 13 | 1.55 | 13 | 1.55 | 11 | 1.30 | 147320 | 40 | 39.0 | not available | |
| 5-240-15-NSP | 27 | 27 | 0.03 | 0.03 | 3.30 | 3.30 | 6 | 0.70 | 6 | 0.70 | 6 | 0.75 | 130564 | 27 | 32.5 | not available | |
| 6-240-15-NSP | 35 | 35 | 0.03 | 0.03 | 4.25 | 4.25 | 12 | 1.40 | 11 | 1.35 | 10 | 1.25 | 142834 | 38 | 36.5 | not available | |
| 1-240-20-NSP | 34 | 34 | 0.05 | 0.05 | 4.50 | 4.50 | 7 | 1.00 | 7 | 1.00 | 7 | 0.90 | 109132 | 30 | 28.5 | not available | |
| 2-240-20-NSP | 42 | 42 | 0.10 | 0.10 | 5.50 | 5.50 | 9 | 1.15 | 9 | 1.20 | 6 | 0.75 | 56000 | 37 | 28.0 | not available | |
| 3-240-20-NSP | 33 | 33 | 0.08 | 0.08 | 4.25 | 4.25 | 17 | 2.25 | 18 | 2.40 | 18 | 2.35 | 65483 | 56 | 55.5 | not available | |

| Specimen no | First-Peak load $P_1$ kN | Peak load Pp kN | Net deflection at first peak load $\delta_1$ mm | Net deflection at peak load $\delta_P$ mm | First-Peak strength $f_1$ Mpa | Peak strength fp Mpa | Residual load at L/600 $P^D_{600}$ kN | Residual strength at L/600 $f^D_{600}$ Mpa | Residual load at L/450 $P^D_{450}$ kN | Residual strength at L/450 $f^D_{450}$ Mpa | Residual load at L/150 $P^D_{150}$ kN | Residual strength at L/150 $f^D_{150}$ Mpa | Modulus of elasticity under bending E Mpa | Toughness $T^D_{150}$ Joule | Equivalent Flexural Strength Ratio $R^D_{T,150}$ % | Fracture offset mm | remark |
|---|---|---|---|---|---|---|---|---|---|---|---|---|---|---|---|---|---|
| 1-240-35-SP | 34 | 34 | 0.01 | 0.01 | 4.45 | 4.45 | 18 | 2.30 | not available | not available | not available | not available | 542114 | 20 | not available | not available | Test discarded due to the error of machine |
| 2-240-35-SP | 39 | 39 | 0.02 | 0.02 | 4.85 | 4.85 | 25 | 3.10 | 25 | 3.10 | 21 | 2.65 | 248989 | 73 | 63.5 | not available | |
| 3-240-35-SP | 37 | 37 | 0.06 | 0.06 | 4.75 | 4.75 | 24 | 3.10 | 24 | 3.05 | 22 | 2.75 | 89909 | 72 | 61.0 | not available | |
| 4-240-35-SP | 33 | 33 | 0.07 | 0.07 | 4.15 | 4.15 | 20 | 2.60 | 21 | 2.60 | 17 | 2.20 | 70466 | 60 | 58.0 | not available | |
| 5-240-35-SP | 33 | 33 | 0.04 | 0.04 | 4.25 | 4.25 | 22 | 2.80 | 21 | 2.65 | 20 | 2.60 | 135972 | 64 | 64.0 | not available | |
| 6-240-35-SP | 23 | 23 | 0.11 | 0.11 | 3.00 | 3.00 | 19 | 2.45 | 20 | 2.55 | 22 | 2.85 | 32371 | 62 | 83.5 | not available | |
| 1-240-40-SP | 37 | 37 | 0.09 | 0.09 | 4.60 | 4.60 | 34 | 4.25 | 35 | 4.35 | 32 | 4.00 | 61212 | 100 | 91.0 | 205.0 | Test discarded due to poor distribution of fiber |
| 2-240-40-SP | 26 | 26 | 0.03 | 0.03 | 3.40 | 3.40 | 12 | 1.60 | 14 | 1.85 | 17 | 2.25 | 149506 | 46 | 59.0 | 151.0 | |
| 3-240-40-SP | 31 | 31 | 0.06 | 0.06 | 3.95 | 3.95 | 17 | 2.20 | 19 | 2.40 | 20 | 2.60 | 71758 | 61 | 66.0 | 180.0 | |
| 4-240-40-SP | 35 | 35 | 0.06 | 0.06 | 4.45 | 4.45 | 21 | 2.70 | 22 | 2.80 | 23 | 3.00 | 91180 | 69 | 66.0 | 220.0 | |
| 5-240-40-SP | 25 | 25 | 0.04 | 0.04 | 3.10 | 3.10 | 13 | 1.65 | 11 | 1.30 | 16 | 1.90 | 76959 | 42 | 54.5 | 159.0 | |
| 6-240-40-SP | 34 | 34 | 0.07 | 0.07 | 4.25 | 4.25 | 21 | 2.60 | 22 | 2.75 | 23 | 2.90 | 70834 | 70 | 67.5 | 191.0 | |
| 1-320-0-NSP | 35 | 35 | 0.05 | 0.05 | 4.55 | 4.55 | 0 | 0.00 | 0 | 0.00 | 0 | 0.00 | 113567 | 1 | 1.0 | 160.5 | |
| 2-320-0-NSP | 37 | 37 | 0.03 | 0.03 | 4.65 | 4.65 | 0 | 0.00 | 0 | 0.00 | 0 | 0.00 | 134427 | 0 | 0.0 | 156.0 | |
| 3-320-0-NSP | 29 | 29 | 0.04 | 0.04 | 3.75 | 3.75 | 0 | 0.00 | 0 | 0.00 | 0 | 0.00 | 119612 | 1 | 0.5 | 160.0 | |

| Specimen<br>no | First-Peak load<br>$P_1$<br>kN | Peak load<br>Pp<br>kN | Net deflection at first peak load<br>$\delta_1$<br>mm | Net deflection at peak load<br>$\delta_P$<br>mm | First-Peak strength<br>$f_1$<br>Mpa | Peak strength<br>fp<br>Mpa | Residual load at L/600<br>$P^D_{600}$<br>kN | Residual strength at L/600<br>$f^D_{600}$<br>Mpa | Residual load at L/450<br>$P^D_{450}$<br>kN | Residual strength at L/450<br>$f^D_{450}$<br>Mpa | Residual load at L/150<br>$P^D_{150}$<br>kN | Residual strength at L/150<br>$f^D_{150}$<br>Mpa | Modulus of elasticity under bending<br>E<br>Mpa | Toughness<br>$T^D_{150}$<br>Joule | Equivalent Flexural Strength Ratio<br>$R^D_{T,150}$<br>% | Fracture offset<br>mm | remark |
|---|---|---|---|---|---|---|---|---|---|---|---|---|---|---|---|---|---|
| 4-320-0-NSP | 34 | 34 | 0.04 | 0.04 | 4.40 | 4.40 | 0 | 0.00 | 0 | 0.00 | 0 | 0.00 | 121569 | 1 | 1.0 | 163.0 | |
| 5-320-0-NSP | 28 | 28 | 0.01 | 0.01 | 3.50 | 3.50 | 0 | 0.00 | 0 | 0.00 | 0 | 0.00 | 471576 | 0 | 0.0 | 186.0 | |
| 6-320-0-NSP | 25 | 25 | 0.03 | 0.03 | 3.10 | 3.10 | 0 | 0.00 | 0 | 0.00 | 0 | 0.00 | 114015 | 0 | 0.5 | 205.0 | |
| 1-320-15-NSP | 34 | 34 | 0.04 | 0.04 | 4.20 | 4.20 | 16 | 2.00 | 16 | 2.05 | 15 | 1.95 | 137667 | 51 | 51.0 | 191.0 | |
| 2-320-15-NSP | 37 | 37 | 0.03 | 0.03 | 4.65 | 4.65 | 15 | 1.85 | 15 | 1.85 | 17 | 2.10 | 156421 | 51 | 46.0 | 173.0 | |
| 3-320-15-NSP | 33 | 33 | 0.01 | 0.01 | 4.05 | 4.05 | 7 | 0.85 | 7 | 0.85 | 7 | 0.90 | 340505 | 29 | 29.5 | 190.0 | |
| 4-320-15-NSP | 34 | 34 | 0.04 | 0.04 | 4.20 | 4.20 | 16 | 2.05 | 16 | 2.00 | 17 | 2.10 | 122999 | 55 | 54.5 | 178.0 | |
| 5-320-15-NSP | 37 | 37 | 0.02 | 0.02 | 4.45 | 4.45 | 13 | 1.60 | 14 | 1.65 | 16 | 1.90 | 199495 | 53 | 47.5 | 187.0 | |
| 6-320-15-NSP | 33 | 33 | 0.09 | 0.09 | 4.10 | 4.10 | 17 | 2.10 | 17 | 2.15 | 17 | 2.10 | 53269 | 51 | 51.5 | 180.0 | |
| 1-320-20-NSP | 40 | 40 | 0.04 | 0.04 | 5.10 | 5.10 | 20 | 2.65 | 20 | 2.55 | 18 | 2.35 | 133401 | 62 | 52.0 | 215.0 | |
| 2-320-20-NSP | 38 | 38 | 0.04 | 0.04 | 4.65 | 4.65 | 17 | 2.05 | 18 | 2.25 | 17 | 2.05 | 120386 | 56 | 49.5 | 167.0 | |
| 3-320-20-NSP | 39 | 39 | 0.07 | 0.07 | 4.85 | 4.85 | 20 | 2.50 | 22 | 2.75 | 21 | 2.65 | 78261 | 68 | 58.5 | 185.0 | |
| 4-320-20-NSP | 31 | 31 | 0.07 | 0.07 | 3.75 | 3.75 | 13 | 1.55 | 12 | 1.50 | 12 | 1.45 | 63493 | 40 | 43.0 | 165.0 | |
| 5-320-20-NSP | 36 | 36 | 0.02 | 0.02 | 4.40 | 4.40 | 15 | 1.85 | 16 | 1.90 | 18 | 2.15 | 248193 | 58 | 53.0 | 175.0 | |
| 6-320-20-NSP | 38 | 38 | 0.08 | 0.08 | 4.65 | 4.65 | 20 | 2.50 | 22 | 2.75 | 22 | 2.65 | 63753 | 69 | 62.0 | 180.0 | |
| 1-320-25-NSP | 33 | 33 | 0.07 | 0.07 | 4.15 | 4.15 | 15 | 1.85 | 15 | 1.90 | 18 | 2.25 | 66922 | 52 | 51.5 | 155.0 | |
| 2-320-25-NSP | 34 | 34 | 0.04 | 0.04 | 4.05 | 4.05 | 19 | 2.30 | 20 | 2.40 | 19 | 2.30 | 111418 | 61 | 61.0 | 205.0 | |
| 3-320-25-NSP | 32 | 32 | 0.08 | 0.08 | 3.85 | 3.85 | 15 | 1.85 | 16 | 1.95 | 18 | 2.15 | 53054 | 52 | 54.5 | 180.0 | |
| 4-320-25-NSP | 28 | 28 | 0.04 | 0.04 | 3.30 | 3.30 | 15 | 1.75 | 15 | 1.75 | 17 | 2.00 | 82249 | 49 | 59.0 | 140.0 | Test discarded due to fracture outside L/3 |

| Specimen<br>no | First-Peak load<br>$P_1$<br>kN | Peak load<br>Pp<br>kN | Net deflection at first peak load<br>$\delta_1$<br>mm | Net deflection at peak load<br>$\delta_P$<br>mm | First-Peak strength<br>$f_1$<br>Mpa | Peak strength<br>fp<br>Mpa | Residual load at L/600<br>$P^D_{600}$<br>kN | Residual strength at L/600<br>$f^D_{600}$<br>Mpa | Residual load at L/450<br>$P^D_{450}$<br>kN | Residual strength at L/450<br>$f^D_{450}$<br>Mpa | Residual load at L/150<br>$P^D_{150}$<br>kN | Residual strength at L/150<br>$f^D_{150}$<br>Mpa | Modulus of elasticity under bending<br>E<br>Mpa | Toughness<br>$T^D_{150}$<br>Joule | Equivalent Flexural Strength Ratio<br>$R^D_{T,150}$<br>% | Fracture offset<br>mm | remark |
|---|---|---|---|---|---|---|---|---|---|---|---|---|---|---|---|---|---|
| 5-320-25-NSP | 33 | 33 | 0.02 | 0.02 | 4.00 | 4.00 | 15 | 1.80 | 15 | 1.75 | 17 | 2.00 | 180358 | 52 | 52.5 | 151.0 | |
| 6-320-25-NSP | 33 | 33 | 0.09 | 0.09 | 4.10 | 4.10 | 20 | 2.50 | 20 | 2.45 | 19 | 2.35 | 52371 | 61 | 61.5 | 160.0 | |
| 1-320-30-NSP | 32 | 32 | 0.07 | 0.07 | 3.90 | 3.90 | 24 | 2.95 | 25 | 3.00 | 23 | 2.85 | 60539 | 73 | 76.0 | 187.0 | |
| 2-320-30-NSP | 34 | 34 | 0.06 | 0.06 | 4.25 | 4.25 | 27 | 3.30 | 26 | 3.25 | 23 | 2.80 | 79851 | 77 | 74.5 | 190.0 | |
| 3-320-30-NSP | 37 | 37 | 0.09 | 0.09 | 4.35 | 4.35 | 19 | 2.30 | 19 | 2.20 | 19 | 2.30 | 53150 | 60 | 54.5 | 170.0 | |
| 4-320-30-NSP | 32 | 32 | 0.08 | 0.08 | 4.05 | 4.05 | 26 | 3.25 | 26 | 3.25 | 22 | 2.70 | 57249 | 72 | 74.5 | 180.0 | |
| 5-320-30-NSP | 36 | 36 | 0.08 | 0.08 | 4.35 | 4.35 | 25 | 3.05 | 25 | 3.05 | 25 | 3.00 | 58773 | 78 | 72.0 | 185.0 | |
| 6-320-30-NSP | 34 | 34 | 0.07 | 0.07 | 4.20 | 4.20 | 19 | 2.35 | 18 | 2.30 | 19 | 2.40 | 70002 | 57 | 56.0 | 168.0 | |
| 1-320-35-NSP | 38 | 38 | 0.06 | 0.06 | 4.65 | 4.65 | 27 | 3.35 | 28 | 3.50 | 28 | 3.45 | 87379 | 85 | 75.5 | 195.0 | |
| 2-320-35-NSP | 30 | 30 | 0.08 | 0.08 | 3.75 | 3.75 | 22 | 2.70 | 23 | 2.85 | 24 | 2.95 | 52749 | 69 | 77.5 | 225.0 | |
| 3-320-35-NSP | 48 | 48 | 0.08 | 0.08 | 5.80 | 5.80 | 32 | 3.90 | 32 | 3.80 | 30 | 3.55 | 83108 | 90 | 62.5 | 157.0 | |
| 4-320-35-NSP | 34 | 34 | 0.05 | 0.05 | 4.35 | 4.35 | 20 | 2.55 | 22 | 2.75 | 21 | 2.60 | 108454 | 66 | 64.0 | 175.0 | |
| 5-320-35-NSP | 37 | 37 | 0.06 | 0.06 | 4.55 | 4.55 | 27 | 3.25 | 27 | 3.35 | 28 | 3.45 | 81640 | 85 | 76.0 | 167.0 | |
| 6-320-35-NSP | 47 | 47 | 0.06 | 0.06 | 5.75 | 5.75 | 29 | 3.60 | 29 | 3.60 | 27 | 3.35 | 114827 | 92 | 66.0 | 185.0 | |
| 1-320-40-NSP | 24 | 24 | 0.01 | 0.01 | 3.00 | 3.00 | 18 | 2.25 | 18 | 2.25 | 19 | 2.45 | 307730 | 55 | 77.0 | 170.0 | |
| 2-320-40-NSP | 30 | 30 | 0.07 | 1.21 | 3.80 | 3.90 | 29 | 3.70 | 29 | 3.70 | 29 | 3.65 | 62294 | 85 | 95.0 | 205.0 | |
| 3-320-40-NSP | 34 | 34 | 0.06 | 0.06 | 4.50 | 4.50 | 25 | 3.30 | 27 | 3.65 | 26 | 3.55 | 82492 | 82 | 80.5 | 180.0 | |
| 4-320-40-NSP | 39 | 39 | 0.04 | 0.04 | 4.90 | 4.90 | 28 | 3.50 | 29 | 3.65 | 30 | 3.75 | 128574 | 88 | 75.0 | 167.0 | |
| 5-320-40-NSP | 22 | 22 | 0.05 | 0.05 | 2.70 | 2.70 | 19 | 2.35 | 18 | 2.20 | 18 | 2.20 | 64375 | 54 | 81.5 | 165.0 | |

| Specimen<br>no | First-Peak load<br>$P_1$<br>kN | Peak load<br>Pp<br>kN | Net deflection at first peak load<br>$\delta_1$<br>mm | Net deflection at peak load<br>$\delta_P$<br>mm | First-Peak strength<br>$f_1$<br>Mpa | Peak strength<br>fp<br>Mpa | Residual load at L/600<br>$P^D_{600}$<br>kN | Residual strength at L/600<br>$f^D_{600}$<br>Mpa | Residual load at L/450<br>$P^D_{450}$<br>kN | Residual strength at L/450<br>$f^D_{450}$<br>Mpa | Residual load at L/150<br>$P^D_{150}$<br>kN | Residual strength at L/150<br>$f^D_{150}$<br>Mpa | Modulus of elasticity under bending<br>E<br>Mpa | Toughness<br>$T^D_{150}$<br>Joule | Equivalent Flexural Strength Ratio<br>$R^D_{T,150}$<br>% | Fracture offset<br>mm | remark |
|---|---|---|---|---|---|---|---|---|---|---|---|---|---|---|---|---|---|
| 6-320-40-NSP | 33 | 33 | 0.05 | 0.05 | 4.05 | 4.05 | 24 | 3.00 | 26 | 3.25 | 28 | 3.45 | 64375 | 80 | 81.0 | 163.0 | |
| 1-320-0-SP | 38 | 38 | 0.06 | 0.06 | 4.90 | 4.90 | 0 | 0.00 | 0 | 0.00 | 0 | 0.00 | 91837 | 1 | 1.0 | not available | |
| 2-320-0-SP | 29 | 29 | 0.09 | 0.09 | 3.80 | 3.80 | 0 | 0.00 | 0 | 0.00 | 0 | 0.00 | 49662 | 2 | 2.0 | not available | |
| 3-320-0-SP | 34 | 34 | 0.03 | 0.03 | 4.50 | 4.50 | 0 | 0.00 | 0 | 0.00 | 0 | 0.00 | 154561 | 0 | 0.5 | not available | |
| 4-320-0-SP | 37 | 37 | 0.05 | 0.05 | 4.95 | 4.95 | 0 | 0.00 | 0 | 0.00 | 0 | 0.00 | 117464 | 1 | 1.0 | not available | |
| 5-320-0-SP | 30 | 30 | 0.05 | 0.05 | 3.90 | 3.90 | 0 | 0.00 | 0 | 0.00 | 0 | 0.00 | 88487 | 1 | 1.0 | not available | |
| 6-320-0-SP | 31 | 31 | 0.04 | 0.04 | 4.05 | 4.05 | 0 | 0.00 | 0 | 0.00 | 0 | 0.00 | 127451 | 0 | 0.5 | not available | |
| 1-320-15-SP | 29 | 29 | 0.01 | 0.01 | 3.65 | 3.65 | 10 | 1.35 | 11 | 1.35 | 12 | 1.60 | 369975 | 38 | 44.0 | 182.0 | |
| 2-320-15-SP | 29 | 29 | 0.03 | 0.03 | 3.70 | 3.70 | 10 | 1.30 | 11 | 1.35 | 12 | 1.50 | 165161 | 38 | 42.5 | 178.0 | |
| 3-320-15-SP | 29 | 29 | 0.06 | 0.06 | 3.70 | 3.70 | 11 | 1.35 | 12 | 1.55 | 12 | 1.50 | 69863 | 42 | 48.0 | 167.0 | |
| 4-320-15-SP | 27 | 27 | 0.02 | 0.02 | 3.40 | 3.40 | 11 | 1.35 | 11 | 1.35 | 12 | 1.45 | 181709 | 38 | 45.5 | 180.0 | |
| 5-320-15-SP | 29 | 29 | 0.05 | 0.05 | 3.55 | 3.55 | 10 | 1.25 | 11 | 1.40 | 11 | 1.40 | 76256 | 36 | 41.5 | 171.0 | |
| 6-320-15-SP | 29 | 29 | 0.03 | 0.03 | 3.60 | 3.60 | 16 | 1.95 | 16 | 2.05 | 14 | 1.75 | 143545 | 47 | 54.0 | 163.0 | |
| 1-320-20-SP | 41 | 41 | 0.06 | 0.06 | 5.20 | 5.20 | 14 | 1.85 | 15 | 1.85 | 14 | 1.70 | 100954 | 49 | 39.5 | 207.0 | |
| 2-320-20-SP | 38 | 38 | 0.03 | 0.03 | 4.85 | 4.85 | 18 | 2.30 | 19 | 2.45 | 21 | 2.70 | 180796 | 62 | 54.5 | 180.0 | |
| 3-320-20-SP | 29 | 29 | 0.04 | 0.04 | 3.80 | 3.80 | 4 | 0.50 | 4 | 0.50 | 4 | 0.50 | 101492 | 18 | 20.0 | 155.0 | Test discarded due to void in beam specimen |

| Specimen | First-Peak load | Peak load | Net deflection at first peak load | Net deflection at peak load | First-Peak strength | Peak strength | Residual load at L/600 | Residual strength at L/600 | Residual load at L/450 | Residual strength at L/450 | Residual load at L/150 | Residual strength at L/150 | Modulus of elasticity under bending | Toughness | Equivalent Flexural Strength Ratio | Fracture offset | remark |
|---|---|---|---|---|---|---|---|---|---|---|---|---|---|---|---|---|---|
| no | $P_1$ | Pp | $\delta_1$ | $\delta_P$ | $f_1$ | fp | $P^D_{600}$ | $f^D_{600}$ | $P^D_{450}$ | $f^D_{450}$ | $P^D_{150}$ | $f^D_{150}$ | E | $T^D_{150}$ | $R^D_{T,150}$ | | |
| | kN | kN | mm | mm | Mpa | Mpa | kN | Mpa | kN | Mpa | kN | Mpa | Mpa | Joule | % | mm | |
| 4-320-20-SP | 42 | 42 | 0.03 | 0.03 | 5.50 | 5.50 | 27 | 3.50 | 26 | 3.35 | 22 | 2.85 | 234152 | 76 | 60.0 | 180.0 | |
| 5-320-20-SP | 37 | 37 | 0.06 | 0.06 | 4.55 | 4.55 | 18 | 2.25 | 19 | 2.30 | 17 | 2.10 | 77759 | 60 | 53.0 | 225.0 | |
| 6-320-20-SP | 41 | 41 | 0.06 | 0.06 | 5.10 | 5.10 | 27 | 3.40 | 27 | 3.35 | 23 | 2.80 | 93612 | 77 | 63.0 | 220.0 | |
| 1-320-25-SP | 37 | 37 | 0.01 | 0.01 | 4.50 | 4.50 | 27 | 3.25 | 30 | 3.60 | 25 | 2.95 | 455107 | 88 | 78.0 | 155.0 | |
| 2-320-25-SP | 37 | 37 | 0.02 | 0.02 | 4.50 | 4.50 | 26 | 3.10 | 27 | 3.25 | 26 | 3.15 | 244790 | 82 | 73.5 | 193.0 | |
| 3-320-25-SP | 41 | 41 | 0.04 | 0.04 | 4.95 | 4.95 | 22 | 2.65 | 23 | 2.70 | 22 | 2.65 | 149763 | 71 | 58.0 | 200.0 | |
| 4-320-25-SP | 37 | 37 | 0.07 | 0.07 | 4.55 | 4.55 | 27 | 3.25 | 30 | 3.70 | 28 | 3.45 | 69323 | 86 | 77.0 | 195.0 | |
| 5-320-25-SP | 36 | 36 | 0.05 | 0.05 | 4.40 | 4.40 | 27 | 3.25 | 28 | 3.45 | 30 | 3.65 | 99481 | 85 | 78.5 | 175.0 | |
| 6-320-25-SP | 39 | 39 | 0.05 | 0.05 | 4.85 | 4.85 | 21 | 2.65 | 23 | 2.85 | 21 | 2.60 | 106603 | 69 | 58.5 | 177.0 | |
| 1-320-30-SP | 32 | 32 | 0.07 | 0.07 | 3.90 | 3.90 | 24 | 2.95 | 25 | 3.00 | 23 | 2.85 | 59738 | 73 | 76.0 | 225.0 | |
| 2-320-30-SP | 34 | 34 | 0.06 | 0.06 | 4.30 | 4.30 | 27 | 3.35 | 26 | 3.30 | 23 | 2.85 | 82509 | 77 | 75.0 | 180.0 | |
| 3-320-30-SP | 37 | 37 | 0.09 | 0.09 | 4.50 | 4.50 | 19 | 2.40 | 19 | 2.30 | 19 | 2.35 | 55954 | 60 | 54.5 | 215.0 | |
| 4-320-30-SP | 32 | 32 | 0.05 | 0.05 | 4.15 | 4.15 | 25 | 3.20 | 25 | 3.25 | 24 | 3.10 | 87115 | 72 | 75.0 | 185.0 | |
| 5-320-30-SP | 34 | 34 | 0.07 | 0.07 | 4.15 | 4.15 | 27 | 3.25 | 26 | 3.20 | 27 | 3.25 | 69427 | 75 | 73.0 | 200.0 | |
| 6-320-30-SP | 32 | 32 | 0.06 | 0.06 | 3.95 | 3.95 | 24 | 3.00 | 24 | 3.00 | 23 | 2.90 | 74473 | 73 | 77.0 | 205.0 | |
| 1-320-35-SP | 35 | 35 | 0.09 | 0.09 | 4.30 | 4.30 | 21 | 2.55 | 21 | 2.65 | 22 | 2.75 | 53330 | 67 | 63.5 | 165.0 | |
| 2-320-35-SP | 36 | 36 | 0.08 | 0.08 | 4.60 | 4.60 | 30 | 3.85 | 31 | 3.95 | 32 | 4.10 | 66904 | 100 | 90.5 | 215.0 | |
| 3-320-35-SP | 40 | 40 | 0.07 | 0.07 | 5.00 | 5.00 | 34 | 4.15 | 35 | 4.35 | 32 | 3.95 | 84096 | 102 | 84.0 | 158.0 | |
| 4-320-35-SP | 33 | 36 | 0.08 | 1.16 | 4.15 | 4.55 | 33 | 4.15 | 35 | 4.40 | 23 | 2.90 | 57162 | 90 | 90.5 | 155.0 | |

| Specimen | First-Peak load | Peak load | Net deflection at first peak load | Net deflection at peak load | First-Peak strength | Peak strength | Residual load at L/600 | Residual strength at L/600 | Residual load at L/450 | Residual strength at L/450 | Residual load at L/150 | Residual strength at L/150 | Modulus of elasticity under bending | Toughness | Equivalent Flexural Strength Ratio | Fracture offset | remark |
|---|---|---|---|---|---|---|---|---|---|---|---|---|---|---|---|---|---|
| no | $P_1$ | Pp | $\delta_1$ | $\delta_P$ | $f_1$ | fp | $P^D_{600}$ | $f^D_{600}$ | $P^D_{450}$ | $f^D_{450}$ | $P^D_{150}$ | $f^D_{150}$ | E | $T^D_{150}$ | $R^D_{T,150}$ | | |
| | kN | kN | mm | mm | Mpa | Mpa | kN | Mpa | kN | Mpa | kN | Mpa | Mpa | Joule | % | mm | |
| 5-320-35-SP | 40 | 40 | 0.08 | 0.08 | 4.90 | 4.90 | 24 | 2.90 | 24 | 2.90 | 19 | 2.30 | 71022 | 72 | 59.5 | 149.0 | Test discarded due to fracture outside L/3 |
| 6-320-35-SP | 35 | 35 | 0.07 | 0.07 | 4.55 | 4.55 | 22 | 2.80 | 22 | 2.90 | 22 | 2.80 | 73848 | 67 | 63.5 | 167.0 | |
| 1-320-40-SP | 29 | 29 | 0.01 | 0.01 | 3.50 | 3.50 | 24 | 2.85 | 24 | 2.85 | 15 | 1.80 | 348195 | 62 | 71.5 | 200.0 | |
| 2-320-40-SP | 40 | 40 | 0.01 | 0.01 | 4.85 | 4.85 | 36 | 4.35 | 37 | 4.50 | 31 | 3.70 | 456981 | 105 | 87.0 | 195.0 | |
| 3-320-40-SP | 44 | 44 | 0.03 | 0.03 | 5.40 | 5.40 | 41 | 4.95 | 41 | 4.95 | 34 | 4.15 | 200114 | 117 | 87.5 | 175.0 | |
| 4-320-40-SP | 45 | 45 | 0.07 | 0.07 | 5.55 | 5.55 | 37 | 4.50 | 38 | 4.60 | 28 | 3.40 | 86781 | 102 | 75.0 | 180.0 | |
| 5-320-40-SP | 29 | 29 | 0.04 | 0.04 | 3.55 | 3.55 | 23 | 2.80 | 24 | 2.90 | 17 | 2.15 | 114116 | 65 | 74.5 | 187.0 | |
| 6-320-40-SP | 44 | 44 | 0.05 | 0.05 | 5.45 | 5.45 | 35 | 4.30 | 36 | 4.40 | 28 | 3.45 | 120071 | 101 | 76.0 | 193.0 | |

*Remarks: the tables below are the results of flexural test on beam specimens.

3 . Tensile test:

| Batch No. | Age (day) | Strength (ksc) | | | |
|---|---|---|---|---|---|
| | | Specimen1 | Specimen2 | Specimen3 | Average |
| 240-0-NSP | 10 | - | - | - | - |
| 240-15-NSP | 10 | - | - | - | - |
| 240-20-NSP | 10 | - | - | - | - |
| 240-25-NSP | 10 | - | - | - | - |
| 240-30-NSP | 10 | - | - | - | - |
| 240-35-NSP | 10 | - | - | - | - |
| 240-40-NSP | 23 | 28.6 | 37.0 | 36.7 | 34.1 |
| 240-0-SP | 22 | 6.0 | 25.2 | - | 25.2 |
| 240-15-SP | 21 | 23.1 | 22.0 | 12.6 | 22.6 |
| 240-20-SP | 7 | 26.2 | 28.2 | 24.8 | 26.4 |
| 240-25-SP | 6 | 20.1 | 20.2 | 10.4 | 20.2 |
| 240-30-SP | 7 | 27.5 | 24.6 | 25.7 | 25.9 |
| 240-35-SP | 7 | 21.8 | 20.8 | 25.7 | 22.8 |
| 240-40-SP | 5 | 25.1 | 25.7 | 14.5 | 25.4 |
| 320-0-NSP | 10 | 32.0 | 32.2 | 28.8 | 31.0 |
| 320-15-NSP | 10 | 28.0 | 34.4 | 32.1 | 31.5 |
| 320-20-NSP | 26 | 31.6 | 37.3 | 39.7 | 36.2 |
| 320-25-NSP | 25 | 31.8 | 33.6 | 31.6 | 32.3 |
| 320-30-NSP | 30 | 36.7 | 37.7 | 37.8 | 37.4 |
| 320-35-NSP | 29 | 27.6 | 33.1 | 35.0 | 31.9 |
| 320-40-NSP | 28 | 29.2 | 27.3 | 29.2 | 28.6 |
| 320-0-SP | 7 | - | - | - | - |
| 320-15-SP | 8 | 37.5 | 33.9 | 33.1 | 34.8 |
| 320-20-SP | 20 | 47.5 | 31.7 | 1.2 | 39.7 |
| 320-25-SP | 19 | 41.0 | 46.6 | 10.4 | 32.7 |
| 320-30-SP | 18 | 35.3 | 34.2 | 30.2 | 33.2 |
| 320-35-SP | 15 | 38.3 | 34.2 | 24.1 | 32.1 |
| 320-40-SP | 14 | 15.8 | 32.1 | 21.8 | 23.3 |

# 4. Young's modulus and Poisson's ratio

Cube at 7 days

| Specimen No. | peak | stress at 40% | strain at 40% stress | E, Mpa |
|---|---|---|---|---|
| 1 | 262.04 | 104.81 | 0.00204 | 5140 |
| 2 | 290.61 | 116.24 | 0.00088 | 13186 |
| 3 | 319.77 | 127.91 | 0.00121 | 10613 |
| average | | | | 9646 |

Cube at 28 days

| Specimen No. | peak | stress at 40% | strain at 40% stress | E, Mpa |
|---|---|---|---|---|
| 5 | 433.0978 | 173.2391 | 0.001334213 | 12984.37 |
| 6 | 424.6799 | 169.872 | 0.002071861 | 8199.005 |
| 8 | 377.5108 | 151.0043 | 0.002052632 | 7356.621 |
| average | | | | 10591.69 |

Cube at 7 days

| Specimen No. | before, mm | | | after, mm | | ΔD | Δa | ∈x | ∈y | v |
|---|---|---|---|---|---|---|---|---|---|---|
| | a | a | D | a | a | mm | mm | | | |
| 1 | 151 | 152 | 153 | 151.1 | 151 | 0.31 | 0.1 | 0.000662 | 0.002026 | 0.326853 |
| 2 | 153 | 151 | 154 | 152 | 150 | N/A | N/A | N/A | N/A | N/A |
| 3 | 150 | 152 | 152 | 150.3 | 151 | 0.82 | 0.3 | 0.002 | 0.005395 | 0.370732 |
| 4 | 151 | 152 | 152 | 151.2 | 151 | 1.3 | 0.2 | 0.001325 | 0.008553 | 0.154865 |
| average | | | | | | | | | | 0.28415 |

Cube at 28 days

| Specimen No. | before, mm | | | after, mm | | ΔD | Δa | ∈x | ∈y | v |
|---|---|---|---|---|---|---|---|---|---|---|
| | a | a | D | a | a | mm | mm | | | |
| 1 | 151.9 | 150.3 | 152 | 152 | 152.58 | 0.58 | 0.1 | 0.000658 | 0.003816 | 0.172527 |
| 2 | 151.4 | 152.2 | 152 | 151.5 | 152.85 | 0.85 | 0.1 | 0.000661 | 0.005592 | 0.118113 |
| 3 | 149.1 | 154.2 | 153.1 | 150 | 153.1 | N/A | N/A | N/A | N/A | N/A |
| 4 | 151 | 152 | 152 | 151.3 | 152.75 | 0.75 | 0.3 | 0.001987 | 0.004934 | 0.402649 |
| average | | | | | | | | | | 0.231097 |

## BIOGRAPHY

Miss. Thipphamala Manivong was born in Sisattanak districk, Vientiane Capital, Lao PDR on 27th November 1988. She received his Bachelor of Engineering in Civil Engineering from National University of Lao in 2010.

In 2010, she applied for AUN/SEED-Net (JICA) scholarship to study Master degree in Geotechnical Engineering at the Department of Civil Engineering of Chulalongkorn University, Thailand. Her advisor was Assistant Professor Dr. Tanate Srisirirojanakorn (Chulalongkorn University).

She has written 1 proceeding. The name of the proceeding is 17th National Conference on Civil Engineering.

Her main research theme was to evaluate the behavior of tunnel lining by using steel fiber reinforced concrete. Her dissertation is completed on 2nd semester of academic year 2555.